

**OBSERVATION METHOD TO PREDICT MEANDER MIGRATION AND
VERTICAL DEGRADATION OF RIVERS**

A Thesis

by

AXEL MANUEL MONTALVO BARTOLOMEI

Submitted to the Office of Graduate and Professional Studies of
Texas A&M University
in partial fulfillment of the requirements for the degree of

MASTER OF SCIENCE

Chair of Committee,	Jean-Louis Briaud
Committee Members,	Kuang-An Chang
	Frederick M. Chester
Head of Department,	Robin Autenrieth

May 2014

Major Subject: Civil Engineering

Copyright 2014

ABSTRACT

Meander migration and vertical degradation of river bed are processes that have been studied for years. These two erosion controlled processes consist of the gradual change of the geometry of the river due to the flow of water eroding the soil. This erosion may cause a shift that could be a threat to existing bridges, highways, and useful lands. Different methods have been proposed to make predictions of the behavior of rivers with respect to these processes. Many of these methods are used to predict the migration rate and the final position of the bankline or centerline of a river, assuming that the erosion rate is constant for a certain time. However, most of these methods ignore one of the three general processes of meander migration and vertical degradation: geometry, flow, and soil. Therefore, there is need for a method that can accurately predict the amount of erosion that may occur in rivers.

Six different sites in Texas were selected for this project. Four of the selected rivers have meander migration problems, and two rivers have vertical degradation problems. Each river has shown erosion problems that have been a threat to the bridges, roads or farm lands. A new method, called the Observation Method, was developed to predict meander migration and vertical degradation by using geometry, water flow, and soil erodibility. Aerial photos and maps from different years were obtained to study the change of the geometry of the rivers. River hydrographs were obtained from the U.S. Geological Survey to estimate the river velocity from daily flow. Soil samples from each site were obtained for laboratory testing, using the Erosion Function Apparatus. A code was written in MATLAB and Excel to estimate the critical velocity by using a model based on the erosion function obtained from the erosion tests. It is important to know where the river was and its history to be able to predict where the river will be. The erosion of each river from the six sites was estimated using the model and predictions were made for 10 years after the last observation for each case. This method proved to be a simple and quick way to obtain results for the movement of one point of the river.

ACKNOWLEDGEMENTS

I would like to thank first and foremost Dr. Jean-Louis Briaud, my committee chair. His guidance, words and time have been very valuable to me. I am always impressed by his knowledge, experience and leadership. His support and patience in tough times will always be appreciated and never forgotten.

Also, I would like to thank Dr. Xiaofeng Liu, professor at University of Texas in San Antonio, for believing in our work. A bright future is ahead for you. Thanks also to my committee members Dr. Chang and Dr. Chester for their help.

My gratitude also goes to the Texas Department of Transportation, for making this project possible. I would like to thank each person at TxDOT that helped me get all the information needed for this project. Thanks to all the faculty and members of the Civil Engineering Department of Texas A&M University for their help in these last few years. Thanks to Dr. Giovanna Biscontin for giving me the opportunity twice to come to Texas A&M, first as an undergraduate student and then for my graduate studies.

Thanks go to all my family and friends. Their support and encouragement made my journey possible.

TABLE OF CONTENTS

	Page
ABSTRACT	ii
ACKNOWLEDGEMENTS	iii
TABLE OF CONTENTS	iv
LIST OF FIGURES	vi
LIST OF TABLES	xii
CHAPTER I INTRODUCTION AND RESEARCH OBJECTIVES.....	1
1.1 Introduction.....	1
1.2 Research Objectives	4
1.3 General Approaches	4
CHAPTER II LITERATURE REVIEW.....	7
2.1 Introduction.....	7
2.2 General Approaches	7
2.3 Factors Affecting River Erosion	20
CHAPTER III RESEARCH APPROACH	22
3.1 Introduction.....	22
3.2 Full Scale Experimental Study.....	22
3.3 Analytical Study	22
CHAPTER IV FULL SCALE EXPERIMENTAL STUDY.....	24
4.1 Site Locations.....	24
4.2 Movement of Rivers	31
4.3 Site Visit.....	45
4.4 Laboratory Testing	71
CHAPTER V ANALYTICAL STUDY	75
5.1 Introduction.....	75
5.2 Meander Program	76
5.3 Observation Method	81

5.4 Methodology Development and Procedure	82
CHAPTER VI OBSERVATION METHOD	101
6.1 Introduction	101
6.2 General Steps	101
6.3 Use of Excel Spreadsheet.....	109
6.4 Use of Matlab Code.....	113
6.5 Prediction Step	117
6.6 Verification of the Observation Method.....	119
CHAPTER VII RESULTS USING THE OBSERVATION METHOD	122
7.1 Introduction	122
7.2 Results for Critical Velocity (Calibration Step).....	122
7.3 Results for Prediction	139
7.4 Discussion of Results.....	143
CHAPTER VIII SUMMARY AND RECOMMENDATIONS	144
8.1 Summary	144
8.2 Recommendations	145
REFERENCES	147
APPENDIX A	149

LIST OF FIGURES

	Page
Figure 1. SH 63 at Sabine River (Google Earth, 2013)	2
Figure 2. SH 34 at North Sulfur River (Google Earth, 2013)	3
Figure 3. Modified Brice classification system for meandering channels (Brice, 1975)	9
Figure 4. Best-fit circles used to observe the change of the bends between 1937 and 1966 (Lagasse et al. 2004).....	10
Figure 5. Best-fit circles for 1937 and 1966 and the predicted circles for 1998 (Lagasse et al., 2004)	11
Figure 6. Aerial photograph of the White River in 1966 with the 1937 bankline in white and the predicted 1998 bankline in black (Lagasse et al., 2004)	11
Figure 7. Three circles (Years 1, 2, 3) with their respective radius of curvature (R) and the magnitude of migration (D) (Lagasse et al., 2004)	13
Figure 8. Predicted circle in Year 4 (Lagasse et al., 2004)	15
Figure 9. Meander migration for the Nueces River at US 90 (Briaud et al., 2001a).....	16
Figure 10. Relationships between catchment area and erosion rate, based on Hooke (Briaud et al., 2007)	18
Figure 11. Data used by Hooke (1980) (Briaud et al., 2007).....	18
Figure 12. Data used by Brice (1982) (Briaud et al., 2007).....	19
Figure 13. Data used by Nanson and Hickin (1983) (Briaud et al., 2007).....	20
Figure 14. Site locations in Texas.....	24
Figure 15. SH 105 at Brazos River (Google Earth, 2013)	25
Figure 16. FM 787 at Trinity River (Google Earth, 2013).....	26
Figure 17. SH 63 at Sabine River (Google Earth, 2013)	27
Figure 18. SH 34 at North Sulfur River (Google Earth, 2013)	28

Figure 19. US 90 at Nueces River (Google Earth, 2013)	29
Figure 20. FM 973 Bridge at Colorado River (Google Earth, 2013).....	30
Figure 21. Meander movement of Brazos River between 1910 and 1999 (Briaud et al., 2001).....	31
Figure 22. Sketch of channel movement.....	32
Figure 23. Flow hydrograph of Brazos River.....	33
Figure 24. Velocity hydrograph of Brazos River	33
Figure 25. Surveying map of Trinity River	34
Figure 26. Flow hydrograph of Trinity River.....	35
Figure 27. Velocity hydrograph of Trinity River	35
Figure 28. Meander movement of Sabine River between 1989 and 2004.....	36
Figure 29. Flow hydrograph of Sabine River.....	37
Figure 30. Velocity hydrograph of Sabine River	37
Figure 31. Vertical degradation of North Sulfur River at SH 34	38
Figure 32. Flow hydrograph of North Sulfur River.....	39
Figure 33. Velocity hydrograph of North Sulfur River	39
Figure 34. Meander movement of Nueces River between 1995 and 2008	40
Figure 35. Flow hydrograph of Nueces River	41
Figure 36. Velocity hydrograph of Nueces River.....	41
Figure 37. Profiles of Colorado River at FM 973 (cross section)	42
Figure 38. Exposure of drilled shafts.....	43
Figure 39. Flow hydrograph of the Colorado River	44
Figure 40. Velocity hydrograph of the Colorado River	44
Figure 41. Location of samples at Brazos River (Google Earth, 2013).....	46

Figure 42. Layers of sand and clay	47
Figure 43. Clay and vegetation at the site	47
Figure 44. Samples S1B1 and S1B2	48
Figure 45. Samples S1B3 and S1B4	49
Figure 46. Samples S1B5 and S1B6	49
Figure 47. Location of samples at Trinity River (Google Earth, 2013).....	50
Figure 48. Trinity River photos	51
Figure 49. Sheet piles and cracks	52
Figure 50. Sample S2B1 and slope next to sheet pile.....	53
Figure 51. Riprap and samples S2B4 and S2B5.....	54
Figure 52. Location of samples at Sabine River (Google Earth, 2013).....	55
Figure 53. Vegetation and concrete next to river	56
Figure 54. Column of the bridge	56
Figure 55. Samples S3B2 and S3B4	57
Figure 56. Concrete blocks at east side of bridge.....	57
Figure 57. Location of samples at North Sulfur River (Google Earth, 2013).....	58
Figure 58. North Sulfur River site photos.....	59
Figure 59. Sample S4B1 and river photo	60
Figure 60. Location of samples at Nueces River (Google Earth, 2013)	61
Figure 61. Nueces River site photos	62
Figure 62. Layers of soil of the river and sample S5B2	63
Figure 63. Obtaining sample S5B7 at meander.....	63
Figure 64. Drilled shafts.....	64
Figure 65. Location of samples (Google Earth, 2013).....	65

Figure 66. Soil sampling	65
Figure 67. Obtaining samples with muffler tube	66
Figure 68. Pocket penetrometer and vane tester.....	68
Figure 69. Erosion categories (Briaud, 2013)	73
Figure 70. EFA test results for erosion rate versus velocity	74
Figure 71. Main interface of the MEANDER program	77
Figure 72. Geometry input	78
Figure 73. Soil data input	79
Figure 74. Water data input	80
Figure 75. Prediction of meander position	80
Figure 76. Gage locations in Texas	84
Figure 77. HEC-RAS interface.....	85
Figure 78. TAMU-FLOW interface.....	86
Figure 79. Flow hydrograph.....	87
Figure 80. Velocity hydrograph.....	87
Figure 81. Erosion Function Apparatus setup and test (Briaud, 2007).....	88
Figure 82. Erosion categories according to soil classification (Briaud, 2013).....	89
Figure 83. Erosion function with erosion rate in mm/hr and velocity in m/s	90
Figure 84. Erosion categories with β values	91
Figure 85. Progress of erosion in Brazos River.....	93
Figure 86. Meander position versus time	94
Figure 87. Observed data (green) and predicted data (blue)	97
Figure 88. Sample of code in MATLAB	98
Figure 89. Estimated erosion progress with time	99

Figure 90. Observed data versus calibrated data	99
Figure 91. USGS website for average daily flow at each state	102
Figure 92. USGS gage selection.....	103
Figure 93. USGS parameters.....	104
Figure 94. Flow hydrograph for a selected period.....	105
Figure 95. Velocity hydrograph for the selected period	106
Figure 96. Erosion function categories spreadsheet	107
Figure 97. Erosion function results and parameters	108
Figure 98. Observed and calibrated data.....	112
Figure 99. Input of erosion parameters, time increments and number of observations.	113
Figure 100. Results of critical velocity and ranking index	114
Figure 101. Movement of point with time	115
Figure 102. Dimensionless EFA curve	115
Figure 103. Velocity hydrograph and critical velocity	116
Figure 104. 1:1 slope line with results of observed data vs. calibrated data.....	116
Figure 105. Predicted data versus time	118
Figure 106. Brazos River verification of prediction with field critical velocity of 0.83 m/s	120
Figure 107. Trinity River verification of prediction with field critical velocity of 0.77 m/s	120
Figure 108. Sabine River verification of prediction with field critical velocity of 0.91 m/s	121
Figure 109. Nueces River verification of prediction with field critical velocity of 0.54 m/s	121
Figure 110. Brazos River meander migration	123
Figure 111. Brazos River meander migration with parameters from EFA curve	124

Figure 112. Brazos River meander migration with parameters from erosion categories chart	125
Figure 113. Trinity River meander migration	126
Figure 114. Trinity River meander migration with parameters from EFA curve	127
Figure 115. Trinity River meander migration with parameters from erosion categories chart	128
Figure 116. Sabine River meander migration	129
Figure 117. Sabine River meander migration with parameters from EFA curve.....	130
Figure 118. Sabine River meander migration with parameters from erosion categories chart	131
Figure 119. North Sulfur River vertical degradation with parameters from EFA curve.....	132
Figure 120. North Sulfur River vertical degradation with parameters from erosion categories chart	133
Figure 121. Nueces River meander migration.....	134
Figure 122. Nueces River meander migration with parameters from EFA curve.....	135
Figure 123. Nueces River meander migration with parameters from erosion categories chart	136
Figure 124. Colorado River vertical degradation with parameters from EFA curve	137
Figure 125. Colorado River vertical degradation with parameters from erosion categories chart	138
Figure 126. Brazos River prediction.....	140
Figure 127. Trinity River prediction.....	140
Figure 128. Sabine River prediction	141
Figure 129. North Sulfur River prediction	141
Figure 130. Nueces River prediction	142
Figure 131. Colorado River prediction	142

LIST OF TABLES

	Page
Table 1. Sample labeling legend.....	68
Table 2. Sample locations	69
Table 3. Field test results	70
Table 4. Soil classification at each site	72
Table 5. Colored cells in Excel for input, output and more	101
Table 6. Example of format for time in years to use in both MATLAB and Excel	104
Table 7. Observed data in a table.....	109
Table 8. Erosion function parameters and increment in time	109
Table 9. Velocity hydrograph input and output of movement	110
Table 10. Observed data.....	110
Table 11. Critical velocity and ranking index	111
Table 12. Calibrated data output.....	111
Table 13. Input data for prediction step	117
Table 14. Input of velocity hydrograph for prediction step	118
Table 15. Brazos River data with parameters from EFA curve	124
Table 16. Brazos River data with parameters from erosion categories chart.....	125
Table 17. Trinity River data with parameters from EFA curve	127
Table 18. Trinity River data with parameters from erosion categories chart.....	128
Table 19. Sabine River data with parameters from EFA curve.....	130
Table 20. Sabine River data with parameters from erosion categories chart.....	131
Table 21. North Sulfur River data with parameters from EFA curve.....	132

Table 22. North Sulfur River data with parameters from erosion categories chart.....	133
Table 23. Nueces River data with parameters from EFA curve.....	135
Table 24. Nueces River data with parameters from erosion categories chart	136
Table 25. Colorado River data with parameters from EFA curve.....	137
Table 26. Colorado River data with parameters from erosion categories chart	138

CHAPTER I

INTRODUCTION AND RESEARCH OBJECTIVES

1.1 INTRODUCTION

Meander migration and vertical degradation are two erosion related processes that occur due to the continuous flow of water in rivers. Both can be slow enough to not cause any problems, but can also be a hazard when floods occur. Bridges, roads, and farm lands that are within the flood zone may all suffer damages. To avoid these types of damages, certain measures can be taken to control problems with erosion, such as improving the location and design of bridges. This in turn prevents costs associated with mitigation and countermeasures taken during the operational life of a bridge or highway. Therefore, it is necessary to know when and if a bridge or highway may be in danger of structural damage during its operational life because of erosion problems. This way, during the design and construction process, preventative measures may be taken and proper solutions may be developed in advance. Two examples of bridges that were in danger of structural damage due to excessive erosion are presented herein.

The Burr's Ferry Bridge on the Sabine River, shown in Figure 1, was built over 80 years ago and is on the state line between Texas and Louisiana. This bridge is above a meander and floods that occurred during the 1990s eroded the bank on both the east and west side of the river. Concrete blocks were used as countermeasures to reduce the erosion along the bank of Louisiana. However, along the bank of Texas, the erosion on the bank of Texas has been a major concern to the Texas Department of Transportation. How close will this meander be to the bridge in 5 or 10 years? If a big flood occurs, how many meters will the river "move" south and get closer to the bridge?



Figure 1. SH 63 at Sabine River (Google Earth, 2013)

Another case is the North Sulfur River at SH 34 in Ladonia, TX, shown in Figure 2. This river used to have meanders but was straightened in the 1920s to avoid floods in the farm lands. The problem at this bridge location was of vertical degradation. A new bridge was built in the early 2000s when it was found that the columns of the old bridge were being exposed due to short length, which could have caused a collapse during a flood because of the erosion at the bottom of the river. Although a collapse was avoided, it was obvious that a method needed to be developed to predict the progression of erosion with time. With such a method, similar problems may be avoided in other rivers.



Figure 2. SH 34 at North Sulfur River (Google Earth, 2013)

The situations of erosion problems discussed above are very common at different locations in Texas. Some bridges were either not designed to account for these problems or erosion could not be controlled with countermeasure or remedies. The most important aspect of this research project is to develop a simple method that can be used to make a representation of the behavior of the river by using an erosion model. This way, predictions of the movement of a point of interest of the river (in reference to time and distance) can be made based on that model.

There are many factors that have an effect on meander migration and vertical degradation. They can be summarized in three general aspects: soil, geometry, and flow. Many methods have been developed to make predictions, but sometimes one of the three aspects has been ignored. For the method developed in this project, each one of these factors has been taken into consideration to develop a simple solution to these problems.

This research project was sponsored by the Texas Department of Transportation (TxDOT) and was conducted by the Texas Transportation Institute at Texas A&M University (College Station, TX). This research is part of the program “Assessment of the Effects of Regional Channel Stability and Sediment Transport on Roadway Hydraulics Structures”. This program is a collaboration between Texas A&M University, University of Texas at San Antonio, and University of Houston. Each university has a team with different tasks and approaches to provide guidelines for the TxDOT, which will be used for the existing bridges and for rivers with similar problems.

1.2 RESEARCH OBJECTIVES

The objectives of this research project are the following:

- Study sites selected by the TxDOT that have problems related to (1) meander migration and/or (2) vertical degradation. Each river is located in the state of Texas and is affected by erosion.
- Perform site and laboratory tests (full scale experimental study).
- Develop a model that relates the soil erodibility, river flow, and past observations with the meander migration and vertical degradation.
- Develop a method (called Observation Method) using computer programming that uses the model to study the movement of a point of interest or critical point in the river.
- Use the Observation Method to be able to make a prediction of the movement of a selected point of interest or critical point for each river.
- Provide the TxDOT with general guidelines to use the Observation Method for the study of other rivers.

1.3 GENERAL APPROACHES

The Observation Method is based on observed data or the history of the river. The following approaches were implemented for this research and used to develop the

Observation Method to predict meander migration and vertical degradation. The Observation Method incorporates the three most important components: soil, flow and, geometry.

1.3.1 Selected Rivers

Six different rivers in Texas were selected to be studied for this project. Four had meander migration problems and two had vertical degradation problems. The rivers are:

- SH 105 at Brazos River (Navasota, TX) – Meander migration
- FM 787 at Trinity River (Cleveland, TX) – Meander migration
- SH 63 at Sabine River (Texas-Louisiana Border) – Meander migration
- SH 34 at North Sulfur River (Ladonia, TX) – Vertical degradation
- US 90 at Nueces River (Uvalde, TX) – Meander migration
- FM 973 at Colorado River (Austin, TX) – Vertical degradation

1.3.2 Research Approach

After the selection of the rivers, the research was divided in two important steps: the experimental study and the analytical study.

- Full scale experimental study – Involved the site investigation and tests conducted at site, laboratory testing, and the study of the movement of the river by observation of maps, aerial photos, or cross-sections of rivers.
- Analytical study – Involved the application of the data collected on the experimental study and used in conjunction with a mathematical model to develop a program that is used to establish the behavior of the river and make predictions. The final product of this part of the project is the “Observation Method”.

1.3.3 Observation Method

The final product of the analytical study of the project is the Observation Method. This method uses:

- observations from aerial photos or maps for meander migration
- cross-sections for vertical degradation
- flow hydrograph converted to velocity from the river under study
- erosion function, which relates erosion rate to velocity, obtained from the erosion tests using the Erosion Function Apparatus (EFA)

The model used to determine the erosion of a river is determined by the following equation:

$$\frac{\dot{z}}{v_c} = \alpha' \left(\frac{v}{v_c} \right)^\beta$$

Where:

\dot{z} : erosion rate

v : velocity

v_c : critical velocity

α' and β : parameters that define the erosion function

This model is dimensionless and is used to determine the erosion per day when an average daily velocity from a river is obtained. The critical velocity, minimum velocity for erosion, is site specific and is found by an iterating process. A simple computer program is used to obtain the critical velocity and to view the movement or position of a point of interest of a river through time. The Observation Method is used for each river selected and the results are incorporated in this report.

CHAPTER II

LITERATURE REVIEW

2.1 INTRODUCTION

River meanders are prone to change due to the action of water. Elevation and horizontal location of the river change because of the centrifugal force that increases the shear stress between the water and soil. There are different methods that have been used to predict the movement or migration of meanders. Meander migration prediction is complicated; there are too many factors that influence this process. There are three general approaches to predict meander migration:

1. Time-sequence maps and extrapolation
2. Empirical equations
3. Fundamental modeling.

2.2 GENERAL APPROACHES

There are three principal factors that have a direct effect on meander migration: the geometry, the flow, and the soil. The geometry of the meander and of the cross-section of the channel has an impact on the shear stress generated between the soil and water. Some of the geometry parameters are: center of meander circle, meander amplitude, channel width, and radius of curvature. The flow velocity of the water also has an effect on the shear stress generated. The soil resists this shear stress and controls the erosion rate.

2.2.1 Time Sequence Maps and Extrapolation

This method was mentioned by Brice (1982) and redefined by Lagasse (2004a and 2004b). This method is one of the most commonly used methods to predict meander migration. This method uses two or more maps of the studied river to determine the rate of the migration and the center and radius of a circle that represents the meander. A map

is obtained for t_1 , which is the first date, and a circle is drawn to match the meander. The radius and center are recorded for this first map, t_1 . Then, a more recent map for t_2 is used and the circle for the meander is drawn, recording radius and center. To predict the position of a meander at t_3 , the distance between center of the second circle and the center of the third circle can be predicted by using the time between t_2 and t_3 and the migration rate between the first two circles. This method assumes that the migration rate is constant. If a map for t_3 is used, a comparison can be made between the actual circle and the predicted circle. This helps to evaluate the accuracy and precision of this method (verification).

This method uses either maps or aerial photos. For rivers, aerial photos with high resolution are preferred. After drawing the lines that define the shape of the river, best-fit circles are drawn at the outer bank of each bend. The radius of curvature (R), average arc and centroid position of each circle have to be defined. The number of circles can be used to classify the river using the following classification system, developed by Brice (1975). Brice developed a classification system based on 125 streams with four main categories: simple, compound, symmetrical and asymmetrical. Figure 3 shows a table with the Modified Brice classifications (Brice, 1975). The classification system has 9 categories for the meander bends. However, sometimes using only one classification may not be enough. The shape of the loops of a river can change from t_1 to t_2 . The number of loops can increase or decrease.










MODIFIED BRICE CLASSIFICATION		SCREEN
	A SINGLE PHASE, EQUIWIDTH CHANNEL INCISED OR DEEP	*
	B ₁ SINGLE PHASE, EQUIWIDTH CHANNEL	*
	B ₂ SINGLE PHASE, WIDER AT BENDS, NO BARS	
	C SINGLE PHASE, WIDER AT BENDS WITH POINT BARS	
	D SINGLE PHASE, WIDER AT BENDS WITH POINT BARS, CHUTES COMMON	
	E SINGLE PHASE, IRREGULAR WIDTH VARIATION	
	F TWO PHASE UNDERFIT, LOW-WATER SINUOSITY (WANDERING)	*
	G ₁ TWO PHASE, BIMODAL BANKFULL SINUOSITY, EQUIWIDTH	*
	G ₂ TWO PHASE, BIMODAL BANKFULL SINUOSITY, WIDER AT BENDS WITH POINT BARS	
NOTE: WHERE SCREEN = *, CLASS FALLS OUT DUE TO IMPLICATIONS OF CONSIDERABLE STABILITY OR EXCESSIVE INSTABILITY		

Figure 3. Modified Brice classification system for meandering channels (Brice, 1975)

The circles are used to compare the bend movement and dimensions of each year. Figure 4 shows a comparison of the best-fit circles. An arrow indicates the magnitude and direction of the movement of the bend centroid. The magnitude and direction of the circle and the change of radius of curvature can be observed with two or more maps and/or photos.

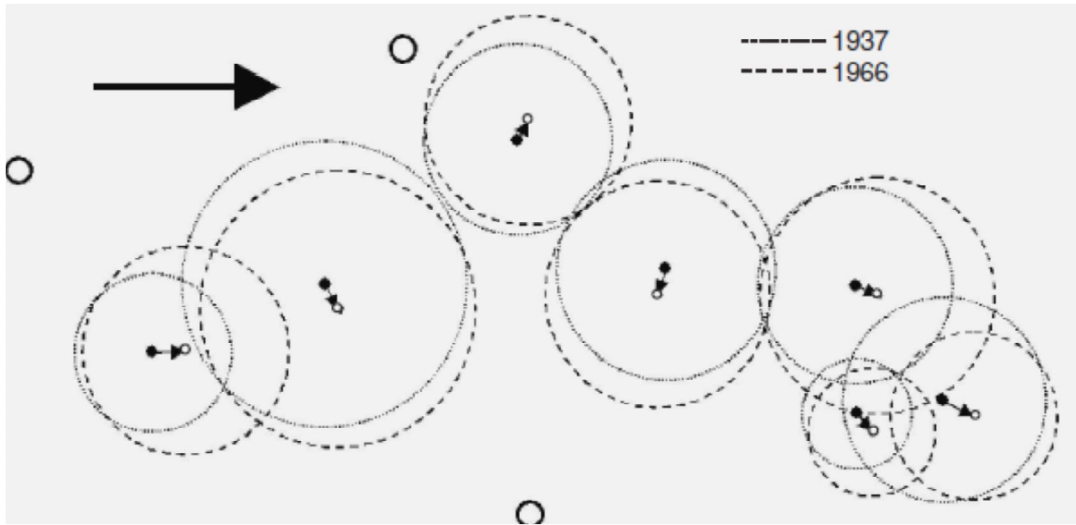


Figure 4. Best-fit circles used to observe the change of the bends between 1937 and 1966 (Lagasse et al. 2004)

A simple extrapolation can be used to predict the position of the bends with the information obtained from these circles. This is assuming that the direction and the rate of the movement are constant during a period. The annual rate of movement can be obtained dividing the distance that the bend has moved by the difference of years between the two photos. With this rate and calculating the radius of the circle, a circle that represents the prediction of the movement of the bend can be drawn (Figure 5). The banklines of the river can be drawn after the extrapolation of the circles (Figure 6).

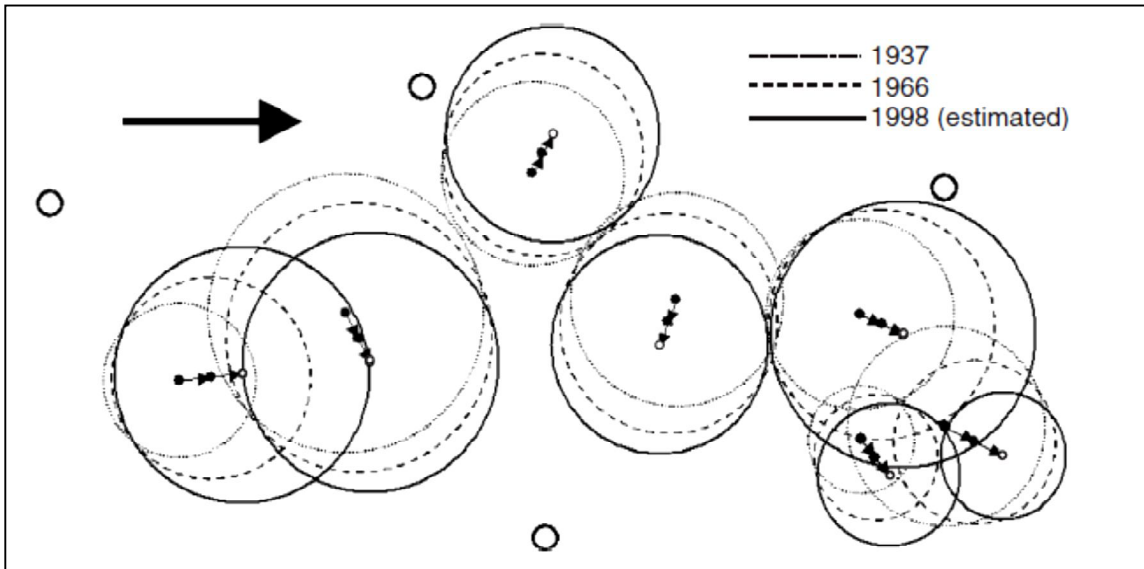


Figure 5. Best-fit circles for 1937 and 1966 and the predicted circles for 1998 (Lagasse et al., 2004)

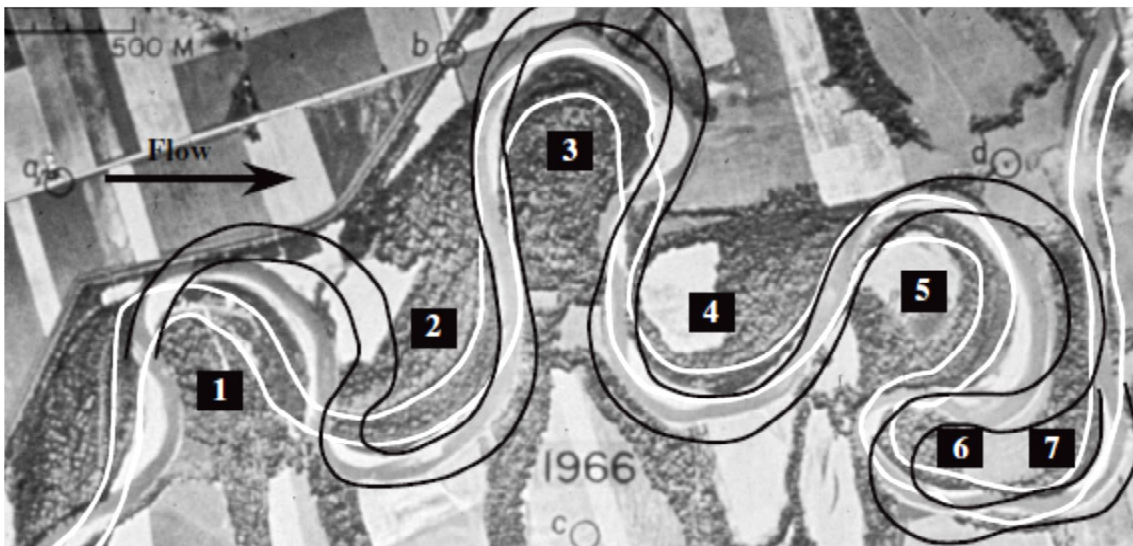


Figure 6. Aerial photograph of the White River in 1966 with the 1937 bankline in white and the predicted 1998 bankline in black (Lagasse et al., 2004)

Sometimes, it is desirable to obtain a prediction of the movement based on more than a single period of analysis. For example, if two periods are obtained (three photos or three maps), two different annual rates are obtained. The following two equations

define the change of radius of curvature per year for a Period A (Year 1 to Year 2) and for a Period B (Year 2 to Year 3).

$$\Delta R_{CA} = (R_{C2} - R_{C1}) / Y_A$$

$$\Delta R_{CB} = (R_{C3} - R_{C2}) / Y_B$$

Where:

ΔR_{CX} : annual rate of change of the radius of curvature for Period X

R_{CX} : radius of curvature in Year X

Y_X : number of years in Period X

The annual rate units are ft/yr or m/yr. These rates indicate how much the circles increase or decrease in size for the period of time. The annual rates of migration are used to predict the distance that the center of the circle has moved in a period. The units of the migration rate are the same units as the rate of change of radius of curvature. The annual rate of migration is obtained by dividing the distance between the centroids of two circles by the total of years. Figure 7 shows three circles that represent two known periods.

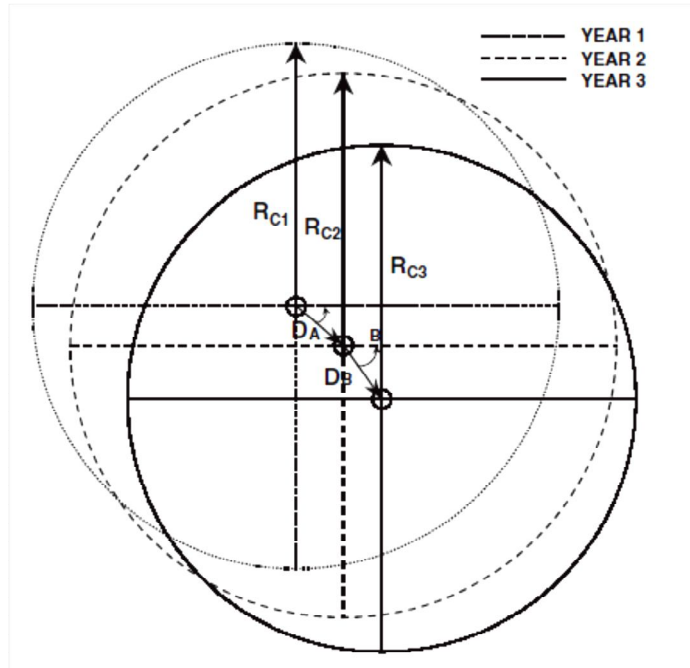


Figure 7. Three circles (Years 1, 2, 3) with their respective radius of curvature (R) and the magnitude of migration (D) (Lagasse et al., 2004)

For a Period C (between Year 3 and 4), a long term average can be used, but in most cases, it is more desirable to use the most recent rate. The next three equations correspond to Figure 8. The magnitude (distance) of migration of the circle is obtained with the following equation:

$$D_c = \left(\frac{D_B}{Y_B} \right) \times (Y_C)$$

Where:

D_x (ft or m): magnitude of the migration (displacement) of the center of the circle

Assuming that the rate used for the prediction is the most recent rate, the radius of the predicted circle is obtained by extrapolation, as defined by:

$$R_{C4} = R_{C3} + \frac{R_{C3} - R_{C2}}{Y_B} \times (Y_C)$$

Where:

R_{C4} (ft or m): predicted radius of curvature of Year 4

R_{C2} (ft or m): radius of curvature for Year 2 (ft or m)

R_{C3} (ft or m): radius of curvature for Year 3

Y_B : number of years of the Period B

Y_C : number of years of the Period C

The angle of migration of the center of the circle, θ , defines the angle of the bend migration. This angle describes the relative direction of the movement of the circles. The angle is obtained from the arrows used to represent the movement of the circle. As the radius of curvature, the predicted angle in a period can be obtained by extrapolation

$$\theta_C = \theta_B + \frac{\theta_B - \theta_A}{Y_B} \times (Y_C)$$

Where:

θ_X : angle of the bend migration for Period X

If the geomorphic and hydrologic conditions have not changed significantly, then the direction can be assumed as the same as in the last period (for example, $\theta_C = \theta_B$) and it would not be necessary to use this equation.

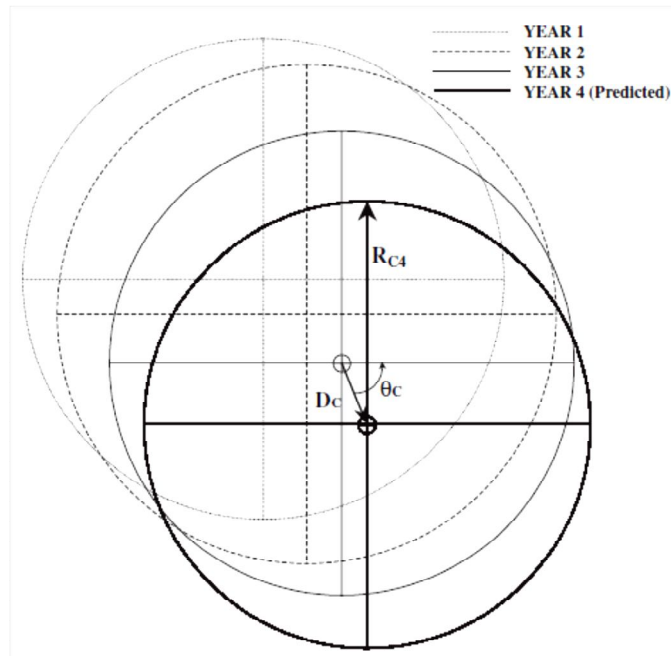


Figure 8. Predicted circle in Year 4 (Lagasse et al., 2004)

Using the meander migration rate and the position of the circles, the meander position can be predicted. Again, the average migration rate or the last migration rate between the last two circles is assumed to be constant and the method can either be conservative or overpredict the results. In Figure 9, circles are drawn to represent the meander at different points in time of the Nueces River

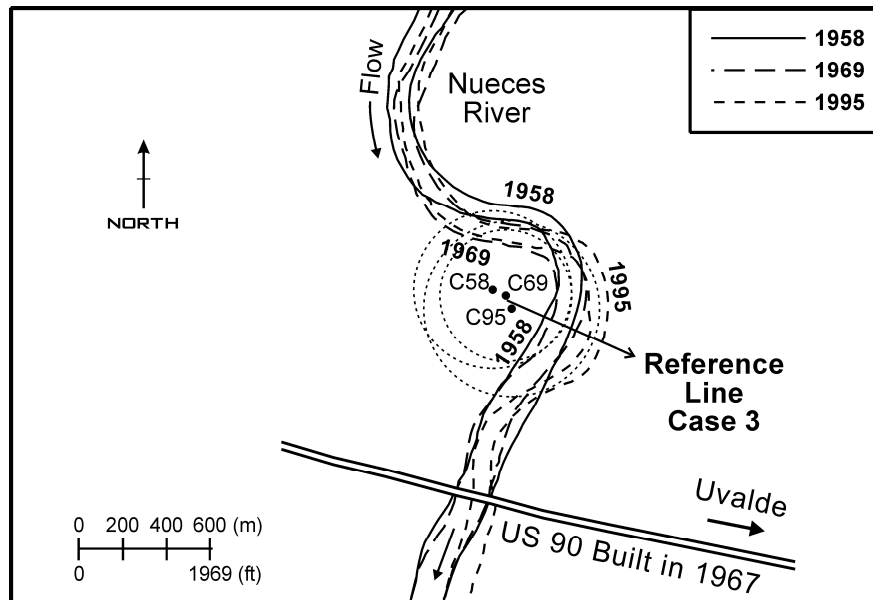


Figure 9. Meander migration for the Nueces River at US 90 (Briaud et al., 2001a)

2.2.2 Empirical Methods

The empirical methods, or empirical equations, use different variables to estimate the meander rate based on experimental data or observation. Each method has one or more variables that determine the meander migration rate. Most of these equations use geometrical parameters or characteristics as their influential factor to predict the meander rate.

2.2.2.1 Keady and Priest (1977)

The data obtained to develop the equation was from the following locations:

- Mississippi River in Tennessee, Louisiana, and Mississippi
- Red River in Arkansas
- Pearl River in Louisiana
- Tombigbee River in Mississippi
- Buffalo River in Louisiana
- Red Deer River in Alberta, Canada

The influencing parameters found by Keady and Priest (1977) are the slope of the river (s) and the amplitude of meander (A). Other variables involved in the equation are the gravity (g) and a function of the slope ($\phi(s)$). The relation is presented in the following equation:

$$\frac{V}{\sqrt{gA}} = \phi(s)$$

Where:

V (ft/yr) = migration rate= dM/dt

g (ft/s²) = acceleration of gravity,

A (ft) = meander amplitude,

S = slope

$\phi(s) = f(s)$ = function of s

2.2.2.2 Hooke, J.M. (1980)

Hooke (1980) analyzed the meander migration rate on rivers in Devon, England from field measurements. These measured rates were compared with the rates obtained from historical maps for the period from 1840 to 1975. He also compared the measured rates with published rates of bank erosion in the literature, and found that the rate in his study followed the general trend of the worldwide values as shown in Figure 10 and Figure 11 . The equation used by Hooke is:

$$M = 2.45A^{0.45}$$

Where:

M (m/year): migration or erosion rate

A (km²): catchment area

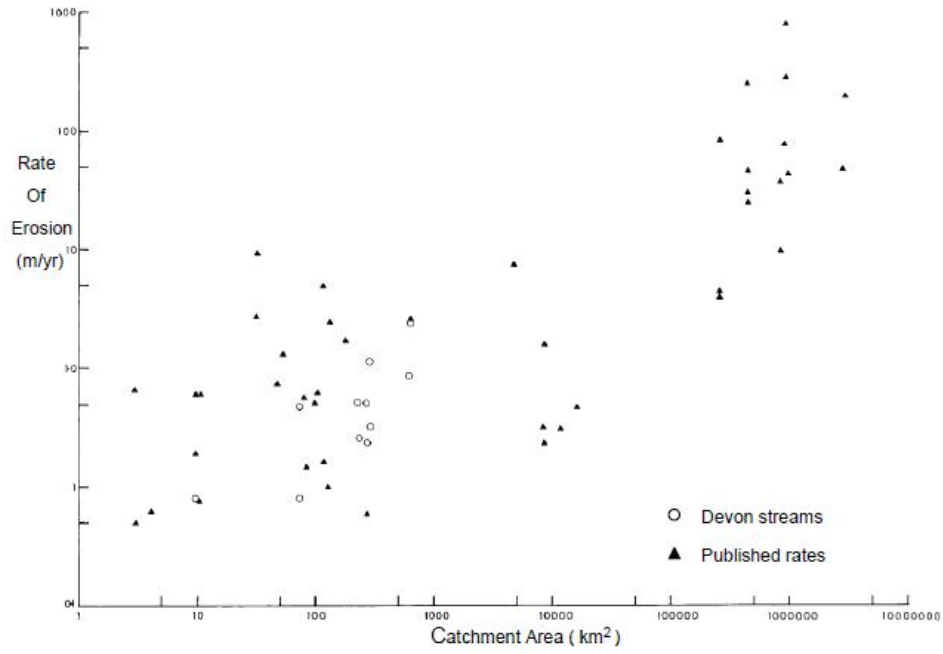


Figure 10. Relationships between catchment area and erosion rate, based on Hooke (Briaud et al., 2007)

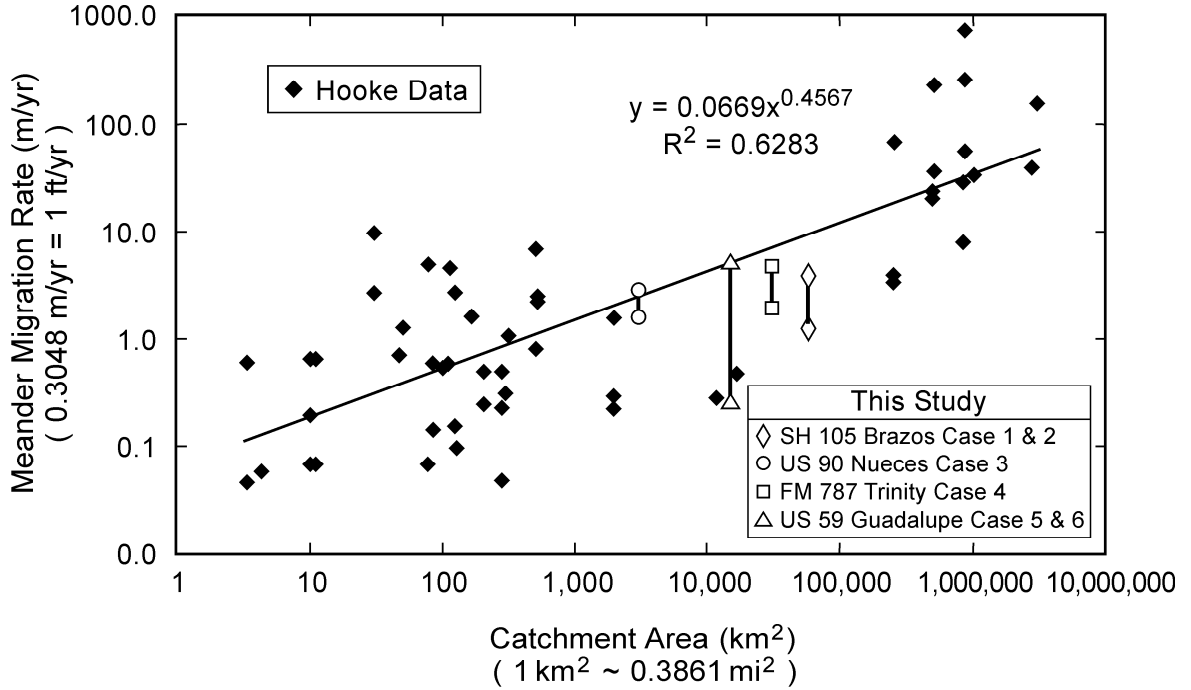


Figure 11. Data used by Hooke (1980) (Briaud et al., 2007)

2.2.2.3 Brice, J.C. (1982)

Brice's data (1982) consisted of 43 data points from four different stream types (equiwidth, wide bend, braided point bar, braided) as shown in Figure 12. Brice proposed that the erosion rate of the bank is related to the width of the channel, as stated in the following equation:

$$Y = 0.01B$$

Where:

Y (m/year): erosion rate

B (m): channel width

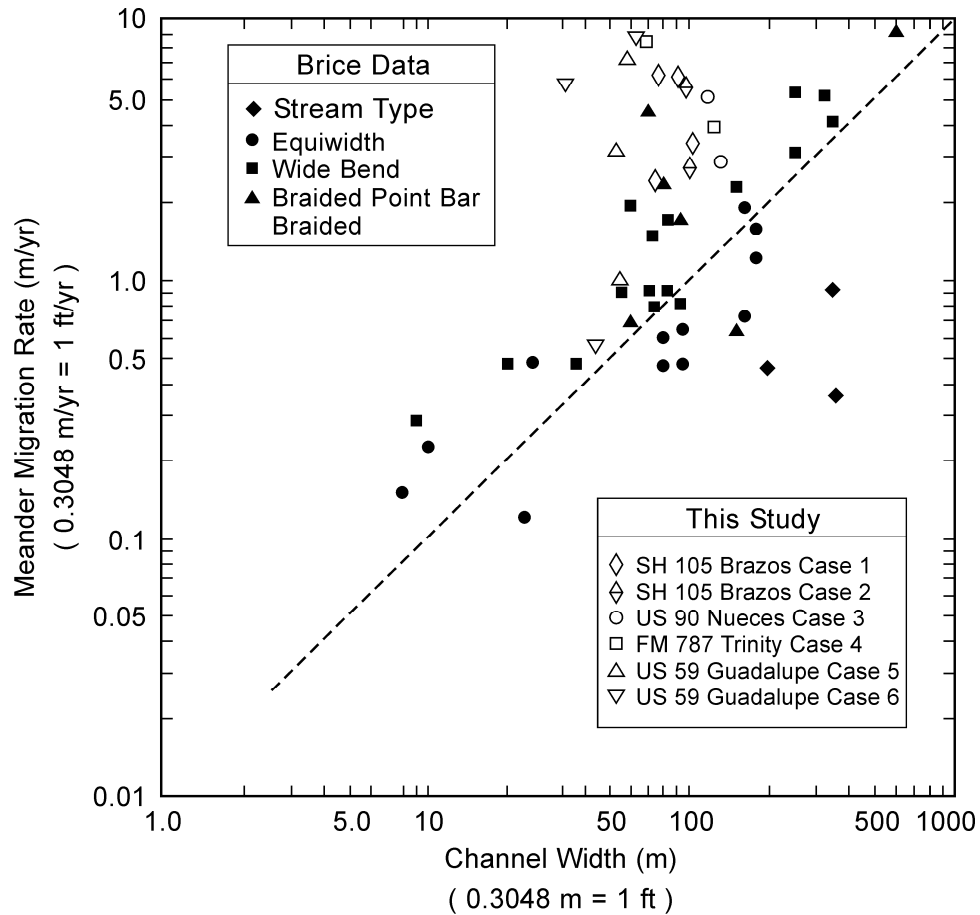


Figure 12. Data used by Brice (1982) (Briaud et al., 2007)

2.2.2.4 Nanson and Hickin (1983)

Nanson and Hickin (1983) determined that the migration rate of a meandering river is influenced by the ratio of radius of curvature to the channel width (R_c/W). This normalized ratio is applied to two equations: one of them when the R_c/W is less than 3 and the other one when the ratio is larger than 3. The ratio of migration rate to channel width (MR/W) is the highest when R_c/W is 3. Figure 13 shows this curve with data obtained from some cases and also includes the data obtained by Nanson and Hickin.

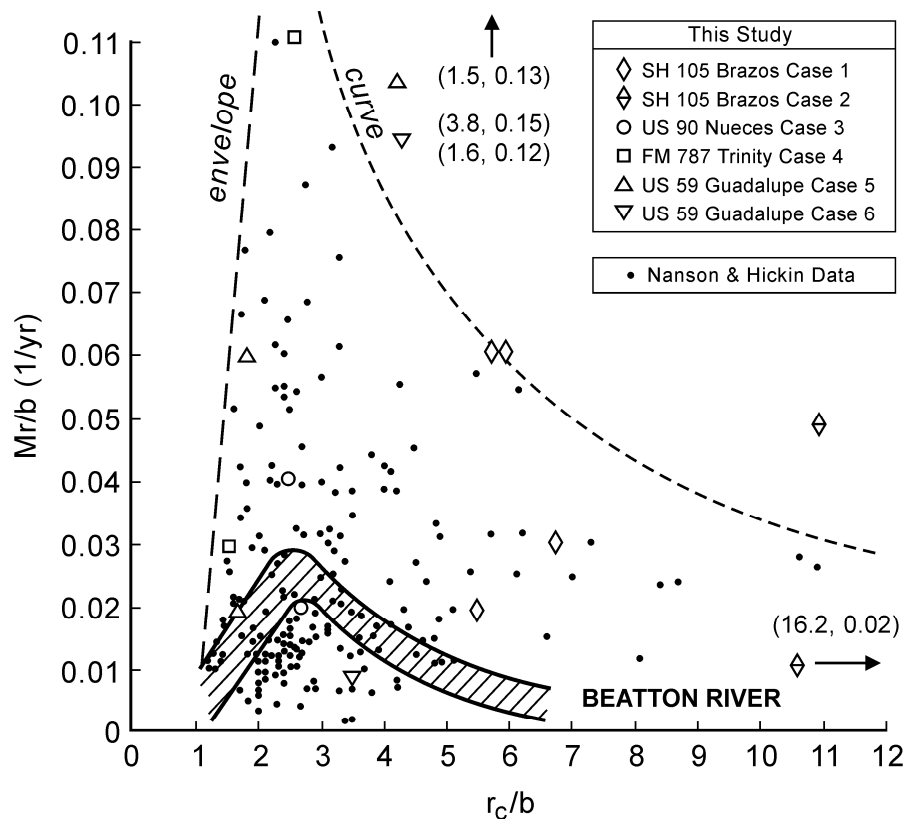


Figure 13. Data used by Nanson and Hickin (1983) (Briaud et al., 2007).

2.3 FACTORS AFFECTING RIVER EROSION

As mentioned before, the meander migration and vertical degradation problems have many influential factors. The three main components are soil, flow and geometry. The erosion rate of one soil type is different from others; the water flow conditions change every day and from river to river; and the geometry of the river affects how the

shear stress of the water acts on the river bend or bank. The geometry and the flow of water are strongly related and this is why most of the methods used to make these predictions do not take into account the erodibility of the soil. It also considers that the migration rate will always be the same for a chosen period of time. However, the list of factors related to the erosion can be more complicated than the three mentioned. As mentioned by Briaud et al. (2001a and 2001b), some of the influencing factors are:

- stream pattern (straight, meandering, braided);
- free surface slope;
- channel roughness;
- sediment load;
- vegetation;
- debris problem;
- channel relocation;
- human activities on the floodplain of rivers.

CHAPTER III

RESEARCH APPROACH

3.1 INTRODUCTION

The approach to solve the issues involving meander migration and vertical degradation of rivers can be separated in two main areas: full scale experimental study and analytical study. The first one involves the site visit and both field and laboratory testing, and the second one involves the methodology and the step by step procedure to solve the problem by using a mathematical solution.

3.2 FULL SCALE EXPERIMENTAL STUDY

The steps involving the experimental study were:

- Selection of the different sites.
- A thorough study of the site before visiting (history, maps, photos, prior issues, etc.). The meander migration or vertical degradation problems were studied.
- Site visit and investigation of the problems and the surroundings
- Perform in-situ testing such as pocket penetrometer or vane tests.
- Obtain soil samples for erosion and classification tests.

The experimental study gives a better idea of the expectations and the results of the research. The information that is obtained from this step is used in the analytical study, and a relationship must be established between the observed data and the predicted data.

3.3 ANALYTICAL STUDY

The steps involving the analytical study are:

- Obtain the maps or aerial photos of the sites.
- Obtain the flow hydrograph of each river and convert the flow to velocity using the characteristics of the river.

- Use the erosion results to obtain the parameters that define the erodibility of the soil.
- Use the observed river movement, velocity and erosion function to develop a model and a program. These will be used to obtain the general behavior of the river and be able to obtain the predicted movement of the river.

The main objective of the analytical study is to obtain a model that can be used to study the behavior of the river with time and make a prediction based on that behavior. Using data from the past (observed data) and a model, the movement of the river could be studied through time in both meander and vertical degradation problems. The most important parameter to find in the analytical study is the critical velocity. This velocity is the minimum velocity that is needed for erosion to occur. The critical velocity can be found in the experimental study when erosion tests are performed using the EFA. This velocity may not necessarily be the same as the critical velocity found in the field. The critical velocity is found for each case selected by using a program that iterates and finds the best results based on a comparison between the calculated data and the observed data. Results are obtained and conclusions are made based on the comparisons between the calculated data and the expected behavior.

CHAPTER IV

FULL SCALE EXPERIMENTAL STUDY

4.1 SITE LOCATIONS

The sites of concern for this project are located at six different rivers in Texas, shown in Figure 14. Each one has had erosion problems and different remedies have been implemented for control purposes in some of them. Meander migration and degradation at the bottom of the rivers are some of the issues of these rivers. In general, for those with meander migration problems, aerial photos of these rivers can be used to compare the river movement due to the erosion and deposition of the soil and sediments. In the following sections, an aerial photo is presented for each site, and the red arrow in each of these figures represents the direction of flow.

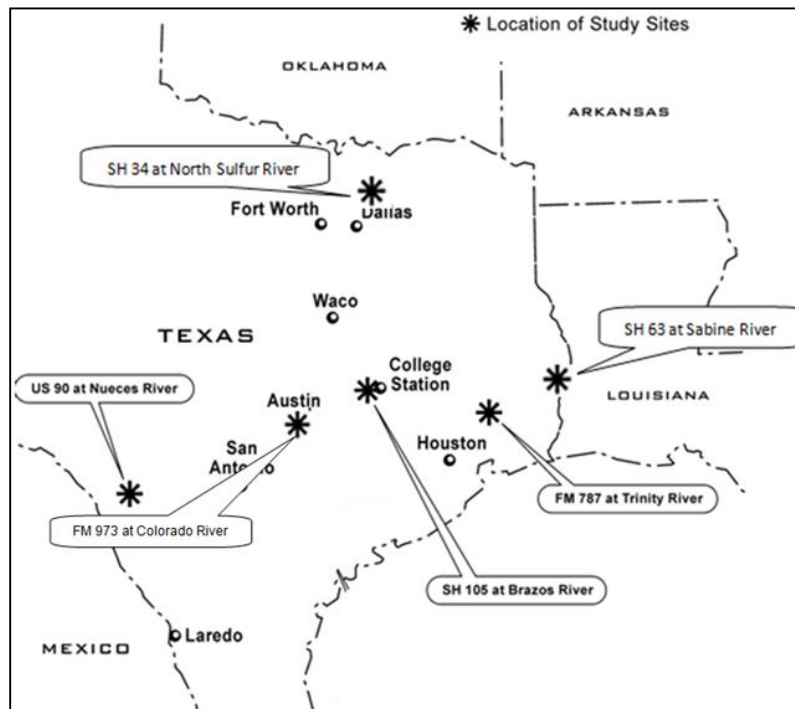


Figure 14. Site locations in Texas

4.1.1 SH 105 at Brazos River (Navasota, TX)

The bridge that crosses the Brazos River is located about 5 miles to the west of Navasota and 3 miles from the Navasota Airport. Figure 15 shows an aerial photo of the site. This bridge at SH 105 has a length of approximately 500 meters. The river meander to the north of this bridge (upstream) has moved to the southeast, getting close to the SH 105 and to farm-to-market road 159. The river is eroding part of a land property. Vegetation at the west side of the river has controlled the rate of erosion. Here it has been slower than the erosion to the east side of the bridge.



Figure 15. SH 105 at Brazos River (Google Earth, 2013)

4.1.2 FM 787 at Trinity River (Cleveland, TX)

The second site is located 30 miles to the northeast of Cleveland, TX, shown in Figure 16. The bridge is located at FM 787 and crosses the Trinity River from east to west. FM 787 connects Cleveland to SH 146. The bridge at this location is approximately 200 meters long. Erosion at this site became a concern as early as 1957, when retards were installed at the western bend, upstream of the bridge. Later the problem was at the east side, right under the bridge. The bridge was extended between 1998 and 2002. Also, the river has moved toward the highway and several sheet piles have been installed. Erosion here occurs approximately 400 meters away from the bridge.



Figure 16. FM 787 at Trinity River (Google Earth, 2013)

4.1.3 SH 63 at Sabine River (Texas-Louisiana Border)

This bridge, known as the Burr's Ferry Bridge, crosses the Sabine River and is at the state line between Louisiana and Texas (Figure 17). After crossing this bridge from Texas, the SH 63 becomes LA 8 (or Nolan Trace Parkway) in Louisiana. This bridge is over 80 years old and it is made of steel, with concrete piers. Erosion has become a serious problem both at the west side and east side of the bridge. The major concern right now is at the west side (Texas), where erosion has progressed in the last 20 years and the river is getting dangerously close to the bridge.



Figure 17. SH 63 at Sabine River (Google Earth, 2013)

4.1.4 SH 34 at North Sulfur River (Ladonia, TX)

The bridge at SH 34 that crosses the North Sulfur River is located at Ladonia, TX, as shown in Figure 18. This town is located 15 miles to the north of Commerce and 75 miles to the northeast of Dallas. The river at this site does not have meander close to this bridge. The problem at this location is that the river was straightened in the 1920s to avoid floods in farm lands and this caused an increase in velocities. Vertical degradation and widening of the river has occurred since. The bridge at this site is approximately 150 meters long.



Figure 18. SH 34 at North Sulfur River (Google Earth, 2013)

4.1.5 US 90 at Nueces River (Uvalde, TX)

The bridges that cross the Nueces River at US 90 are located in Uvalde, TX (Figure 19). Uvalde is located 85 miles to the west of San Antonio. Two bridges are at this location, one for each direction. Each bridge is 7 miles to the west of this town. The older one, from west to east, was built in the 1930s and is made of steel trusses. This bridge has only one lane. The other one is made of concrete and has two lanes. In 1998, a big flood occurred and the riprap at the west side of the bridges failed. Vertical degradation and a shift to the west were noticeable since 1996, before this event. Also the meander at the north has moved to the east, in a similar fashion as the Brazos River.



Figure 19. US 90 at Nueces River (Google Earth, 2013)

4.1.6 FM 973 at Colorado River (Austin, TX)

The Colorado River flows through the city of Austin and is one of the longest rivers in Texas. The Texas Department of Transportation has detected problems of vertical degradation at one of the bridges that crosses this river. This bridge is located 5 minutes away from the Austin-Bergstrom International Airport and it is about 450 feet long. Inspections of this bridge have shown that the drilled shafts of the piers have been exposed due to the erosion of the river bed. The location of this river can be seen in Figure 20. Reparations of this bridge or the construction of a new one have been considered.



Figure 20. FM 973 Bridge at Colorado River (Google Earth, 2013)

4.2 MOVEMENT OF RIVERS

4.2.1 SH 105 at Brazos River (Navasota, TX)

Figure 21 shows the evolution of the meander migration of the Brazos River towards SH 105. This is between 1989 and 2010. Also, there has been channel movement at the bridge. Figure 22 shows a sketch of the movement at the bridge. A flow hydrograph and velocity hydrograph of this river are shown in Figure 23 and Figure 24, respectively.

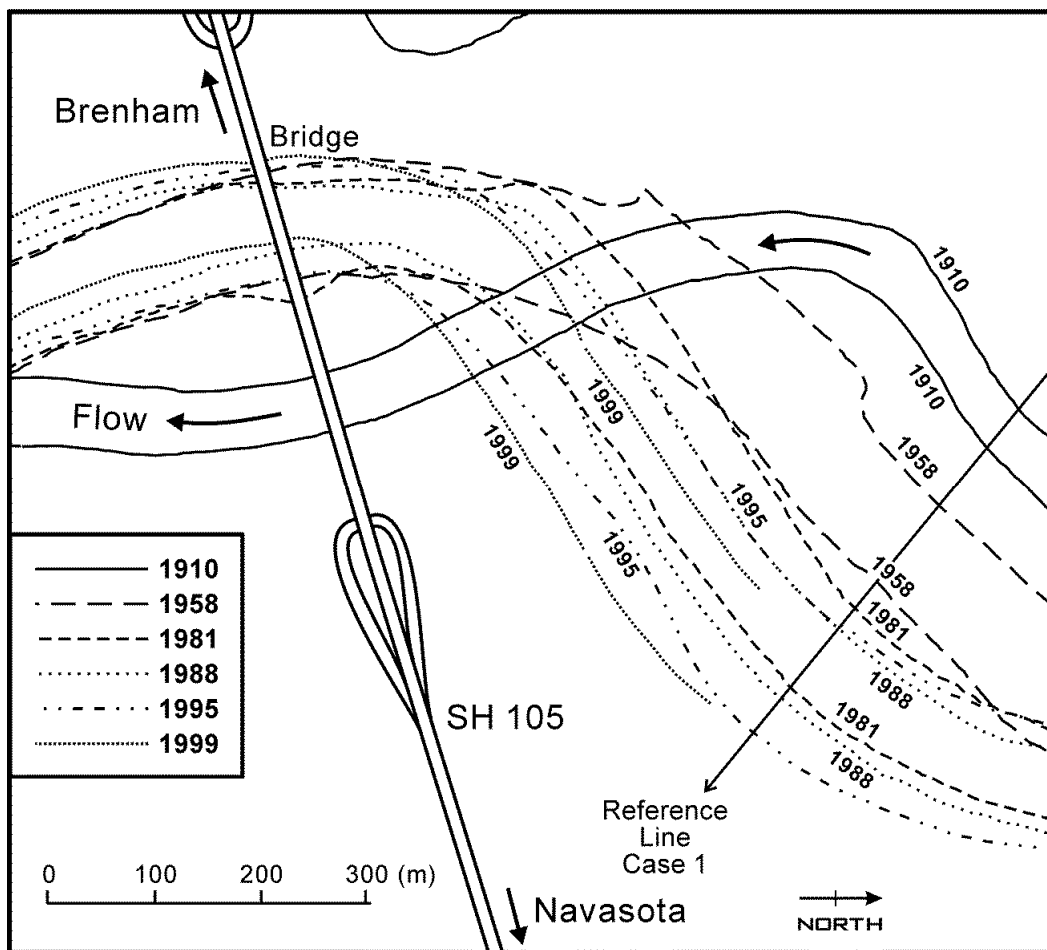


Figure 21. Meander movement of Brazos River between 1910 and 1999 (Briaud et al., 2001)

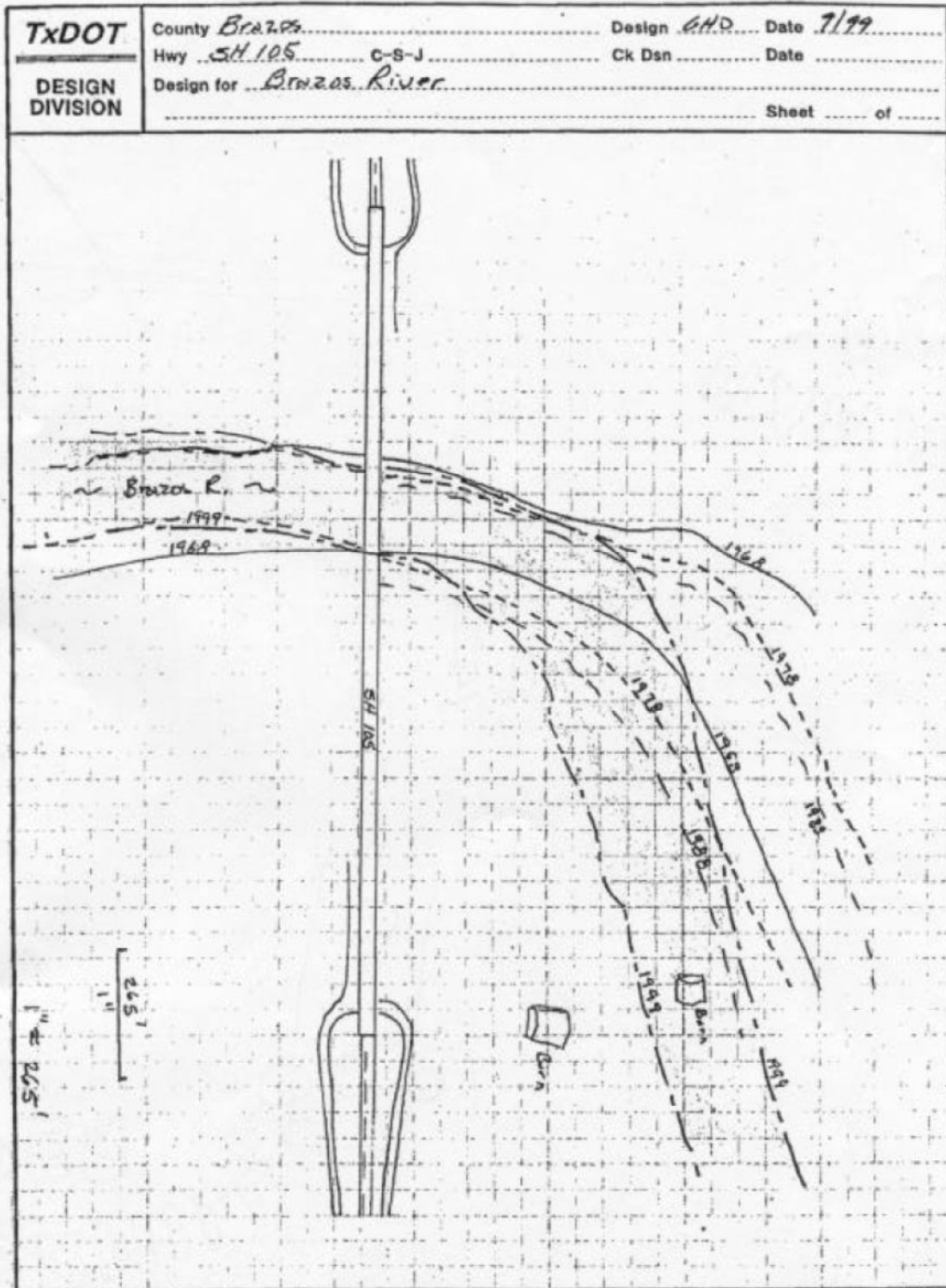


Figure 22. Sketch of channel movement

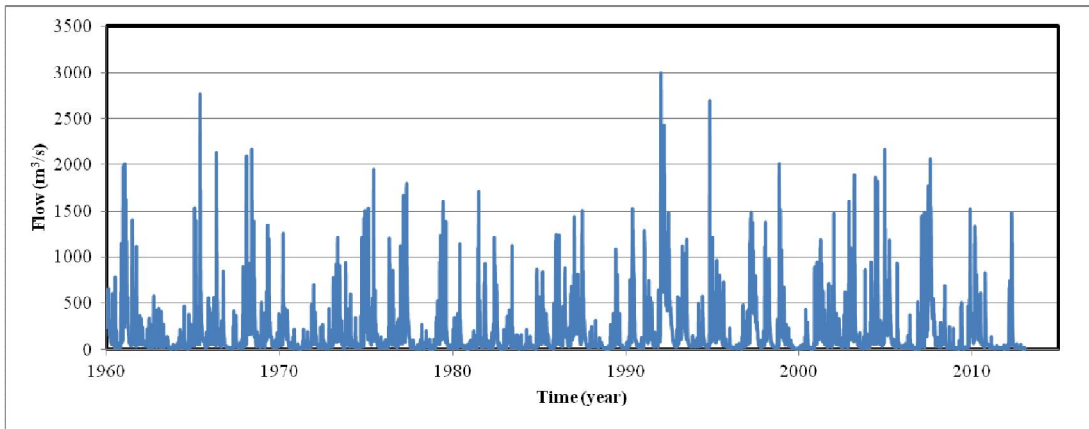


Figure 23. Flow hydrograph of Brazos River

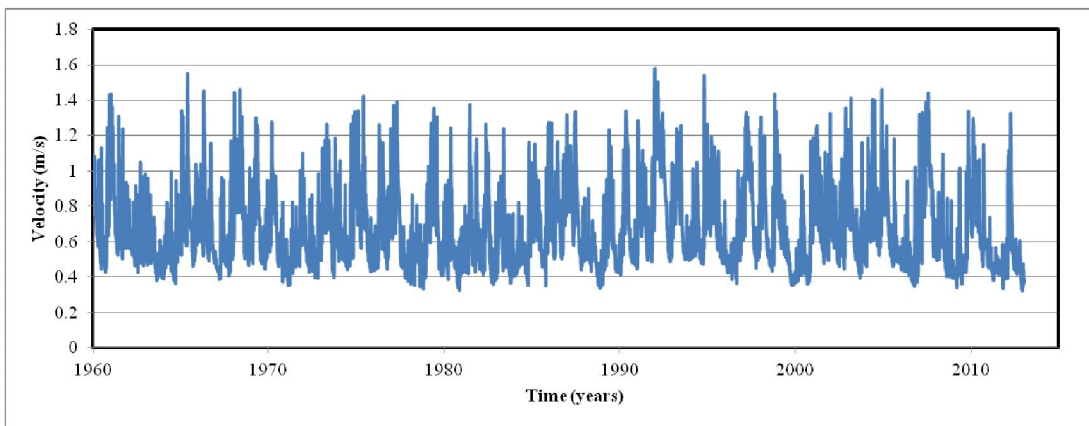


Figure 24. Velocity hydrograph of Brazos River

4.2.2 FM 787 at Trinity River (Cleveland, TX)

Erosion here occurs parallel to the FM 787 and next to the bridge. Figure 25 shows the movement of the river. This drawing was generated by surveying in this area. The surveying in this area was done between 1991 and 1995, before the extension of the bridge at the site. Aerial photos of this river do not show the erosion at the site as well as this figure. Figure 26 and Figure 27 show flow and velocity hydrographs, respectively, of this river between 1960 and 2013.

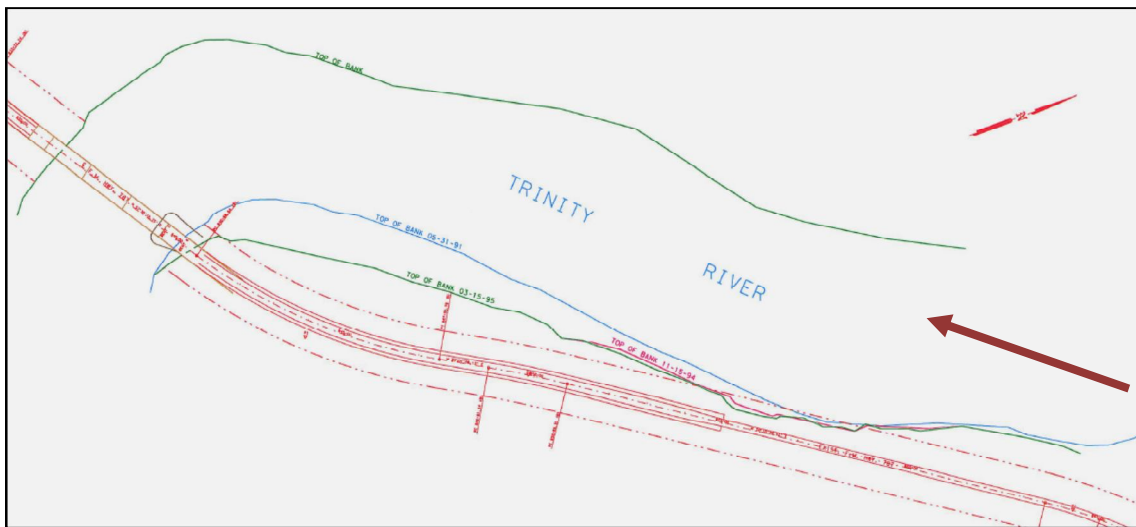


Figure 25. Surveying map of Trinity River

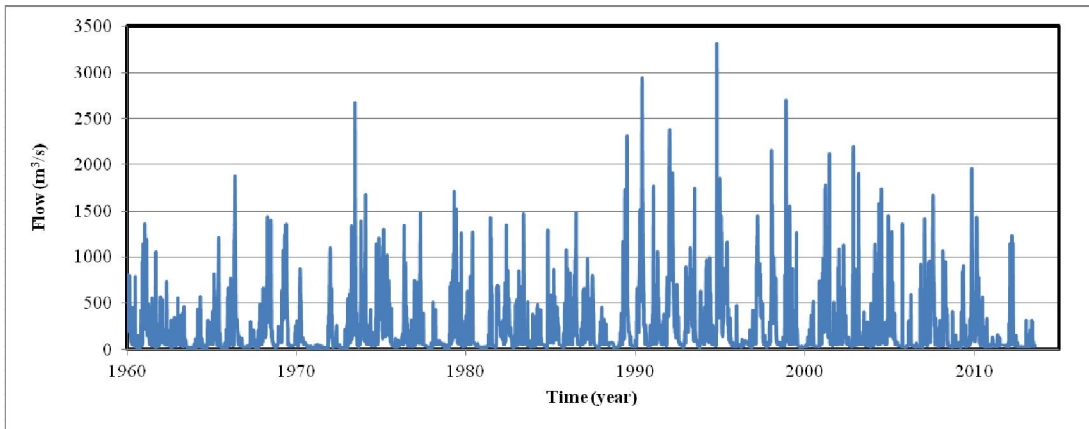


Figure 26. Flow hydrograph of Trinity River

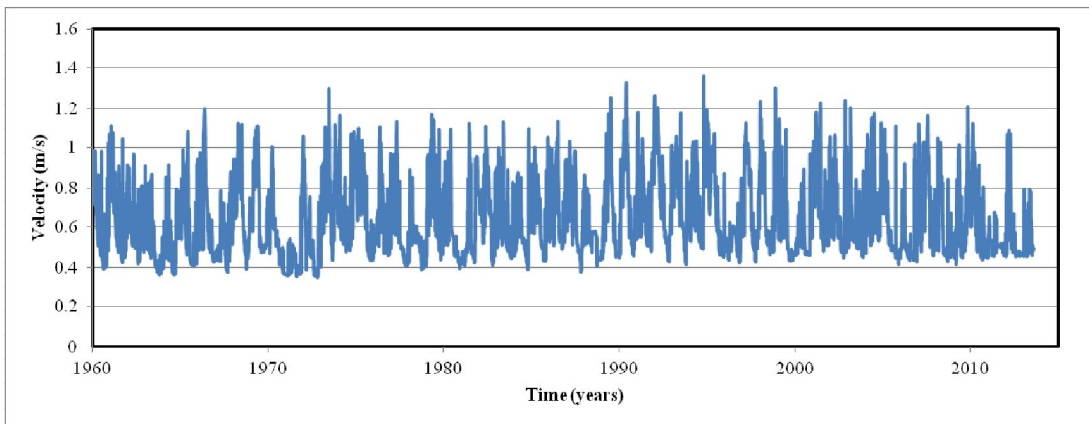


Figure 27. Velocity hydrograph of Trinity River

4.2.3 SH 63 at Sabine River (Texas-Louisiana Border)

Erosion next to the bridge on the west side has been progressively getting closer to the foundations of the bridge. Figure 28 shows the progression of the erosion between 1989 and 2004. Flow and velocity hydrographs are shown in Figure 29 and Figure 30, respectively.

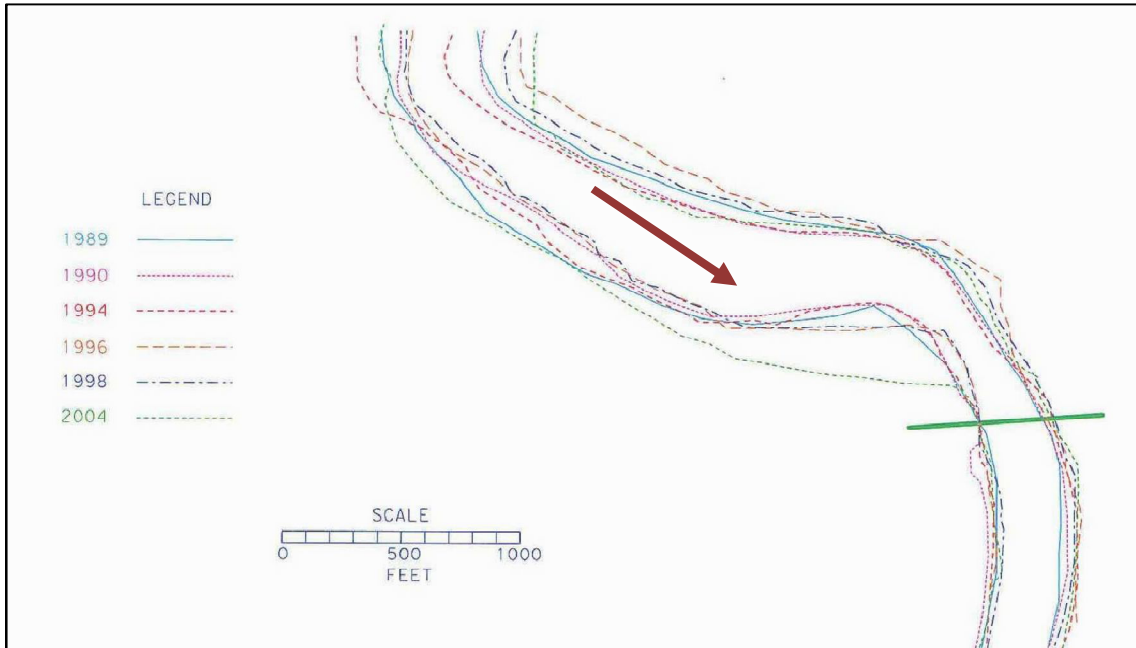


Figure 28. Meander movement of Sabine River between 1989 and 2004

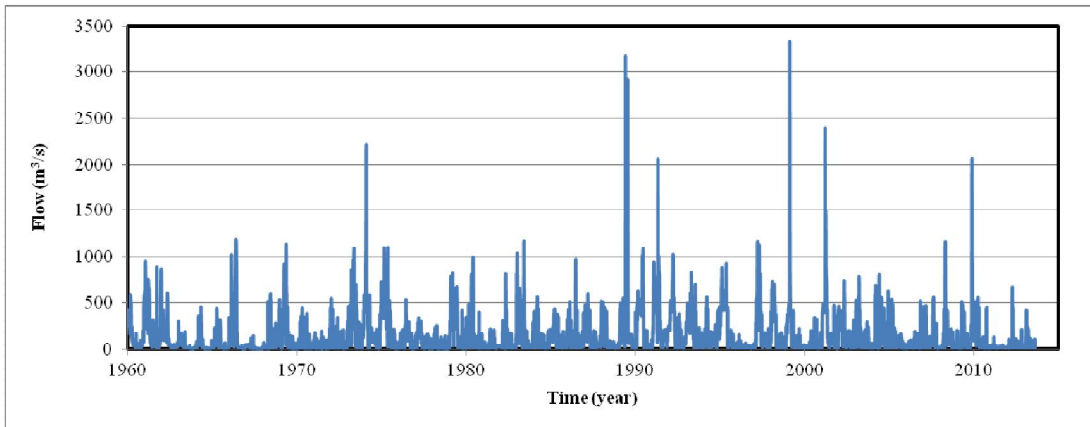


Figure 29. Flow hydrograph of Sabine River

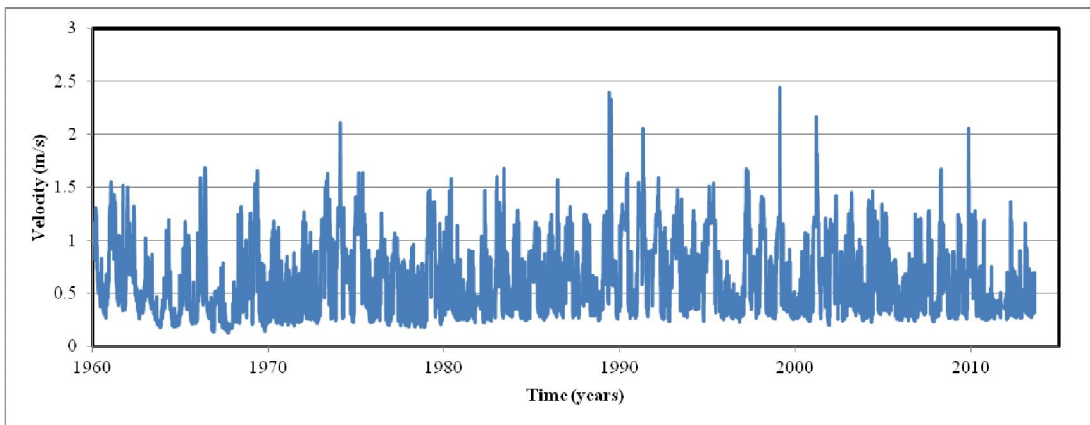


Figure 30. Velocity hydrograph of Sabine River

4.2.4 SH 34 at North Sulfur River (Ladonia, TX)

Figure 31 shows the vertical degradation of the North Sulfur River at the bridge in SH 34. This site has no meander and the erosion is because of straightening of the river in the 1920. Clay at the bottom of the river eroded and blue shale was exposed. The sediments of the river then were deposited on top of the blue shale. Figure 32 and Figure 33 show flow and velocity hydrographs, respectively, for this river.

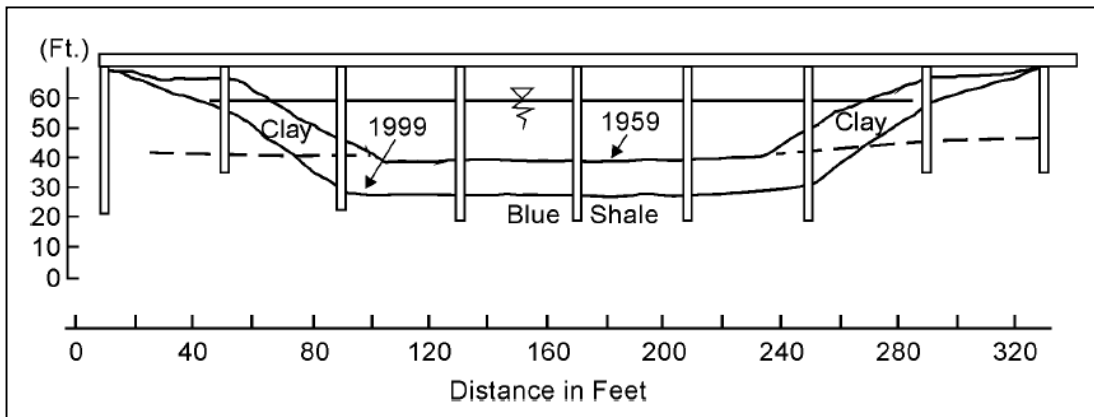


Figure 31. Vertical degradation of North Sulfur River at SH 34

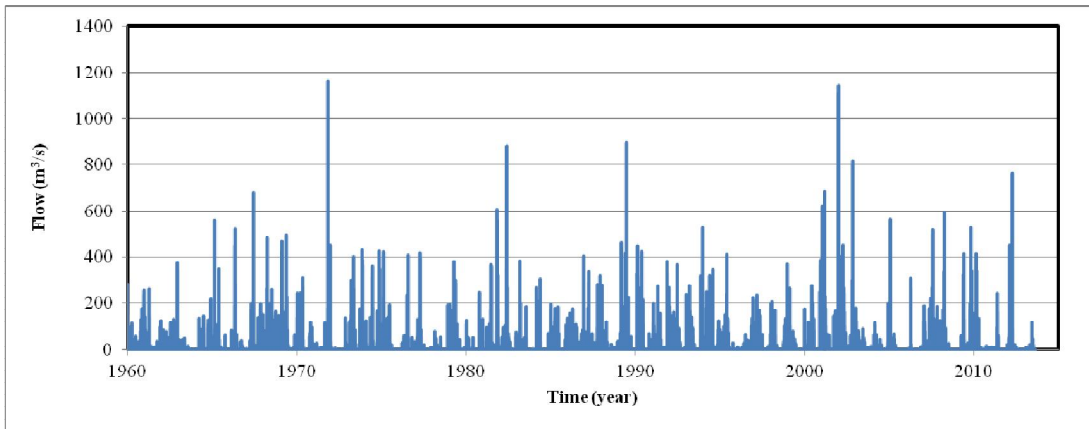


Figure 32. Flow hydrograph of North Sulfur River

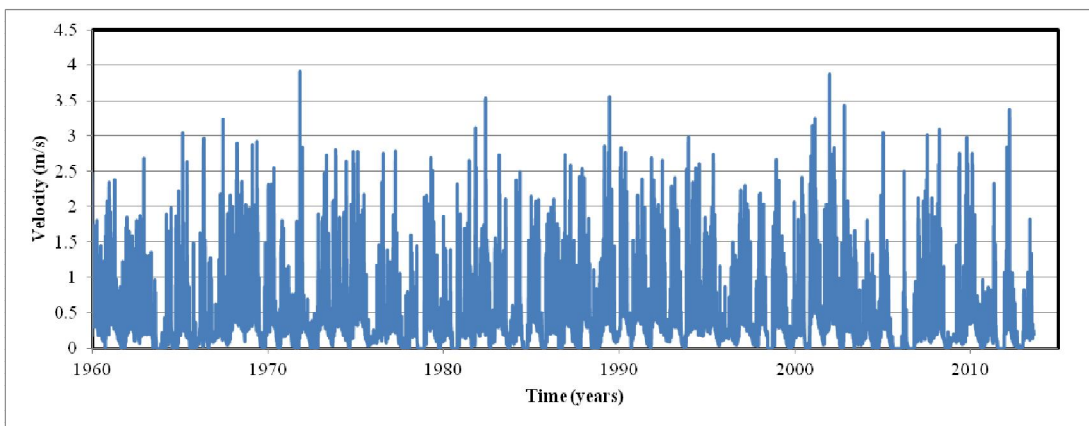


Figure 33. Velocity hydrograph of North Sulfur River

4.2.5 US 90 at Nueces River (Uvalde, TX)

The erosion at the Nueces River is in the same fashion as in the Brazos River. Erosion occurs at the meander to the north of the bridge. However, there are two big differences at this site. First, this river is dry most of the year. Only certain times during the year there is flow of the river and also during big floods. Second, there is a big concern of erosion at the bridge. In 1998 there was a big flood that resulted in failures in the riprap at the west side of the bridge. Figure 34 shows the progression of erosion at this site between 1995 and 2008. A flow hydrograph is shown in Figure 35 and a velocity hydrograph is shown in Figure 36.

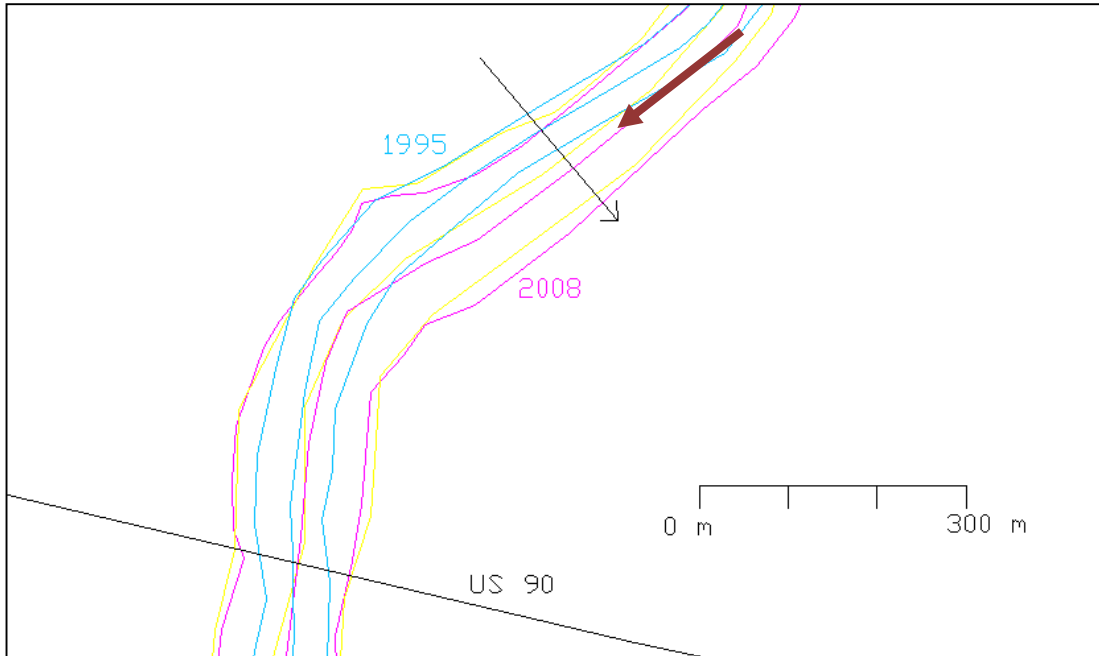


Figure 34. Meander movement of Nueces River between 1995 and 2008

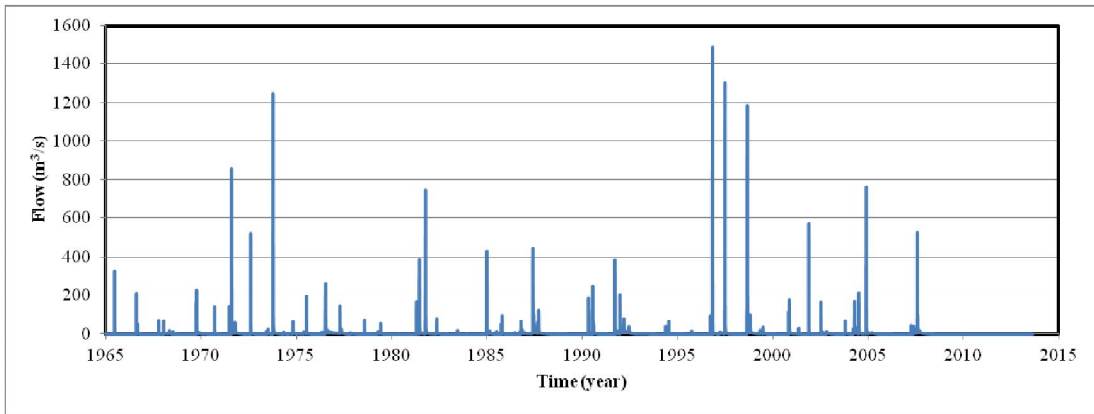


Figure 35. Flow hydrograph of Nueces River

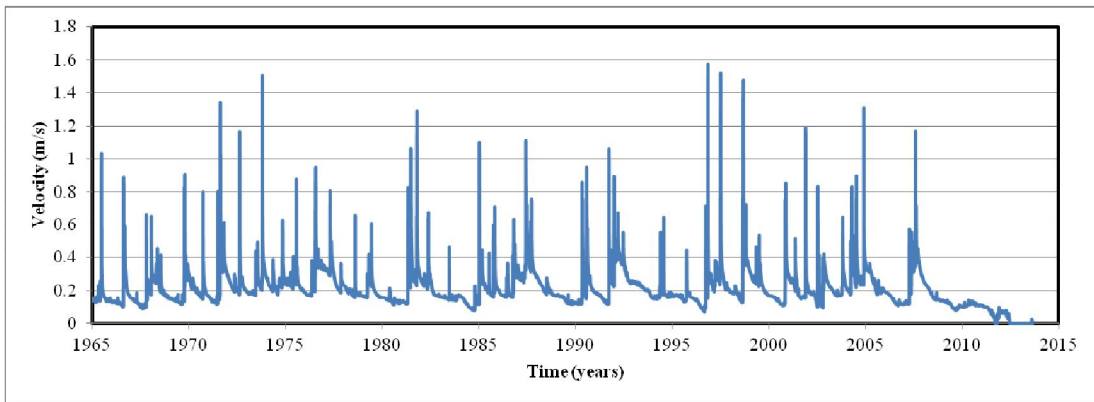


Figure 36. Velocity hydrograph of Nueces River

4.2.6 FM 973 at Colorado River (Austin, TX)

Figure 37 shows the change of the bottom of the river between two different profiles: one in 1991 and the other in 2005. The black line corresponds to the river in 1991 and the red line corresponds to an inspection in 2005. Data from inspections after 2005 shows that there are not significant changes since. The measurements to get these profiles were done from the top of the river. The north points from left to right in this figure. Figure 38 shows a table of the exposure of the drilled shafts in feet from an inspection 2005. Figure 39 and Figure 40 show the flow and velocity hydrographs of this river, respectively.

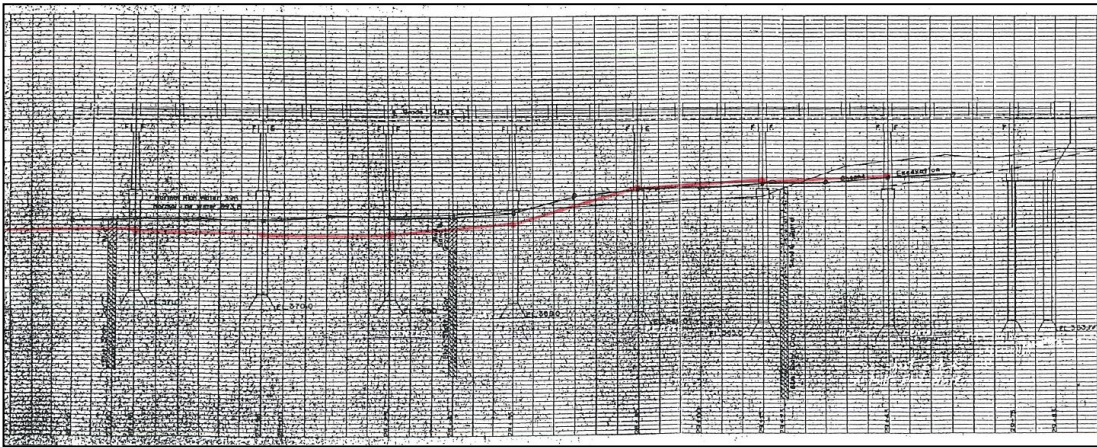


Figure 37. Profiles of Colorado River at FM 973 (cross section)

Exposure of Drilled Shafts below Bottom of Pier Base Cap

Pier No. (from South)	West Shaft (ft)	Center Shaft (ft)	East Shaft (ft)
<i>Bent 6</i>			
1 2		6.8	7
2 3	8	9	9
<i>Drift</i> 3 4	7	9	9.5
<i>Drift</i> 4 5	11	12	11.5
5 6	11.5	12	12
6 7	11.5	12	11.5
7 8	10.5	11	12
<i>Drift</i> 8 9	8.5	9.5	12
<i>Drift</i> 9 10	5.5	6	8
<i>Drift</i> 10 11	5	6	6.5
11 12	3	5.5	6

2011 QTS

Figure 38. Exposure of drilled shafts

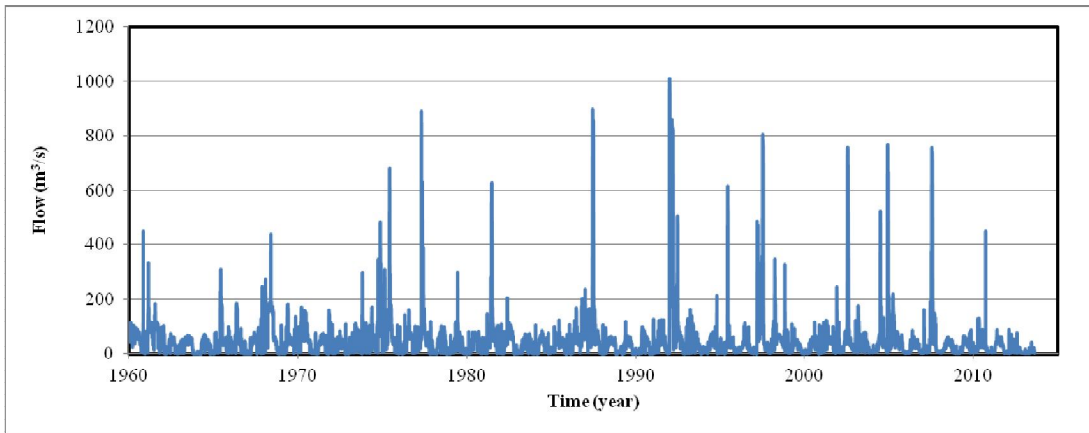


Figure 39. Flow hydrograph of the Colorado River

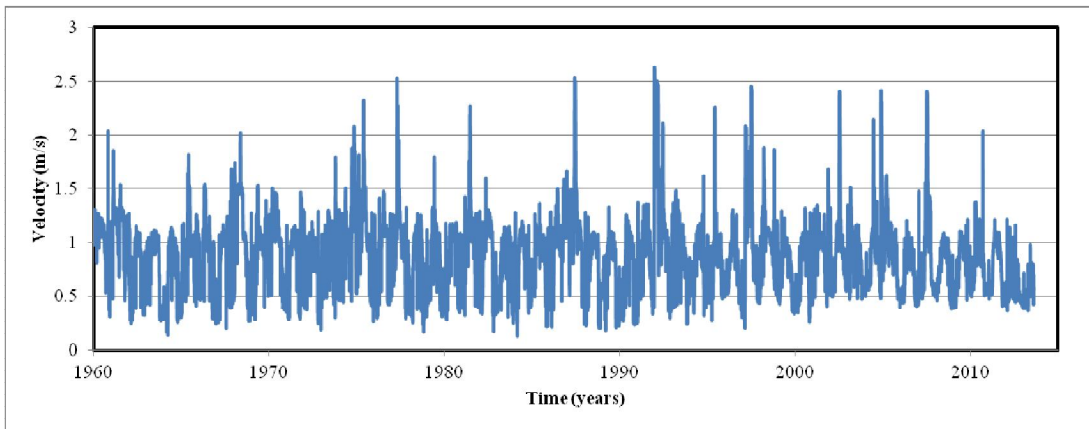


Figure 40. Velocity hydrograph of the Colorado River

4.3 SITE VISIT

Five of the six sites previously mentioned were visited in a week, from June 4 through June 11, 2012. Each visit consisted of: taking soil samples in 6-inch modified Shelby tubes that are used for erosion testing, taking bulk samples of the soil next to where the tube samples were extracted, and general exploration of the sites (photos, notes, etc.). The last site was visited after it was added to the project. The schedule of the site visits was the following:

- SH 105 at Brazos River (Navasota, TX) - June 4, 2012
- FM 787 at Trinity River (Cleveland, TX) – June 5, 2012
- SH 63 at Sabine River (Texas-Louisiana Border) – June 6, 2012
- SH 34 at North Sulfur River (Ladonia, TX) – June 7, 2012
- US 90 at Nueces River (Uvalde, TX) – June 11, 2012
- FM 973 at Colorado River (Austin, TX) – April 23, 2013

The exploration team was divided in two groups during these visits. The first group had the task to collect soil samples that were be used for erosion tests and classification of soils. The graduate students Axel Montalvo and Ghassan Akrouch, from Texas A&M University, were part of the first group. The second group had the task to collect sediments from the eroded areas and samples from the bottom of the river for other purposes. The members of this second group were Dr. Kyle Strom from University of Houston, Dr. Xiaofeng Liu from University of Texas at San Antonio, and Rusen Sinir, graduate student from University of Texas at San Antonio.

4.3.1 SH 105 at Brazos River (Navasota, TX)

This site was visited on Monday, June 4, 2012. The bridge of interest is located on SH 105, to the west of Navasota. There are accesses to get under the bridge on both east side and west side of the bridge. The first five soil samples were obtained from the east side of the bridge, one under the bridge next to the water and the other one from the west side of the bridge. Figure 41 shows the exact location of the samples. These locations were obtained with the coordinates given by a GPS. The velocity of the river

was very low and seemed like the water was not moving this day. The depth of the river could vary between 3-5 feet. Currently, only one column of the bridge is under the water.



Figure 41. Location of samples at Brazos River (Google Earth, 2013)

At first sight, it was noticed that on the west side of the bridge there was a lot of vegetation, compared to the east side. The high velocities during floods erode both sides under the bridge, but also it can be noticed that the meander to the north of the bridge has been eroded. The soil to the south of the bridge on the west side looked like the soil at the meander. No samples were obtained to the south of the bridge. At the top of the cliffs that have been formed with the erosion, the soil looks more clayey and at the middle it is more sandy (Figure 42). Erosion has progressed during the years, as pipes that are supposed to be underground were exposed. It was not possible to get to the top because it was very steep.

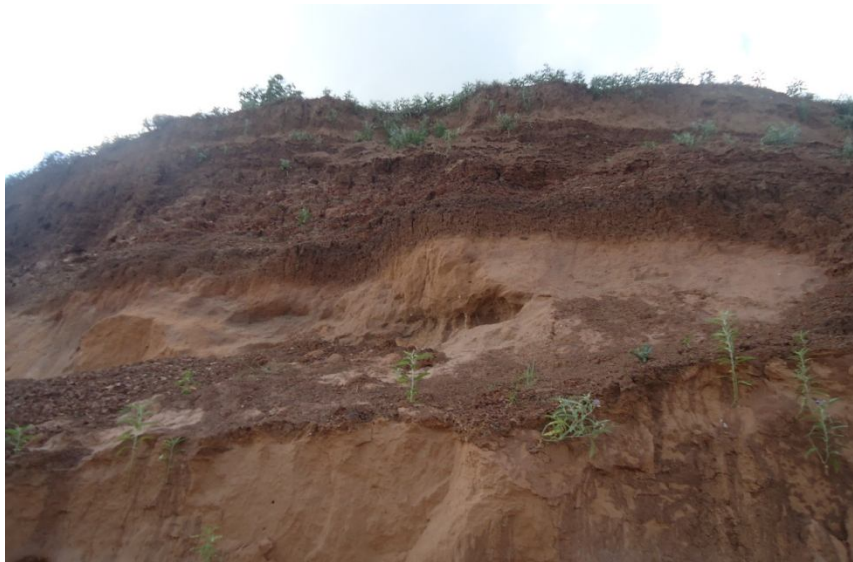


Figure 42. Layers of sand and clay

When a big flood comes, the sandy soil is washed away and the clay layer at the top falls. Big chunks of clay that look like rocks have been accumulated and have dried over time (Figure 43a). Vegetation has grown on this soil, at the side of the meander (Figure 43b). This may indicate that a big flood has not occurred recently.



a. Chunks of clay



b. Vegetation

Figure 43. Clay and vegetation at the site

The first two soil sample from this site, S1B1 (Figure 44a) and S1B2 (Figure 44b) were obtained at halfway between the outer bank of the meander to the north of the bridge and the bridge itself. The first sample was obtained by driving the tube in the soil

that looked more sandy/silty. This sample is representative of soil that erodes easily at high velocities. The color of this soil was between orange and brown. This soil is generally fine grained and barely had cohesion. A hole was dug to penetrate the tube. The second sample was a sample of the clay. This clay looked very similar to the clay layer at the top. The clay was wetter than the soil from the first sample, even though they were at the same height from the river. This sample was obtained from the surface. Both tubes were driven on a vertical position.



a. Sample S1B1

b. Sample S1B2

Figure 44. Samples S1B1 and S1B2

For the third sample, S1B3, was driven in a more loose sand (Figure 45a). This soil was similar to the one obtained in the first sample, but is not more representative of the soil on this area. This sand looked like the sand sediment at the point bars, but it looked like this was part of the natural soil and not sediments. The color and texture of this sand was similar to beach sand, but with finer particles. Compaction at the site was necessary for this sample. The soil for S1B4 (Figure 45b) was very similar to the one obtained in S1B1. These two samples are the best representation of the soil of this area. These tubes were particularly easy to drive in the soil.



a. Sample S1B3

b. Sample S1B4

Figure 45. Samples S1B3 and S1B4

S1B5, the fifth sample (Figure 46a), is from the soil beneath the bridge, next to the water. It was not possible to extract a sample from the bottom of the river, so this is the closest that could represent it. The soil here was wet, as it was less than 10 feet from the water. The soil here was more clayey and different from the other 4 samples. The last sample, S1B6 (Figure 46b), was obtained from the west side of the bridge. This side of the river has a lot of vegetation and the soil is like mud. This sample was the hardest to obtain, in terms of the soil conditions and the effort to drive the tube into the soil. The soil here was clay and very wet. At the surface it has a brown color, but when after digging, it has a darker color and small roots were found almost anywhere.



a. Sample S1B5

b. Sample S1B6

Figure 46. Samples S1B5 and S1B6

4.3.2 FM 787 at Trinity River (Cleveland, TX)

This site was visited on June 5, 2012. The problem of erosion at this site is different when compared to the first site. Here the road is parallel to the river and the distance between them is very short. Many countermeasures have been installed at this site to prevent erosion. The most noticeable were the ripraps along the river and beneath the bridge, and the sheet piles. The rocks were placed mainly under the bridge and at some points along the river. Several sheet piles have been installed; some of them are newer than others. At this site, two samples were extracted in tubes at a critical point of erosion next to the road. Also one sample was placed in bags to compact in the laboratory. Finally, two tubes were driven to obtain samples from the west side of the bridge. Figure 47 shows the location of the samples.

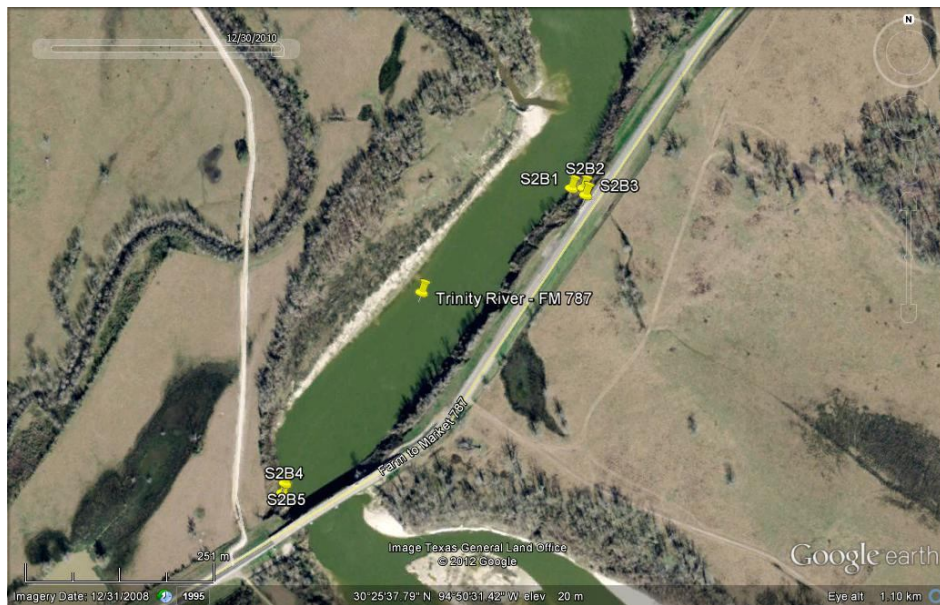


Figure 47. Location of samples at Trinity River (Google Earth, 2013)

In the past, erosion at the bridge was a big security issue and the bridge had to be extended. This was part of a big project to save this bridge and the road. Figure 48a shows the extended part of the bridge (east side of the bridge). Also, sheet piles have been used to protect the road from erosion, but some of them have not been effective and newer ones have been installed. Figure 48b shows an example of a sheet pile that failed

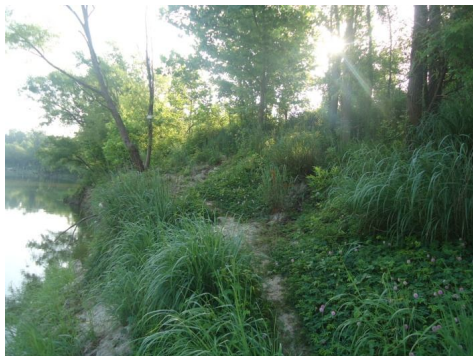
at this site. It has to be mentioned that a lot of vegetation has grown between the river and the road (Figure 48c). Big trees have grown in this area. However, when a big flood comes, the water can wash away the soil. There was a difference of elevation of approximately 25 feet between the road and the water level of the river at the moment of the visit. Figure 48d shows the side of the road on the right and the vegetation that is between the river and the road on the left.



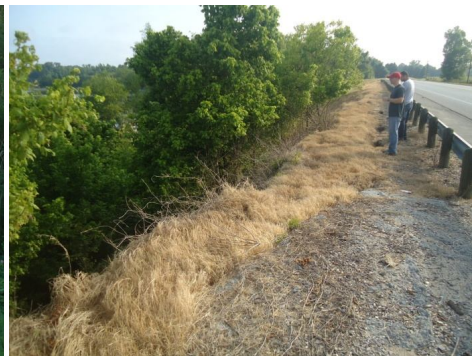
a. Looking to the west



b. Failed sheet pile



c. Vegetation along Trinity River



d. Vegetation next to the FM 787 road

Figure 48. Trinity River photos

A big crack on the pavement can be seen in Figure 49a and Figure 49b. This crack has exposed the newest sheet pile used to protect the road. This has been a big concern because the crack has been getting bigger and a failure of the road may happen in the future. Approximately 15 feet away from this sheet pile, an old sheet pile could be seen. Only a few pieces of this sheet pile were still there, as they were removed when the new sheet pile was installed (Figure 49c and Figure 49d).



a. Sheet pile inside the crack



b. Crack next to the road



c. Old sheet pile



d. Old sheet pile

Figure 49. Sheet piles and cracks

The first three samples (S2B1, S2B2 and S2B3) were obtained from the most critical part of erosion at this moment. As seen in Figure 47, the three samples were taken from the same area. These three samples are a good representation of the soil of this area. The first two samples were extracted with the tubes (Figure 50a). As mentioned before, there is a lot of vegetation in this area. Some roots can be found in these samples. The soil here was sandy and was a light brown color. For the third sample (Figure 50b), the soil was put in two big bags because it was not possible to drive a tube in the slope.



a. Sample S2B1

b. Soil of slope

Figure 50. Sample S2B1 and slope next to sheet pile

The last two samples (S2B4 and S2B5) were obtained from the west side of the river. From this side, the riprap can be seen on Figure 51a (east side of bridge) and Figure 51b (west side of the bridge). The size of these rocks varied from 0.5'-2'. The soil at the west side of the bridge was a combination of sands, clays, and organic material (Figure 51c and Figure 51d). Here the soil samples had more roots beneath the surface than the other three samples that were obtained from the other side of the river, even though there was less vegetation.



a. Riprap on the east side of the bridge



b. Riprap on the west side of the bridge



c. Sample S2B4



d. Sample S2B5

Figure 51. Riprap and samples S2B4 and S2B5

4.3.3 SH 63 at Sabine River (Texas-Louisiana Border)

The site at the Sabine River was visited on June 6, 2012. The bridge at this location, the Burr's Ferry Bridge, was built in 1925 and connects the SH 63 of Texas with the LA 8 of Louisiana. The bridge is made of steel, with concrete columns. The flow of the water is mainly controlled by the Toledo Bend Dam. The Sabine River is the boundary between the two states. Only 4 samples were collected at this site. All of the samples were obtained at the west side of the bridge (Texas). No samples were collected from the east side (Louisiana). The soil at the west side of the river has been eroding and could be a danger in the future. Figure 52 shows the exact location of each soil sample.



Figure 52. Location of samples at Sabine River (Google Earth, 2013)

This river, as seen in aerial photos, has changed a lot due to the erosion and it can be seen at the place where the samples were collected. The soil here is sand and seems highly erodible. There is a lot of vegetation in this area (Figure 53a). Blocks and broken pieces of concrete have been placed as riprap to help to control the erosion (Figure 53b). However, it looks like it has not worked very well and they have not put enough. It looks like they put it as an emergency mitigation and not a long term solution to the problem.



a. Vegetation and concrete

b. Concrete blocks at the curve

Figure 53. Vegetation and concrete next to river

As seen in Figure 54, the water level at this point is very low compared to what happens during a big flood. The graffiti also show that the water has washed the paint off the wall. The soil around the column is exposed, but this area floods sometimes when the gates of the dam are opened, usually during afternoons, as we were told by local fishermen. The soil around the column is sand.



Figure 54. Column of the bridge

The first three samples (S3B1, S3B2 and S3B3) were collected from the curve next to the bridge. The soil, as specified before, was sand. Some roots could be found due to the vegetation of the area. It was relatively easy to drive the tubes into the soil (Figure 55a). The fourth sample (S3B4) was collected from the soil under the bridge, next to the column. The soil here was sand too. However, it was different than the other first three. Here the sand had two different colors and was wetter (Figure 55b).



a. Sample S3B2

b. Sample S3B4

Figure 55. Samples S3B2 and S3B4

On the east side of the bridge, the erosion has been controlled by huge blocks of concrete (Figure 56). These have been placed by the Louisiana Department of Transportation. No samples could be obtained from this side because of the difficult access, the vegetation and the concrete blocks. Currently, there is no major concern of erosion at this side of the bridge.



Figure 56. Concrete blocks at east side of bridge

4.3.4 SH 34 at North Sulfur River (Ladonia, TX)

This site was visited on June 7, 2012. The Texas Department of Transportation is concerned about the vertical degradation of the soil beneath the bridge, rather than meander migration. This river is very straight at the location of this bridge. Five samples were collected at this site. Figure 57 shows the location of each sample. Contrary to the previous rivers, the North Sulfur River at this site was almost dry. Water could only be seen at some parts. It had been raining for 24 hours and at the time of the visit it was raining too, so this rain could have contributed to the small flow of water. Ponds of accumulated water could be seen at the area. Also concrete blocks were apparently placed next to the columns. It seems that they are used to change the direction of the flow. Part of the columns has been exposed due to the erosion (Figure 58).



Figure 57. Location of samples at North Sulfur River (Google Earth, 2013)



a. Looking to the west



b. Bridge at SH 34



c. Column of the bridge



d. Column exposed

Figure 58. North Sulfur River site photos

Five soil samples were collected at this site. One of them was to the west of the bridge, as seen in Figure 59a. Water flows in this river from west to the east. Three samples were obtained beneath the bridge: one at each side of one of the columns and one below the center of the bridge. The last one was obtained by driving the tube into the soil at one of the sides of the river (Figure 59b). The soil of the first four samples was similar. It was sand, clay and sediments of different sizes of the river. Also, the soil here was very wet. Digging holes was necessary to obtain these samples. The sample from the side of the river was very stiff clay. The soil at this site was dark.



a. Sample S4B1



b. Side of the river, looking to the east

Figure 59. Sample S4B1 and river photo

4.3.5 US 90 at Nueces River (Uvalde, TX)

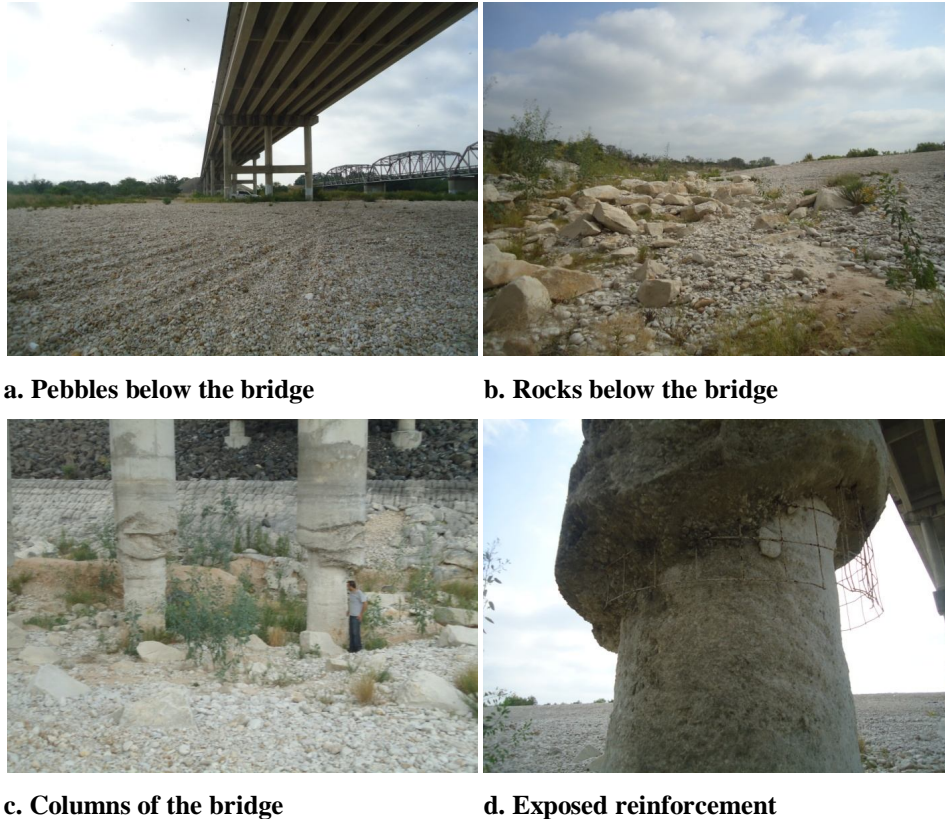
The last site of the first exploration, at the Nueces River, was visited on June 11, 2012. There are two bridges at this site, one for each direction. This river is located to the west of Uvalde. The shape of this river in aerial photos looks similar to the Brazos River in Navasota. A meander to the north of the bridge has been migrating to the southeast. Also the erosion at the west side of the bridge has been a concern for the Department of Transportation. Several countermeasures have been installed here. This river could be accessed from either side of the bridge. The water flows from north to south at this location. The weather here is drier than in the other four locations. No water could be seen in the river. The location of these samples can be seen in Figure 60.



Figure 60. Location of samples at Nueces River (Google Earth, 2013)

The first thing that can be noticed below the bridge is that instead of soil, there are many rocks or pebbles of different sizes (Figure 61a and Figure 61b). The size of most of the rocks was from 3”-6”, but there were others that were bigger. No samples of these rocks were taken. Also, it can be noticed that that the water has eroded the bottom of the columns of the bridge. A thinner part of the column of approximately 10 feet high

is exposed (Figure 61c and Figure 61d). The steel reinforcement of these columns has been exposed too.



a. Pebbles below the bridge

b. Rocks below the bridge

c. Columns of the bridge

d. Exposed reinforcement

Figure 61. Nueces River site photos

The first three samples (S5B1, S5B2 and S5B3) from the west side of the river. Under the bridge, the soil is protected by riprap made of rocks and concrete blocks, so the samples had to be taken from uncovered parts. The soil was very dry as expected and it was sandy. The particle size of this soil was very fine. Layers of this soil could be seen, with rocks in between (Figure 62a). This soil seems highly erodible. No tubes could be driven in this soil, as it was very hard and lack of moisture does not help. The soil was put in plastic bags and then compacted in the laboratory for erosion tests (Figure 62b).



a. Layers of soil and gravel

b. Sample S5B2

Figure 62. Layers of soil of the river and sample S5B2

The last sample, S5B7, was obtained at the meander to the north of the bridge. As can be seen in the tree on Figure 63a, erosion has progressed with time. Figure 63b shows the soil at the wall, which was sand like in the first three samples, but with no gravel in it. Three bags were filled with this soil for erosion tests.



a. Erosion next to a tree

b. Digging for collecting sample S5B7

Figure 63. Obtaining sample S5B7 at meander

4.3.6 FM 973 at Colorado River (Austin, TX)

The bridge can be seen and accessed from the north side. The drilled shafts below the bottom of the pier base cap have been exposed, as can be seen on Figure 64. The condition of these drilled shafts varies and it looks like the concrete has also failed in some of them.



Figure 64. Drilled shafts

Because the samples could not be obtained from the bottom of the river, they were taken from as close as possible from the water. The exact location of the samples can be seen in point A in Figure 65. The soil samples were obtained from this point because the soil was wetter and the tubes were easier to drive into the soil. The soil was sandy with some plasticity (Figure 66).



Figure 65. Location of samples (Google Earth, 2013)



Figure 66. Soil sampling

4.3.7 Obtaining Samples at Each Site

Each soil sample was collected in two ways: driving a modified Shelby tube and putting the soil in bags. At each location, a muffler tube was driven into the ground using a 4x4 piece of wood with handles, as shown in the photos of Figure 67. Most of the samples were obtained from the ground surface. However, others had to be obtained after digging with shovels because of vegetation or to find a more uniform soil that could represent the area. The samples inside the tubes are tested in the EFA. For each tube that was driven, a soil from that same area was put inside bags. These samples are used for the following tests: size distribution using sieves and hydrometer, and Atterberg limits.



Figure 67. Obtaining samples with muffler tube

4.3.8 Field Testing at Each Site

At each site, two in-situ tests were performed to have an idea of the strength of the soil. The first one is the pocket penetrometer test, which is used to have an estimate of the unconfined strength of the soil. The second one is the vane shear test, which gives an estimate of the undrained shear strength of the soil. Below is a detailed description of each device. Figure 68 shows photos of both devices.

- Vane Tester: The vane test (Briaud, 2013) consists of pushing by hand the vane into the soil and rotating until the shear strength is reached when it does not keep increasing. The indicator at the top of the vane stays at the maximum value reached during the rotation and this indicates the shear strength of the soil.
- Pocket Penetrometer: The pocket penetrometer test or PP (Briaud, 2013) consists of pushing the end of a cylinder of 6.35 mm in diameter into the soil until the ultimate bearing pressure is reached. The tip of the PP has a spring and the ultimate pressure is reached when the reading stops increasing. This test gives a quick indication of the soil strength, but the area tested is small and the results must not be used for design purposes.

These tests give estimates and should not be substituted by a proper laboratory test, such as a triaxial test. Table 1 shows the labeling method for every site, as mentioned in the site visit section. Table 2 shows the exact locations where the samples were obtained. A description of each sample and the results of the field tests are shown in Table 3. As seen in this table, no tube samples were collected at the Nueces River or Colorado River sites and no in-situ test were performed. The soils at these sites were either very dry or very wet. Therefore, soil samples were collected in bags at these rivers. Also, in-situ tests were not performed at these sites.



Figure 68. Pocket penetrometer and vane tester

Table 1. Sample labeling legend

S1	Brazos River	S4	North Sulfur River
S2	Trinity River	S5	Nueces River
S3	Sabine River	S6	Colorado River

Table 2. Sample locations

River	Sample	N	W
SH 105 at Brazos River	S1B1	30°21'49.20"N	96° 9'8.50"W
	S1B2	30°21'49.20"N	96° 9'8.60"W
	S1B3	30°21'52.10"N	96° 9'4.70"W
	S1B4	30°21'47.50"N	96° 9'12.10"W
	S1B5	30°21'41.60"N	96° 9'18.90"W
	S1B6	30°21'41.80"N	96° 9'21.00"W
FM 787 at Trinity River	S2B1	30°25'42.70"N	94°50'50.30"W
	S2B2	30°25'42.70"N	94°50'49.70"W
	S2B3	30°25'42.40"N	94°50'49.60"W
	S2B4	30°25'29.61"N	94°51'4.69"W
	S2B5	30°25'30.00"N	94°51'4.60"W
SH 63 at Sabine River	S3B1	31° 3'51.90"N	93°31'13.50"W
	S3B2	31° 3'52.14"N	93°31'13.02"W
	S3B3	31° 3'51.96"N	93°31'12.12"W
	S3B4	31° 3'51.60"N	93°31'11.70"W
SH 34 at North Sulfur River	S4B1	33°27'22.26"N	95°56'32.28"W
	S4B2	33°27'21.84"N	95°56'30.54"W
	S4B3	33°27'22.02"N	95°56'30.36"W
	S4B4	33°27'22.44"N	95°56'30.72"W
	S4B5	33°27'21.54"N	95°56'30.18"W
US 90 at Nueces River	S5B1	29°12'28.62"N	99°54'12.66"W
	S5B2	29°12'29.10"N	99°54'12.54"W
	S5B3	29°12'32.70"N	99°54'10.50"W
	S5B4	29°12'23.76"N	99°54'12.18"W
	S5B5	29°12'23.70"N	99°54'12.18"W
	S5B6	29°12'23.82"N	99°54'12.24"W
	S5B7	29°12'39.30"N	99°53'53.34"W
FM 973 at Colorado River	S6B1	30°12'30.23"N	30°12'30.31"N
	S6B2	97°38'16.79"W	97°38'16.73"W

Table 3. Field test results

Sample	Pocket Penetrometer Reading (kg/cm ²)	Undrained Shear Strength, PP Reading x 30 (kPa)	Vane Test: Undrained Shear Strength (kPa)	Description
S1B1	3.25	97.5	38	sandy soil, fine grained, dug 1 foot, orange/brown color
S1B2	-	-	25	wet clay, 9 feet away from S1B1, halfway from river to top
S1B3	0.5	15	18	sand, looks like sediment from point bars, not representative
S1B4	-	-	40	same soil as in S1B1, not too much effort to drive
S1B5	1	30	10	10 feet away from water, beneath the bridge, dark color, muddy
S1B6	-	-	-	from west side of river, clayey, dark color, muddy
S2B1	0.75	22.5	13	sandy soil, has vegetation, 20 feet away from river, light brown
S2B2	1.2	36	20	sandy soil, has vegetation, 25 feet away from river, light brown
S2B3	-	-	-	sandy soil in bag, from cliff, has roots
S2B4	0.5	15	25	dark soil from west side, clay and sand, has roots
S2B5	1.5	45	25	dark soil from west side, clay and sand, has roots
S3B1	1	30	14	sandy soil, tube inserted horizontally, light brown color
S3B2	0.6	18	18	sandy soil, tube inserted horizontally, close to the river
S3B3	0.5	15	24	sandy soil, tube inserted horizontally
S3B4	1.1	33	20	sand from under the bridge, layers of different colors
S4B1	1.25	37.5	35	away from bridge, different sizes, wet, clay and sand
S4B2	1.25	37.5	24	under the bridge, next to column, wet, sand with different sizes
S4B3	2.25	67.5	-	under the bridge, next to column, wet, sand with different sizes
S4B4	-	-	-	under the bridge at center, wet, sand with different sizes
S4B5	-	-	-	at side of the river, wet clay, hard to drive, dark gray
S5B1	-	-	-	very fine grained with a few pebbles, light brown color
S5B2	-	-	-	very fine grained with a few pebbles, light brown color
S5B3	-	-	-	very fine grained with a few pebbles, light brown color
S5B4	-	-	-	from bottom of bridge, sand and small rocks, dry
S5B5	-	-	-	from bottom of bridge, sand and small rocks, dry
S5B6	-	-	-	from bottom of bridge, clayey, brown color, wet
S5B7	-	-	-	light brown color, 3 bags
S6B1	-	-	-	sandy silt with some plasticity
S6B2	-	-	-	sandy silt with some plasticity

4.4 LABORATORY TESTING

4.4.1 Particle Size Analysis

One of the most important aspects of soils is the size distribution of its particles. As we know, soil is the product of physical and chemical degradation of rock. Depending on how this degradation occurs, the particles and grains of soil will have different sizes. Two standard tests to determine the size distribution of soils are performed in the laboratory according to the ASTM standard D 422-63 (2007). The first test is a sieve analysis, in which the soil is separated by a stack of sieves. Each of these sieves has a number that represents the amount of openings per lineal inch. The second test is the hydrometer analysis, which is a test used for particles smaller than 0.075 mm (particles that pass sieve #200). In this test the soil is mixed with water and a dispersing agent, and the distribution is obtained by a process of sedimentation. The results from both tests are plotted and then used to obtain the classification of the soil, with the Atterberg limits of the soil.

For the sieve analysis, 5 sieves and a pan are put together and the soil is shaken in the sieves for a period of time to separate the coarse soil particles from the fines. The fines are those particles that have a diameter smaller than 0.075mm. The hydrometer was conducted for the soil samples after the sieve analysis test. The soil retained in the pan was analyzed with the hydrometer test. There are other different ways to perform the soil particle size analysis such as performing the hydrometer first and then the sieve or performing a wet sieve analysis. For the soils obtained at the sites, the soil was dried and then separated in the sieves. Only the particles that passed the #200 sieve were tested with the hydrometer test.

4.4.2 Atterberg Limits

The Atterberg limits are parameters used to describe the transition of a soil to different states. The liquid limit and the plastic limit are determined according to ASTM D 4318. A soil can be classified with the Unified Soil Classification System specifications with the results of the Atterberg limits and the particle size analysis. This

test is important to determine if the fines from the hydrometer test are either silts or clays. Silts found at these sites have a low plasticity. Using the results of the particle size analyses and Atterberg limits tests, it is possible to classify the soils. Table 4 shows the classification of some of the soil samples.

Table 4. Soil classification at each site

River	Sample	N	W	Soil Classification
SH 105 at Brazos River	S1B1	30°21'49.20"N	96° 9'8.50"W	SM
	S1B4	30°21'47.50"N	96° 9'12.10"W	SM
	S1B5	30°21'41.60"N	96° 9'18.90"W	SP-SM
	S1B6	30°21'41.80"N	96° 9'21.00"W	CL
FM 787 at Trinity River	S2B1	30°25'42.70"N	94°50'50.30"W	SM
	S2B2	30°25'42.70"N	94°50'49.70"W	SM
	S2B4	30°25'29.61"N	94°51'4.69"W	SC
	S2B5	30°25'30.00"N	94°51'4.60"W	SP
SH 63 at Sabine River	S3B1	31° 3'51.90"N	93°31'13.50"W	SM
	S3B2	31° 3'52.14"N	93°31'13.02"W	SP
	S3B3	31° 3'51.96"N	93°31'12.12"W	SM
SH 34 at North Sulfur River	S4B1	33°27'22.26"N	95°56'32.28"W	SP-SC
	S\$B3	33°27'22.02"N	95°56'30.36"W	SP-SC
	S4B4	33°27'22.44"N	95°56'30.72"W	SP
	S4B5	33°27'21.54"N	95°56'30.18"W	SC
US 90 at Nueces River	S5B1	29°12'28.62"N	99°54'12.66"W	SP
	S5B2	29°12'29.10"N	99°54'12.54"W	SM
	S5B3	29°12'32.70"N	99°54'10.50"W	SM
	S5B7	29°12'39.30"N	99°53'53.34"W	SM
FM 973 at Colorado River	S6B1	30°12'30.23"N	30°12'30.31"N	SC
	S6B2	97°38'16.79"W	97°38'16.73"W	SC

4.4.3 Erosion Function Apparatus

The EFA test is used to obtain an erosion curve, where the engineer can obtain a critical velocity and erosion rate for a given river velocity (Briaud, 2013). The soil sample, in the Shelby tube, is raised and water erodes the top of the sample at certain rate. Soil can be classified, according to its erodibility, in one of six categories. Non-plastic silt and fine sand are classified in the Category I (Very High Erodibility), whereas intact rocks or jointed rocks are classified in the Category VI (Non-Erosive). The erosion charts were developed and proposed based on more than 15 years of research using the EFA. Figure 69 shows the EFA erosion categories. Figure 70 and show the EFA test results for erosion rate versus velocity for some of the samples collected at the sites.

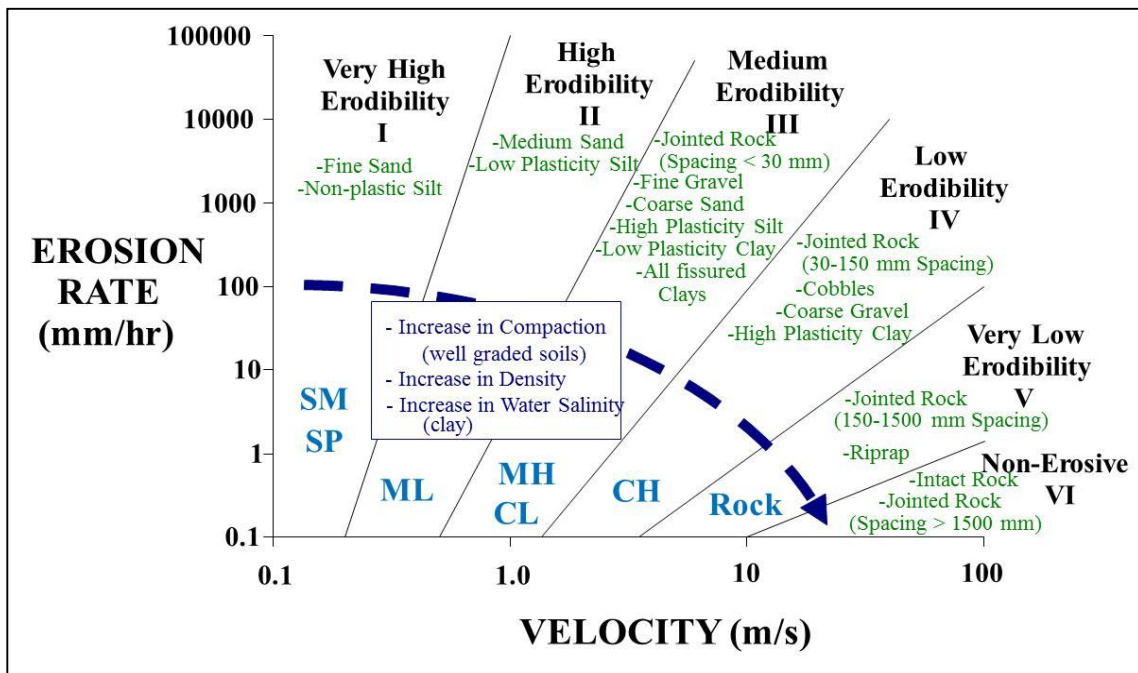


Figure 69. Erosion categories (Briaud, 2013)

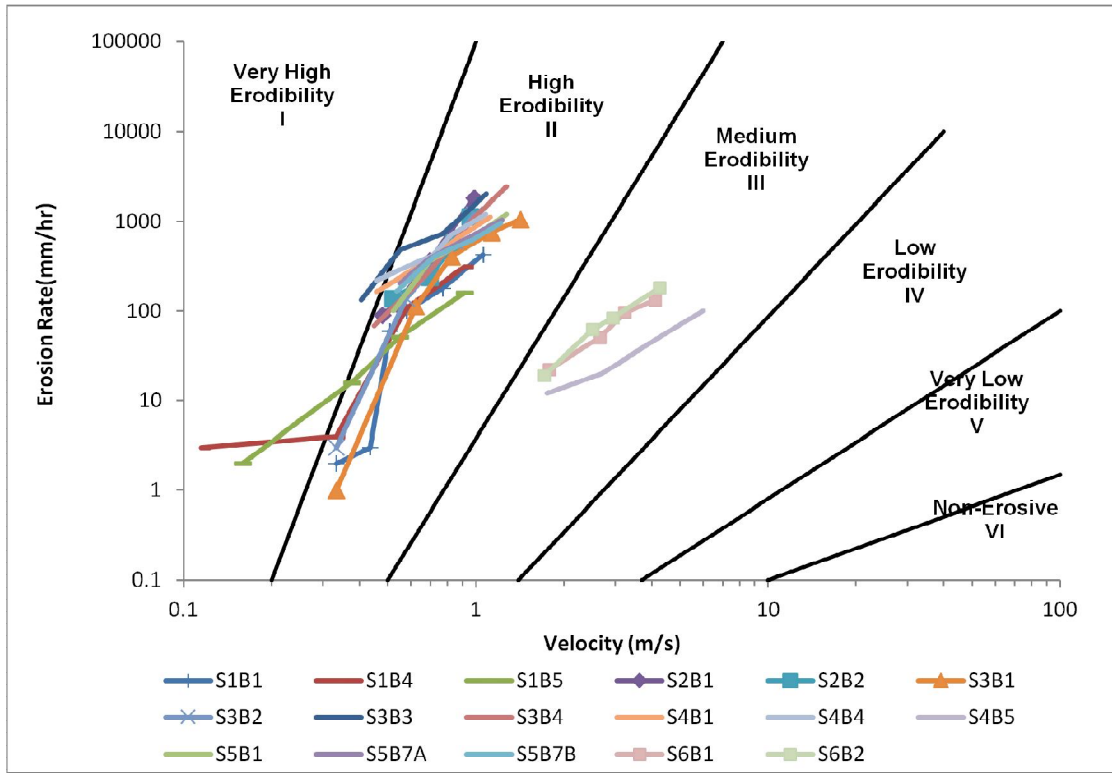


Figure 70. EFA test results for erosion rate versus velocity

CHAPTER V

ANALYTICAL STUDY

5.1 INTRODUCTION

Meander migration is a process that has been studied for years and different methods have been proposed to predict it. The flow of water gradually erodes the banks and can cause a shift that could be a threat to existing bridges, highways and useful lands. Different approaches and procedures can be found in literature. Many of these methods are used to predict the migration rate and the final position of the bankline or centerline of a river. Some of these existing techniques used for meander migration that have been developed are summarized in the Technical Reports 2501-1, 2502-2 and 4378-1 of the Texas Transportation Institute (TTI). Some of the rivers in this project have been studied before and information can be found in these reports.

As mentioned before, there are different approaches to the meander migration problem. Some of these methods consist of numerous studies that result in empirical equations used to obtain the rate of migration. Other methods are based on the hydrologic characteristics of the stream. Techniques based solely on geometry of the bends have also been suggested. All of the proposed methodologies use different variables and consider that one or more of these variables are the most influencing parameters in the prediction.

In the past, TTI has developed different programs. Some of these programs are: SRICOS-EFA, used to predict scour depth at bridge piers (Briaud, et al. 2004); TAMU-FLOOD, used to the recurrence interval of floods that a bridge has experienced since its construction (Briaud, et al. 2009); and MEANDER, used to predict meander migration. A methodology and a program for this project need to be proposed, which will include most of the important influencing factors in meander migration. This method will combine flow and velocity data of the river, soil erodibility, and observations from aerial photographs and/or maps.

5.2 MEANDER PROGRAM

The TTI developed the software called MEANDER, which is used to predict meander migration. MEANDER was developed in 2005 and the TTI Report 4378-1 explains in detail the development of this method. This program is available online and is free of charge. A tutorial to use the program is also included with the software. This software is based on a combination of review of existing knowledge, large flume experiments in two different soil types (i.e., sand and clay), three-dimensional numerical simulations, a hyperbolic model, and a risk analysis. The program consists of two major components: graphic user interface (GUI) and numerical implementation. The program uses the current or past geometry of the river, soil data obtained from erosion tests (EFA test results), and flow data. These also are the three aspects that are considered in the Observation Method developed in this project.

Figure 71 shows the interface of the MEANDER program when opened. The user buttons (command buttons) from left to right correspond to the interfaces that open when clicked: Units, Geometry input, Soil input, Water input, Table input, Plot input, Run function, and Plot output. The two unit systems, the metric system and U.S. system, can be used. The user needs to input the average river width and the path of coordinate file. The coordinate files correspond to the points that define the geometry of the river (initial conditions). If the “Fit Circles” button is clicked, circles will be fitted and drawn on the dialog.

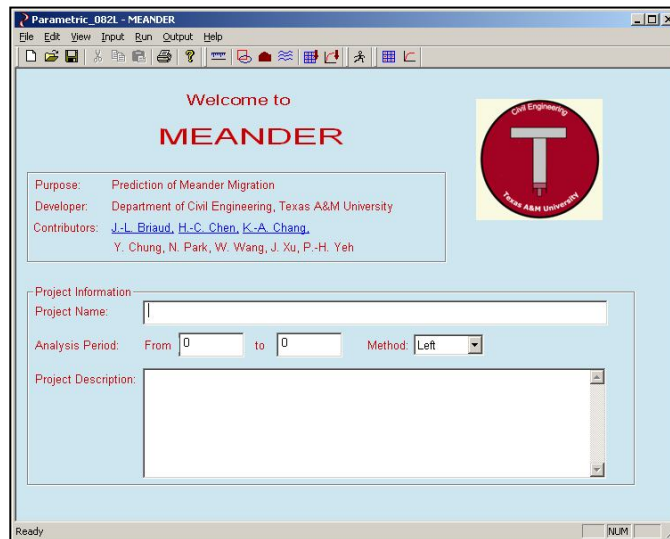


Figure 71. Main interface of the MEANDER program

Before curve fitting is done, the center line or bank of the river is divided into many segments. The three numerical methods used to fit the circles are Criterion Line, Alpha Method and Change of Sign (Figure 72). Only one can be selected and the user is free to change the method as desired, to get better results.

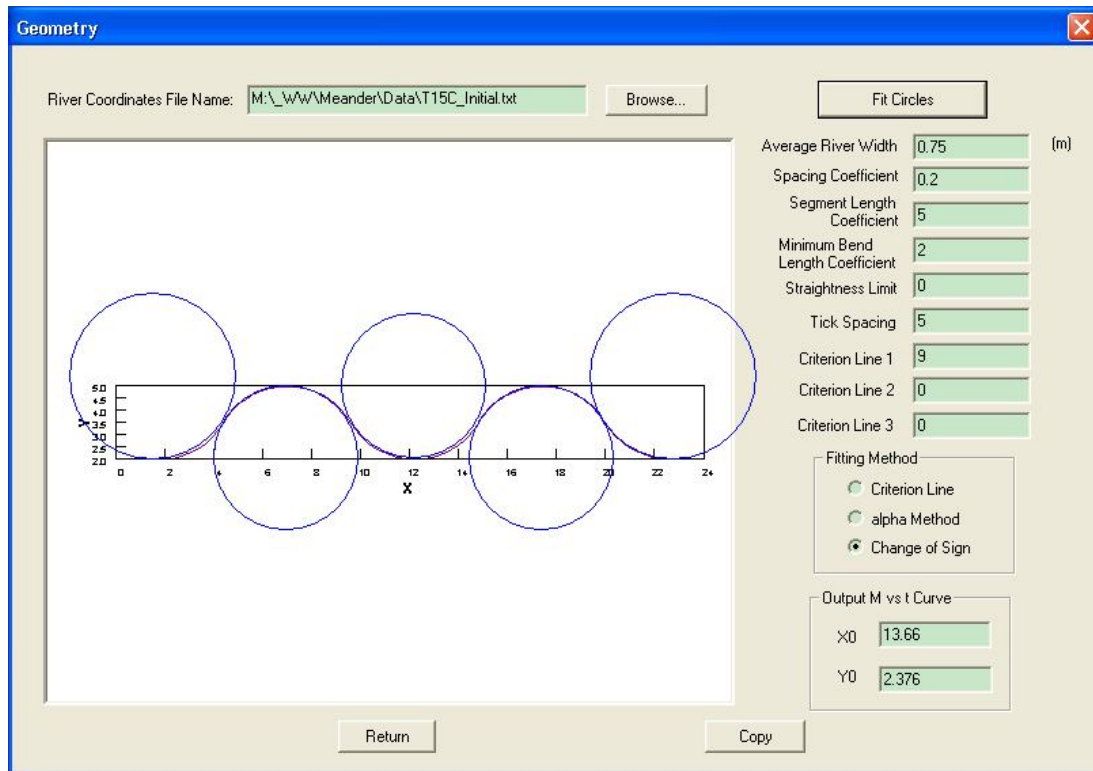


Figure 72. Geometry input

Figure 73 corresponds to the soil data input interface. The first item is critical shear stress, which corresponds to erosion rate of 0.1 mm/hr. The number of points on an EFA curve needs to be specified and a table with the data is created. Since the equations for the modeling used for sand and clay are different, the two options for choosing the type of soil are also provided.

The dialog box titled "Soil Data" contains the following fields and table:

Erodibility Properties
 Critical Shear Stress: N / m²
 Points on EFA Curve:

Point No	Shear Stress (N/m ²)	Scour Rate (mm/hr)
1	0.012	0.1
2	0.04	1
3	0.12	4
4	0.2	12
5	0.28	70
6	0.5	700
7	0.9	1200

Soil
 Sand Clay

OK Cancel

Figure 73. Soil data input

The interface for entering flow conditions is shown in Figure 74. The flow can be in terms of flow or velocity. Three types of analyses are available for the prediction: constant flow, hydrograph, and risk analysis. Risk analysis takes as input either a 100-year and 500-year flood or a hydrograph. One of the choices can be used to calculate the probability associated with the migration movement of the river over a period of time. If the input is flow or discharge, the Discharge versus Velocity table and Discharge versus Water depth table are required by MEANDER. All these tables can be obtained from simulation programs such as HEC-RAS by the U.S. Army Corps of Engineers (Brunner, 2002) or TAMU-FLOW.

Water Data X

Critical Froude Number: s/m^{1/3}

Time Step: hr

Input Hydrologic Data

Discharge vs. Time
 Velocity vs. Time

Constant
 Hydrograph
 Risk Analysis

Velocity: m/s

Time: Day

No. of Points on Curve

Velocity vs. Water Depth:

Velocity vs. Water Depth		
Point No	Velocity (m/s)	Water Depth (m)
1	0	2.5
2	10	2.5

Figure 74. Water data input

The Output Plots box is the final user interface and contains the following buttons: “Center Line or One Bank”, “Both Banks, Risk Analysis”, and “M vs. t for one point”. The program has options such as: show the migrated channel of each step for the center line or a bank; show initial banks, predicted final banks, and measured final banks; or run a risk analysis. The migration process is shown on Figure 75.

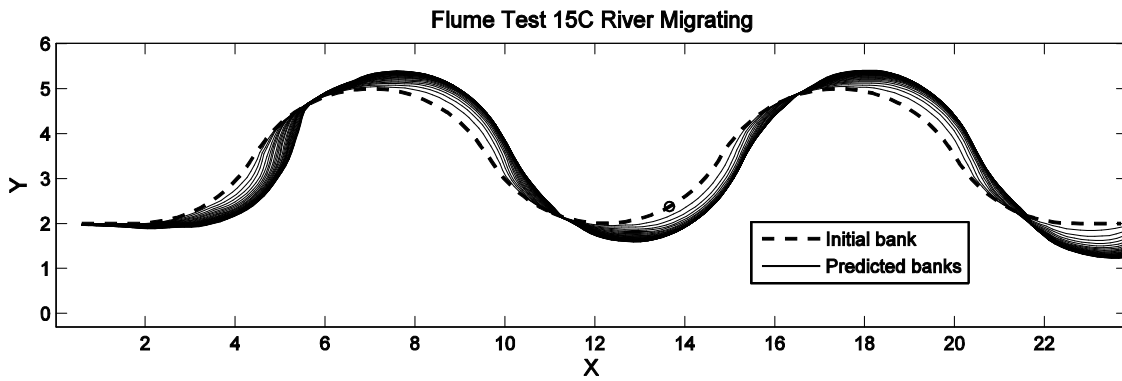


Figure 75. Prediction of meander position

5.3 OBSERVATION METHOD

The observation method for predicting meander migration and vertical degradation is a much simpler method that considers the three variables mentioned before: soil, flow, and geometry. The necessary information to use the model is similar to the steps used in the MEANDER program.

Data of the variation of the discharge of a river can be obtained from the United States Geological Survey. Gage stations in Texas provide daily information of flow of a river. A hydrograph can be used to study the average daily flow of water over a period of time. Also, a graph of velocity versus time can be obtained from a hydrograph, considering the geometry, cross section and roughness of the river. This helps to study the variation of velocity for a determined period of time. With this information we can also know if there was a sudden increase (spike or peak) in the velocity of the river due to a flood or any other event which may have caused it.

Floods can significantly alter a steady flow rate of a river. Therefore, the migration rate (migration movement with time) of a meander can increase drastically. The extrapolation method used with aerial photographs assumes that the flow hydrologic conditions of the river will be the same every year during a period of several years. This is not true when a flood occurs. Floods can be observed on a hydrograph as high peaks in a period of time. The hydrograph and aerial photographs help to determine if there was a significant movement of the meander in the period that the flood occurred.

A prediction of a future flood is important to predict the movement of the meander. These predictions can be obtained with sufficient data. In this case, the worst scenario could be a 100-year flood or a 500-year flood. If no probabilistic approach is used, previous data from the flow could be used. Periods of flow from 10 years were used in this project to make predictions. These periods were used from the same data used to construct a future hydrograph for the prediction.

The migration rate can be related or compared to the erosion of the soil of the bank. Many of the methods used to predict meander migration do not consider the erodibility of the soil. For a complete study of the migration, erosion tests must be

performed. The EFA is used to obtain a curve that relates erosion rate to velocity and erosion rate to shear stress. The critical velocity for erosion can be obtained from the curve. The critical velocity at the site may not be the same and has to be found. If no erosion tests could be performed, the erosion categories can be used using the classification of the soil at the site.

Using the hydrographs of a river, observed data from maps, aerial photos and cross sections, and the erodibility of the soil, a method to predict the meander position and vertical degradation has been developed. This method has been called the Observation Method because it is based on real, observed data to make a prediction of the river in the future.

5.4 METHODOLOGY DEVELOPMENT AND PROCEDURE

The procedure used to predict the meander position during a period of time and where it will be is explained in the following sections. A similar approach is applied for vertical degradation of the bank of the river for these cases. Two software programs were used to verify the Observation Method: MATLAB and Microsoft Excel. A code was written for both programs and a step-by-step example is explained in the next chapter.

5.4.1 Site Selection

The sites of concern for this project are located at six different rivers in Texas. Each one has had erosion problems, and in some of them, different remedies have been implemented for control purposes. Meander migration and degradation at the bottom of the rivers are some of the issues of these rivers. In general, aerial photos of these rivers can be used to compare the river movement due to the erosion and deposition of the soil and sediments. Cross sections from different years can be used to see the progress in vertical degradation at the bridge location. Again, the sites selected for the project and for which each one has been used to design the model were:

- SH 105 at Brazos River (Navasota, TX) – Meander migration
- FM 787 at Trinity River (Cleveland, TX) – Meander migration
- SH 63 at Sabine River (Texas-Louisiana Border) – Meander migration
- SH 34 at North Sulfur River (Ladonia , TX) – Vertical degradation
- US 90 at Nueces River (Uvalde, TX) – meander migration
- FM 973 at Colorado River (Austin, TX) – vertical degradation

5.4.2 Obtaining the River Hydrographs

The first step for the Observation Method is to obtain a hydrograph of the rivers from the USGS stations. The average daily flow can be obtained for a period specified by the user in the USGS website. In some cases, the bridge of interest has no gage installed. A gage downstream or upstream has to be used instead. Figure 76 shows the interface of the USGS website for the gages located in Texas. The data used from each gage is the average daily data. It is important to have the data starting from the date of the first map or photo. The period is selected and ends with the date of the last map or photo. To observe the daily flow, the data is copied in Excel and used in a chart of flow versus time. This generated graph of flow versus time is known as hydrograph. The flow, however, has to be converted to velocity to be used in this method.

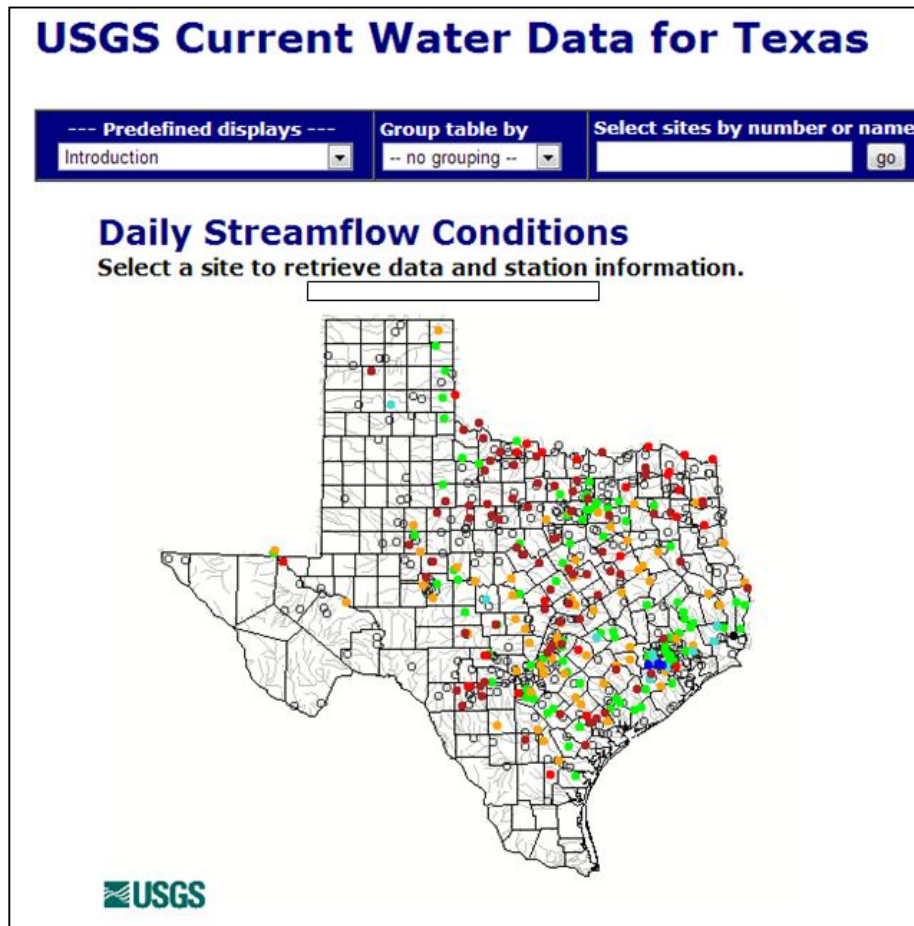


Figure 76. Gage locations in Texas

There are several ways to obtain the velocity of the river from the flow. The most precise way is to obtain the geometry and cross sections of the river and simulate the river in programs such as HEC-RAS or TAMU-FLOW. HEC-RAS was developed by the US Army Corps of Engineers and TAMU-FLOW by Texas A&M University. Both of these programs can be obtained online with no cost. The first one is a robust program that has many functions and could be more complicated to obtain the velocities. This program needs the geometry from the top view, cross sections, roughness and slope of the river. Figure 77 shows the interface of HEC-RAS.

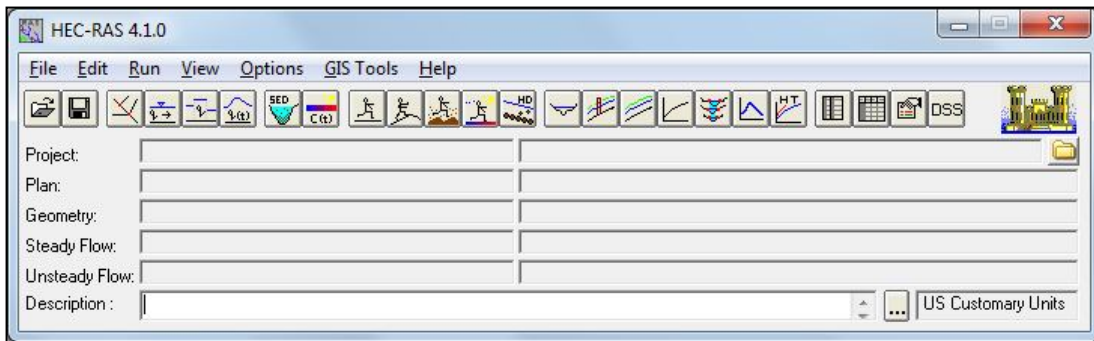


Figure 77. HEC-RAS interface

TAMU-FLOW is a much simpler program and can be used solely for this specific task. The user interface (Figure 78) is simplistic and the only purpose of the program is to obtain the velocity by using only one cross section. The cross section of the river can be assumed to be constant along the river for simplification or the cross section at the area of interest of the river can be used. The coordinates of the cross section of the river are put in the program and then after running the simulation, a curve of velocity versus time can be obtained. The data is saved as a text file that can be opened in Excel. The manual of TAMU-FLOW can be accessed directly from the Help tab. Some of the variables used to run the simulation are the Manning's coefficient and the slope of the river. Any custom or trapezoidal cross-section can be drawn or imported into the TAMU-FLOW program.

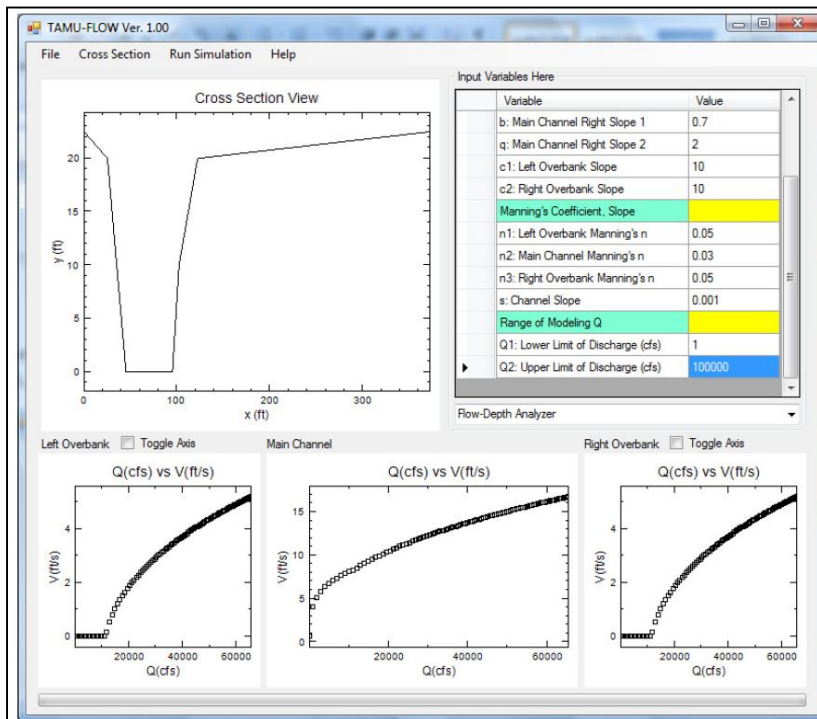


Figure 78. TAMU-FLOW interface

Another way of obtaining the velocity is to use an equation that relates flow with velocity from observed data of a similar river. Rivers that are similar may have a similar relationship between velocity and time. This can be done if a quick verification of the data wants to be obtained, but is not recommended.

In general, after obtaining the relationship between velocity and flow, the velocity and flow are plotted versus time (Figure 79 and Figure 80).

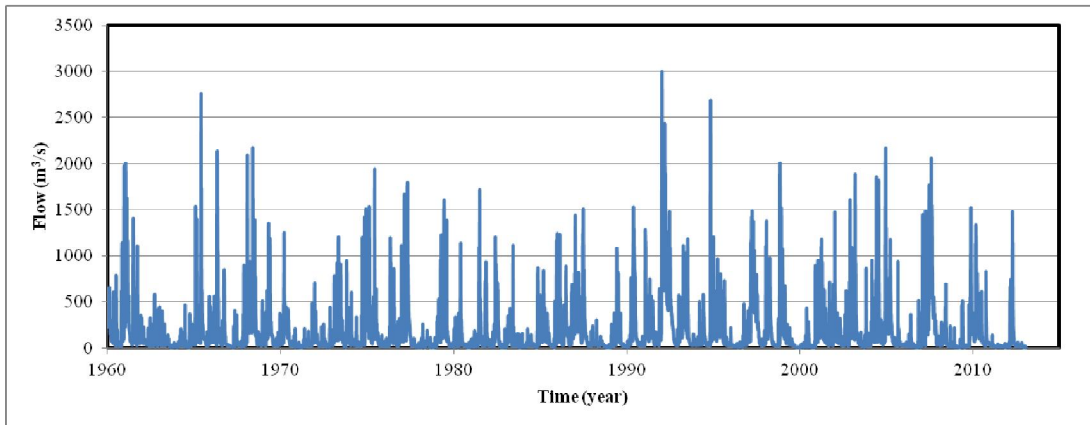


Figure 79. Flow hydrograph

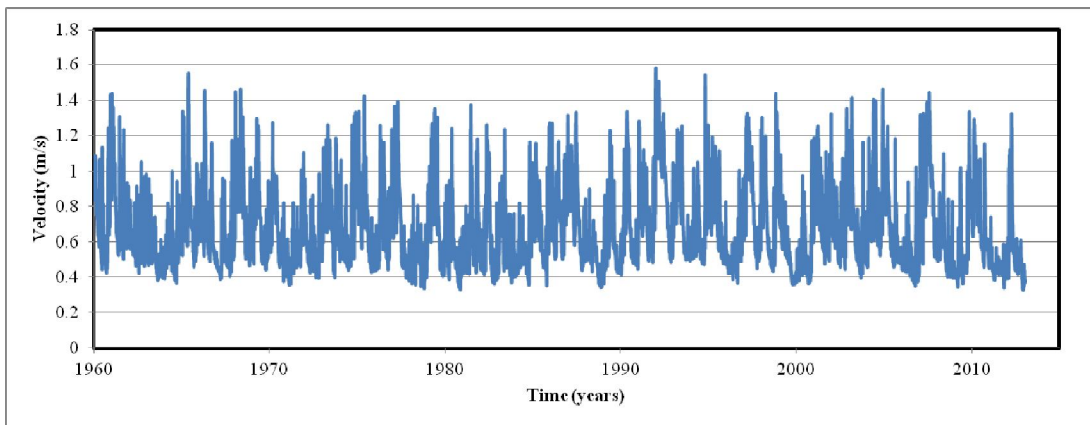


Figure 80. Velocity hydrograph

5.4.3 Generate the EFA Curve

After collecting the soil samples from the field, laboratory testing is necessary to study the erodibility of the soils and their soil classification. The EFA (Figure 81) is used to obtain the erosion function and to classify the soil according to its erodibility. The soil is pushed out of the Shelby tube as it is being eroded. The soil can be classified in one of six categories. If no soil can be tested in the EFA, the engineer can make an assumption of an erosion curve by using the soil classification and its corresponding erosion category.

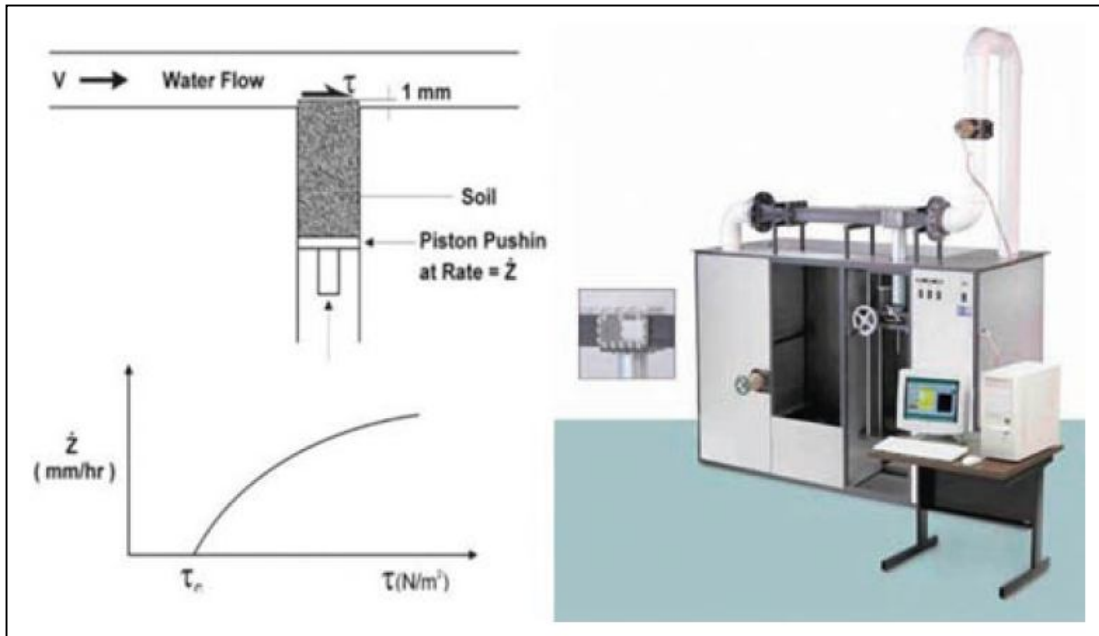


Figure 81. Erosion Function Apparatus setup and test (Briaud, 2007)

Sieve analysis, hydrometer and Atterberg limits tests are used for the classification of soils. Several EFA tests have been performed to obtain the erodibility of the soil of the rivers selected for this project. Not all of the soil samples in the sampling tubes are tested, but only those that represent well the general conditions at each site and where the most critical erosion occurs. Again, the erosion categories according to the soil classification are shown in Figure 82.

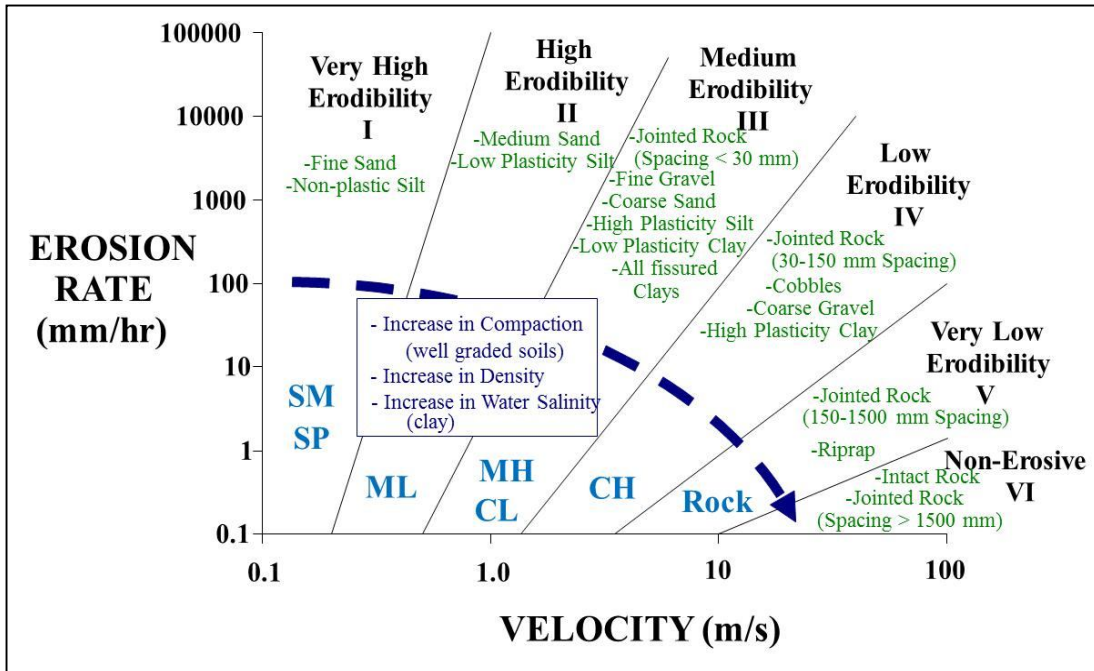


Figure 82. Erosion categories according to soil classification (Briaud, 2013)

The EFA curve, which describes the relationship of the erosion of the soil to the water velocity, is represented as a line in a log-log scale graph. Several readings from an EFA test are used to generate this line. The erosion of the soil sample is measured in millimeters and then these readings are converted to erosion rate in millimeters per hour (mm/hr). A typical EFA curve obtained from the test has erosion in units of millimeters per hour versus the velocity in meters per second (Figure 83). Generally, this kind of test is run to obtain at least 8 points that are used to generate the curve. However, for these samples only between 3 to 6 points could be obtained because of the length of the sample and the erodible material tested.

For the Observation Method, the erosion is first converted from millimeters per hour to meters per second. This information is later used to know how many meters the soil erodes per second because the average flow obtained from the USGS is in meters per second as well. The consistency in the units is very important to calculate the erosion and the critical velocity from the model.

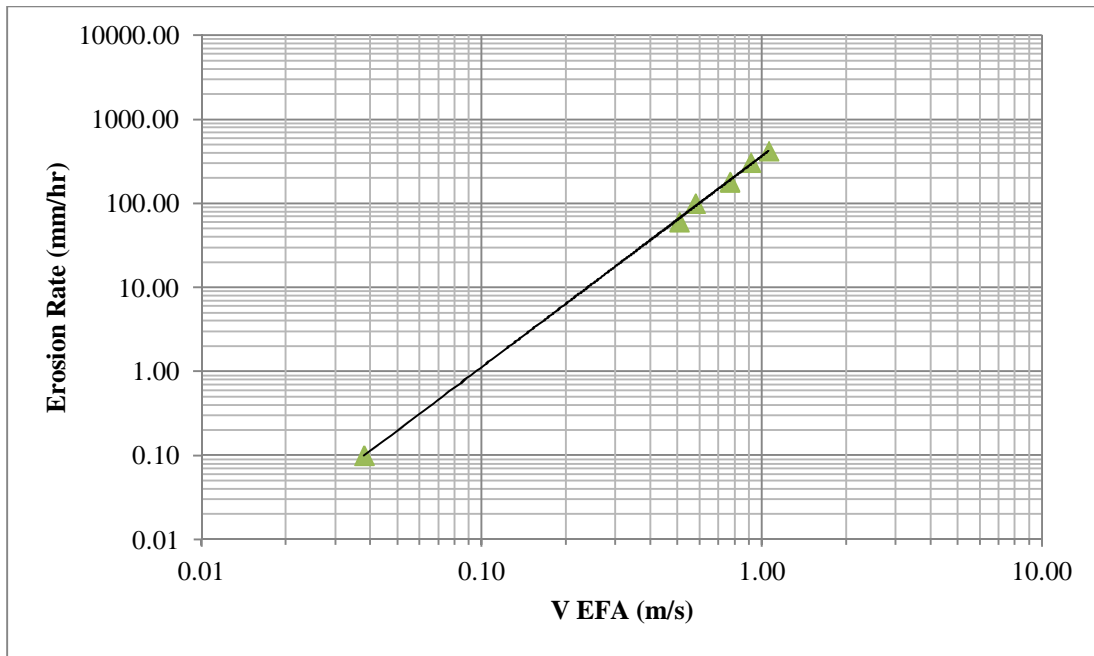


Figure 83. Erosion function with erosion rate in mm/hr and velocity in m/s

A coefficient and an exponent can be obtained from the general equation of an EFA curve, which have been called α and β . A regression line can be obtained using Excel by using the curve fitting option in the graph and both parameters can be seen in the equation of the curve above. The equation for the erosion function is:

$$\dot{z} = \alpha v^\beta$$

Where:

\dot{z} : erosion rate

v : velocity

α and β : parameters.

α is a coefficient and is β an exponent that corresponds to the slope of the line in log-log scale. The α and β are obtained when the units of erosion rate and velocity are both the same. In the case of this project, the units used were in meters per second. Although, the objective of obtaining an equation that could be used with *any* units is the base of the Observation Method. For this reason, the α coefficient is not used, as it changes with a change of units. The slope value of β does not change when both axes have the same units.

Figure 84 shows the classification of the soils and the β exponent that define the divisions between the erosion categories. Using an average line, a line that divides two categories or a user-selected line can be another option if an EFA curve is not obtained or if an EFA test is not performed.

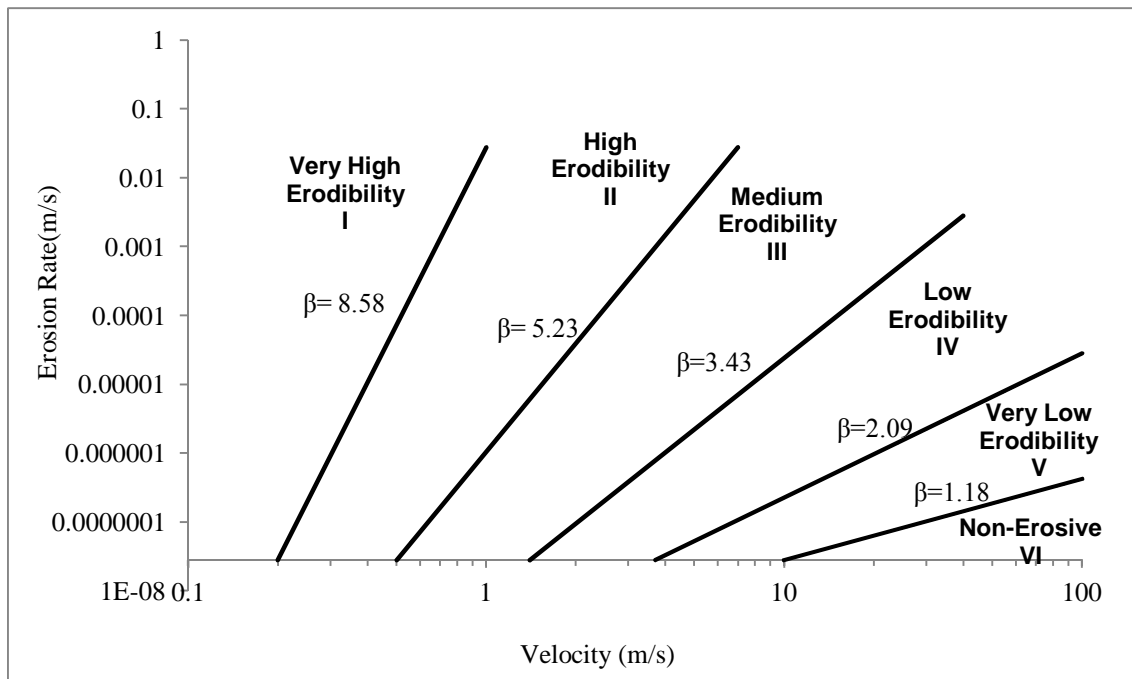


Figure 84. Erosion categories with β values

Sometimes in hydraulics and other fields of science, it is preferred to have the equations with no units on both sides of the equation. The model used in the Observation Method uses the critical velocity, v_c , from the EFA curve to obtain a new equation. Dividing both the erosion rate and the velocity by the critical velocity from the EFA curve, the equation obtained is

$$\frac{\dot{z}}{v_c} = \alpha \left(\frac{v}{v_c} \right)^\beta$$

This equation is the dimensionless EFA curve equation. The critical velocity v_c used in the equation corresponds to an erosion rate of $2.78\text{e-}8$ m/s or 0.1 mm/hr. The α ' coefficient is not the same α coefficient from the EFA curve (which depends on the units

used). To obtain this new parameter, which is dimensionless and does not change with a change of units, the equation used is

$$\alpha' = \frac{\dot{z}_c}{v_{cEFA}}$$

Where:

v_{cEFA} : critical velocity from the EFA curve

\dot{z}_c : erosion rate at critical velocity (typically 2.78e-8 m/s or 0.1 mm/hr)

The critical velocity of the soil sample tested in the EFA can be estimated after performing the erosion test. However, it can be argued that this critical velocity from the sample does not necessarily correspond to the minimum velocity for erosion to occur at the site. It has been proved that shear stresses imposed by small scale testing apparatuses, such as the EFA, can be significantly larger than those stresses observed in the rivers (Perri et al., 2010). There are many factors that could increase the critical velocity at the site such as the vegetation, geometry, compaction, countermeasures, etc.

Also, sometimes the critical velocity cannot be observed during an EFA test and has to be extrapolated. This may result in an inaccurate result. It was found that that the critical velocity occurred at a very low velocity when extrapolating. This is why the critical velocity and the equation used for the Observation Method cannot be applied to each of the velocities obtained from the velocity hydrograph. Erosion occurs at a certain minimum velocity at a site and below that velocity no erosion occurs. The critical velocity at the site must be found.

5.4.4 Observed River Movement

The fourth step of the Observation Method is related to the movement of the river in terms of meander migration or vertical degradation. The movement of the meander can be analyzed with several aerial photographs and/or maps. The aerial photos can be obtained online from different websites or programs such as Google Earth. The aerial photos from Google Earth are limited because it only contains photos from the early 1990s to present time. Other sources have to be used to obtain older photos. Also,

there are databases and libraries that store maps from different years that can be used for this purpose. High resolution photos are always desired and preferred over maps because sometimes the details in topographic maps along the slopes of the river cannot be distinguished as easily as in a photo. However, maps are easier to find than photos for dates from 30 years ago or earlier. The maps and/or photos are overlaid, using the same principle of the extrapolation method by putting together many of them and seeing the progress of the meander migration. Two or more reference points, that have not changed their location, are used to overlay the photos or maps. Different colors or line styles can be used to differentiate the different years in drafting software such as AutoCAD and make a visual comparison of the progress of the erosion. Figure 85 shows an example of the river movement of the Brazos River. The red arrow here is used to show the most critical direction and the movement is then recorded from this reference line.

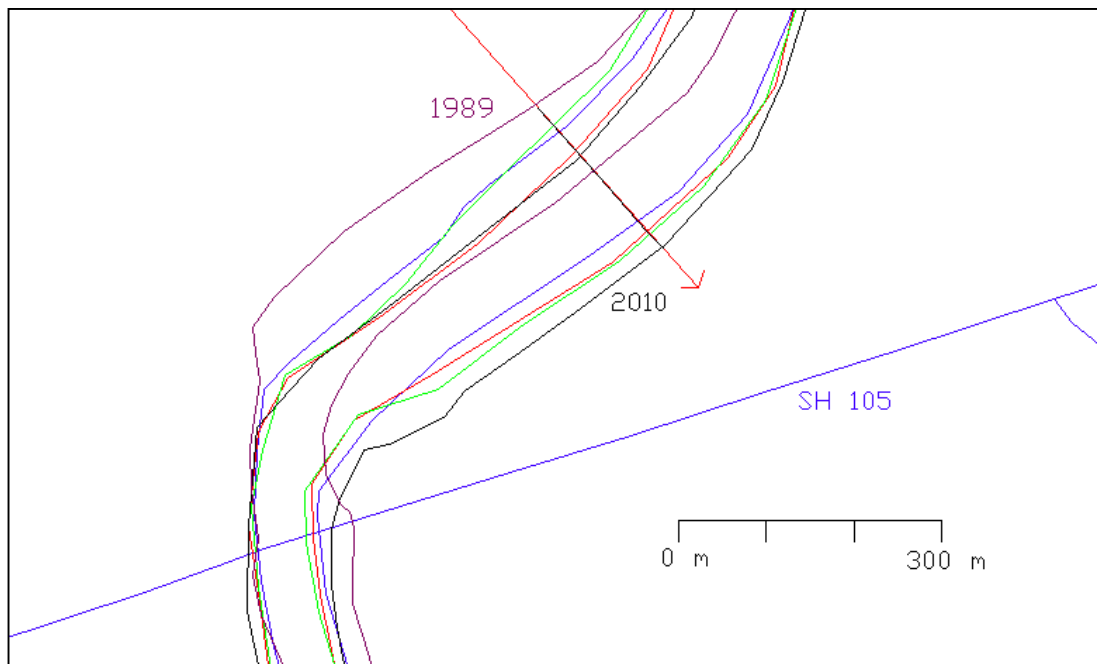


Figure 85. Progress of erosion in Brazos River

A point of reference (or interest) of a meander is used to study its displacement with time. In the case of Figure 85, the red arrow represents the most critical direction of

erosion and a point of reference moves along this direction during the period of years used in the maps. This point could either be in the centerline or in the outer bend of the river. With this information, the movement can be plotted in a graph of the meander position (or displacement) of this point with time.

After obtaining the data of the average daily flow from USGS, only the period between the first and last map, photo or cross section is used. The point of reference is used to represent the movement of a critical area of the meander with time. It would be tempting to estimate the migration rate of the river as the slope of the meander position versus time, but the migration rate is not constant as it was mentioned before. The units of the migration rate are distance over time. Figure 86 shows an example of the magnitude of migration versus time for a certain point.

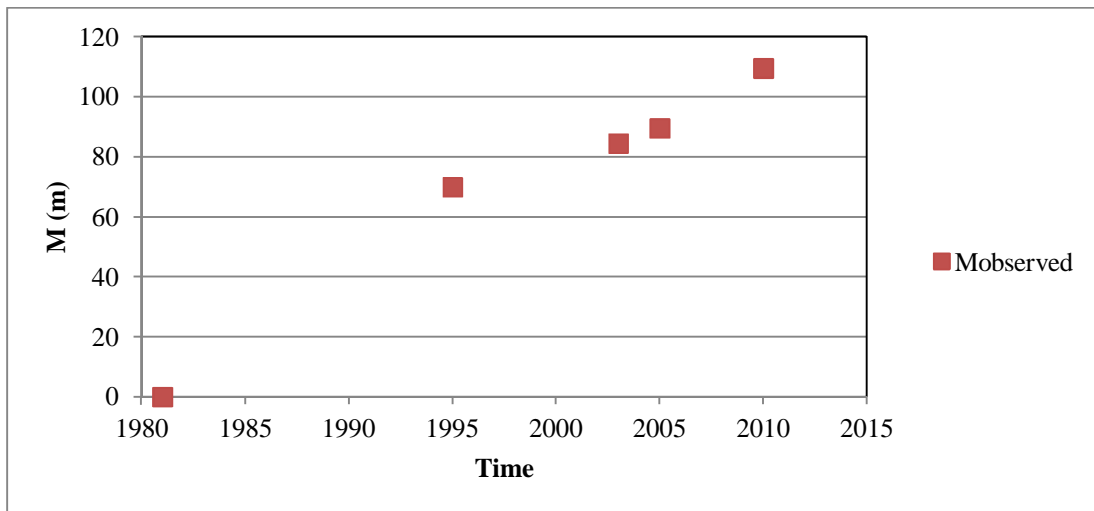


Figure 86. Meander position versus time

5.4.5 Obtain the Critical Velocity by Regression (Calibration Step)

The most important part of this method is to obtain the critical velocity of the river (or site critical velocity). As said before, the critical velocity obtained from the EFA test does not necessarily correspond to the minimum velocity of erosion that occurs at the site. Also, this critical velocity will only correspond to the point along the critical direction mentioned in the previous step.

The critical velocity of the site is used in the equation of the model from the step 3 and it is assumed that the river will not erode below this velocity. To obtain this velocity, a code was written in MATLAB and Excel using the equation of the model. The input data used in the code are:

- the β exponent from the erosion function of the soil at the site, which corresponds to the slope of the curve
- the average velocities (in meters per second) for the period that is being considered and the time (in years) corresponding to each day
- the observed data, which is the movement of the point from the meander position or bottom of the river when vertical degradation occurs. The initial value for river position can be 0 or other depending on the reference used. The precision of the critical velocity will increase when more data is accumulated from different maps or photos.

The code calculates the migration in meters as a function of time over the duration of the hydrograph by using β values from the EFA results but for a chosen range of trial and error critical velocities (v_c). The α' coefficient is calculated every time the program uses a different critical velocity. Every time a new erosion function with slope β is generated, the original erosion function is displaced and the α' has to be calculated because it is obtained by dividing the erosion rate at critical velocity (\dot{z}_c) by the critical velocity (v_c). The EFA curve maintains the slope, but the α' coefficient changes every time the critical velocity changes on each iteration.

The step where the critical velocity and the α' coefficient are found is called the calibration step. During the calibration step, the magnitude of migration or degradation (M) is estimated for each day by using the velocity assigned for each day from the hydrograph. The velocity data and each day (each day in units of years) are imported and then the code iterates multiple times (in the case of MATLAB), using the range of critical velocities. The user selects the velocities manually if using a spreadsheet. This range can be between the minimum and the maximum velocity found in the velocity hydrograph for the river being studied. The equation used to find the daily erosion and

the progress of the movement of the point of reference in the river is based on the dimensionless EFA curve model equation from step III.

$$M = \alpha' \left(\frac{v}{v_c} \right)^\beta \times v_c \times \Delta t$$

where Δt is in days. This equation is obtained by multiplying the model equation by time and critical velocity on both sides of the equation. The increment of each step for the calculation of M is one day or 86400 seconds. Erosion will only occur when the ratio $v/v_c \geq 1$ or $v \geq v_c$.

The results obtained from the previous equation are the same as those that would be obtained from the original equation

$$\dot{z} = \frac{M}{\Delta t} = \alpha v^\beta$$

that after multiplying both sides by the Δt ,

$$M = \alpha v^\beta \times \Delta t$$

where M is in units of length, as well. Because of the correspondence between both equations (one without any units and the other one with units), both model equations can be used to predict the meander migration. However, the method was developed to use the dimensionless EFA curve in order to be able to use velocities and measurements in both SI and English units. The α coefficient changes when the units are changed, but the α' coefficient can be used with any units when using the dimensionless EFA equation. The slope of both equations in log-log scale is the same, thus the β does not change.

The code compares the magnitude M with the observed data for each critical velocity from the range. If only five points were obtained from the maps, the code will only compare the migration estimated with the model for the last four points. The precision of this method is improved with the quantity of observed data (Figure 87).

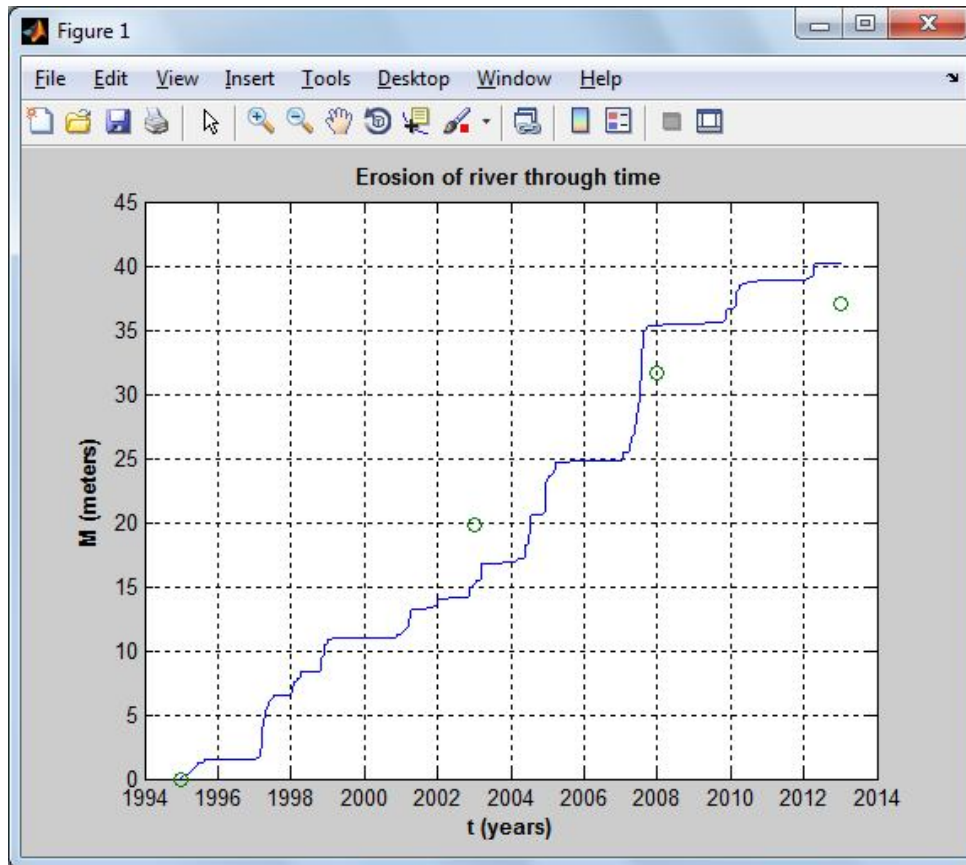


Figure 87. Observed data (green) and predicted data (blue)

The program (in MATLAB) runs until the difference between the points of observed data and the points generated is the smallest for a certain date. The method used to minimize the difference is by obtaining a Ranking Index (RI). The precision of the points is better when the RI is the smallest that it can be (Briaud and Tucker, 1988). The RI is calculated with the following equation

$$RI = |\mu(a)| + \sigma(a)$$

Where:

μ : mean value

σ : standard deviation

a : ratio of the calibration or generated value of meander position over the observed (M_c/M_o).

After finding the smallest RI for a selected range of velocities, the critical velocity is obtained, and the meander position is generated versus time. Figure 88 shows a sample of how the code looks in MATLAB and the iteration process used.

```

for i=1:length(vec)
a=zdotc/vec(i);
    for j=1:length(t)

        if (v(j)/vec(i))>1
            M(j)=a*((v(j)/vec(i))^B)*vec(i)*deltat;
        else
            M(j)=0;
        end

        Ma(1)=M(1);
    end

    for j=2:length(t)

        Ma(j)=Ma(j-1)+M(j);

    end

td(1,:)=[t(1),Ma(1)];

for k=1:(length(t0)-1);

    td(k+1,:)=[t(t0(k+1)*365-t0(1)*365),Ma(t0(k+1)*365-t0(1)*365)];
end

Mcp=[td(:,2)];
Mco=[tomo(:,2)];

```

Figure 88. Sample of code in MATLAB

Figure 89 shows the progress of the erosion of the river when plotted with time. The line shows the position of the river from the reference direction selected in step IV. As seen, the river position can be stable and sudden big jumps may occur. This happens when a big flood occurs for consecutive days and the velocity of the river increases abruptly. This proves that big changes occur at rivers when big floods occur. In a matter of 24 or 48 hours, the river can even move from 5 to 20 meters when large volume of

water during a flood (and the high velocities that come with) washes away the soil from the banks of the river.

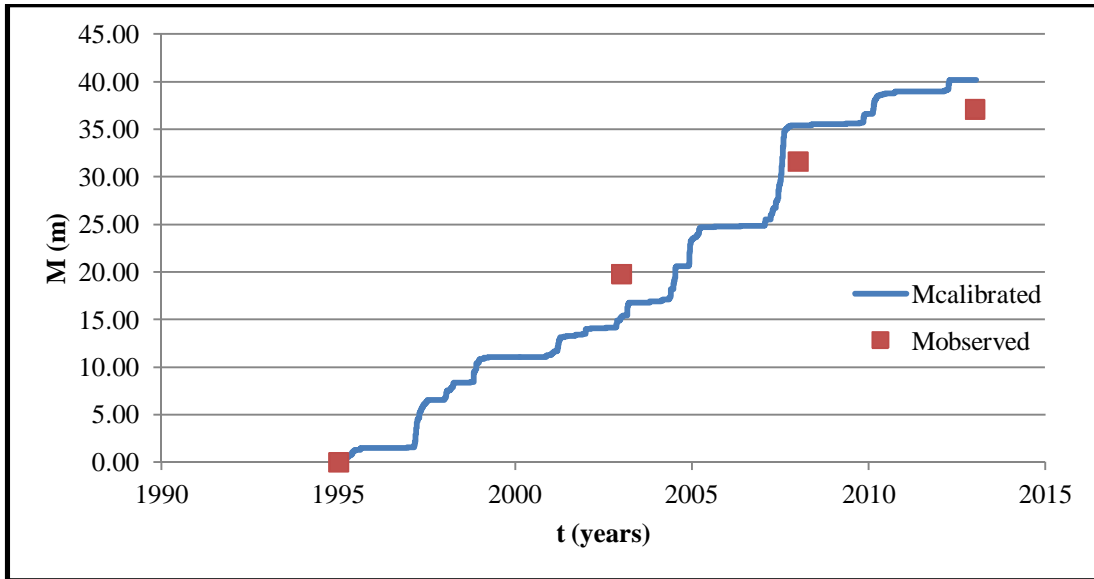


Figure 89. Estimated erosion progress with time

The calibrated values and the observed values can be compared to see how different they are. A fitted line can be drawn in a graph of M_c versus M_o (Figure 90).

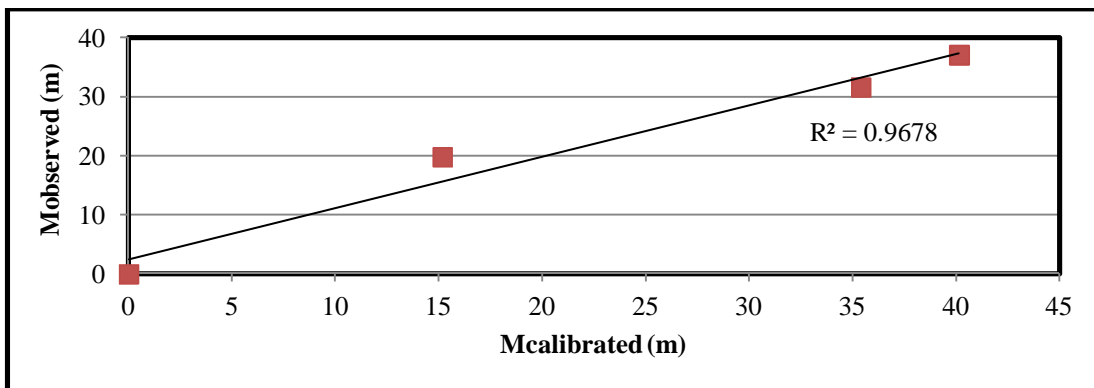


Figure 90. Observed data versus calibrated data

5.4.6 Use the Model to Predict Meander Migration (Prediction Step)

The program (or the user) stops the iterating process when the critical velocity is found with the smallest RI. This is the end of the calibration step. This critical velocity and its corresponding alpha prime coefficient are then used on the next step to predict the position of the meander or the vertical degradation in the future by using either a full hydrograph or a single value of velocity. After generating the data from the calibration step and using the critical velocity, a prediction of the meander can be performed by using velocities that could occur in the future. As expected, big floods are responsible for big changes in the meander position. Using a user generated hydrograph of velocities or repeating the recent data, the position of the meander can be calculated and an approximation can be obtained.

Also, the calibration step approach could be used to verify the model. For example if data between 1990 and 2000 is used, the critical velocity can be obtained from the back calculation process and then used to estimate the position of the river after the year 2000. Then, the hydrograph for the period between 2000 and 2010 can be used with the critical velocity to estimate the position of the river in the year 2010. Because this also is a date from the past, the observed data from 2010 can be compared with the estimated position of the river for the 2010. The model can be verified and it can be seen how precise the approximation of the data used was if done this way. Examples of this verification step can be seen in Section 6.6.

CHAPTER VI OBSERVATION METHOD

6.1 INTRODUCTION

The Observation Method is used to be able to find the critical velocity in the field and determine the erosion in function of the river velocity. As said before, the Observation Method is based on observed data. It is important to generate the history of the movement of the river. Based on the principles explained on the previous chapter, a step-by-step example is explained in this chapter using the two codes developed in this project. One code was written in MATLAB and the other one in Visual Basic for Applications for Microsoft Excel. The Brazos River case is used as an example.

6.2 GENERAL STEPS

The following steps are performed first before using either the MATLAB code or the Excel spreadsheet. The Excel spreadsheet is used for the erosion function results, even if MATLAB is used later to perform the calibration and prediction steps. The colors of the boxes in Excel (Table 5) are used not only to distinguish the input from the output, but also from calculations and others. The yellow cells with blue font correspond to input. The blue cells with red font correspond to output. The white boxes with green font are used for calculations and automatic counting and should not be edited. The orange cells indicate that the selection of a range of cells has to be modified for the calculations to work. These cells are also output values.

Table 5. Colored cells in Excel for input, output and more

INPUT
OUTPUT
CALCULATIONS, ETC.
MODIFY RANGE (OUTPUT)

1. Select a river and find the nearest USGS station.
 - a. The USGS contains information of stations that measure the average daily flow in the United States at http://waterdata.usgs.gov/nwis/dv/?referred_module=sw. Select here by State/Location and then select Texas (Figure 91).

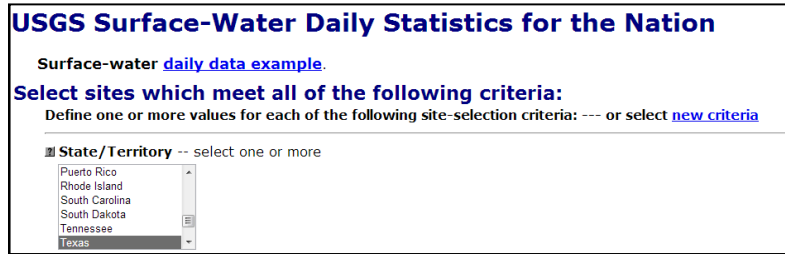


Figure 91. USGS website for average daily flow at each state

- b. A list of all the gage stations and their locations show up. Select the gage station that corresponds to the river. Most of these bridge locations have a gage station nearby. Data from a gage station nearby is used when there is no gage station at the location. If there is insufficient data but there is a gage at the site (gage station not working anymore or only recent data is available), a gage station from upstream or downstream from the same river has to be used to complete the hydrograph. This happens for the Brazos River. For this case, the closest gage stations corresponding to the Brazos River for this case are 8110200 and 8111500. The 8110200 is at the location, but it was operating only in the 1970s and 1980s. The 8111500 station is located downstream in Hempstead, TX. An estimation of the flow can be obtained if the drainage area at the gage stations is known. The following formula can be used to estimate the flow when data at the gage station of the bridge is missing.

$$Q_2 = Q_1 \frac{A_2}{A_1}$$

Where Q is flow and A is the drainage area, which can also be obtained from the USGS data. In this case, Q_2 corresponds to the unknown data and Q_1 to the known. The USGS provides the drainage area at the gage station, but if there are no gage stations, then the drainage area has to be estimated using other methods. Geographic Information Systems (GIS) can be used to get the drainage area at a point of interest.

- c. After selecting the gage station, select at the top Time-Series: Daily Data (Figure 92). Also a Map of the location of the gage is available here.

USGS Surface-Water Daily Statistics for the Nation
 USGS 08108700 Brazos Rv at SH 21 nr Bryan, TX

Available data for this site Time-series: Daily data GO

Site Selection
 Select sites which meet all of the following criteria: ---- or select [new criteria](#)

Check one or more boxes to select sites/parameters for further display--below

USGS 08108700 Brazos Rv at SH 21 nr Bryan, TX					
	Parameter Code	Parameter Name	Period of Approved Daily-Mean Data		Count
			From	To	
<input type="checkbox"/>	00060	Discharge, cubic feet per second	1993-07-14	2013-04-24	7225
<input type="checkbox"/>	00065	Gage height, feet	1993-07-15	2013-04-24	5882

Figure 92. USGS gage selection

- d. Select Discharge under Available Parameters, Tab-separated under Output Format and set the Date Range (Figure 93). Click Go and the Data should show up. Click File > Save As... and save the information in a text file. Open the text file from Microsoft Excel to view the information.

Figure 93. USGS parameters

- e. Convert all the dates from the column of time in years. To do this, you have to remember that every day is 1/365 years (approximately, one day is 0.0027 years). The code does not recognize the format of the dates and they have to be converted to a number. Table 6 shows example of the format of the each date.

Table 6. Example of format for time in years to use in both MATLAB and Excel

Time (Days)	Time (Year)	Gauge Station	Date
1	1960.00274	8109000	1/1/1960
2	1960.005479	8109000	1/2/1960
3	1960.008219	8109000	1/3/1960
4	1960.010959	8109000	1/4/1960
5	1960.013699	8109000	1/5/1960
6	1960.016438	8109000	1/6/1960
7	1960.019178	8109000	1/7/1960
8	1960.021918	8109000	1/8/1960
9	1960.024658	8109000	1/9/1960

- f. Plot the flow hydrograph, as in Figure 94, to get a better understanding of the river flow in flow versus time format and select the time range that will be used.

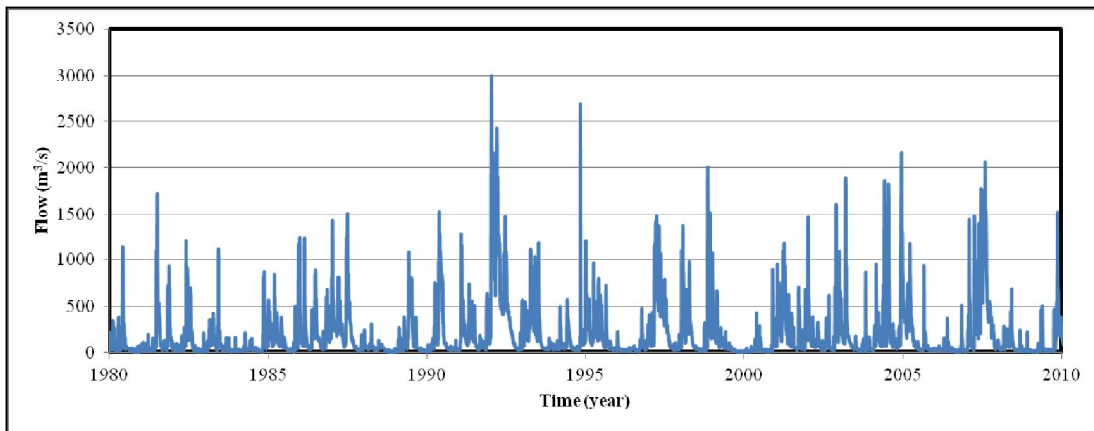


Figure 94. Flow hydrograph for a selected period

2. Convert the flow hydrograph to velocity hydrograph.
 - a. As explained in section 5.4, the flow hydrograph has to be converted to velocity using one of the following methods:
 - i. TAMU-FLOW: This software is available online, free of cost at: https://ceprofs.tamu.edu/briaud/research_wip.html
An easy, step-by-step instruction manual is included with the software. Velocity is obtained from one cross section of the river.
 - ii. HEC-RAS: This software is available online, free of cost at: <http://www.hec.usace.army.mil/software/hec-ras/>
 - iii. Other similar software or using an equation to convert from flow to velocity from a similar river.
 - b. The flow is converted to velocity (in m/s) and the dates are reduced to the range of interest (Figure 95).

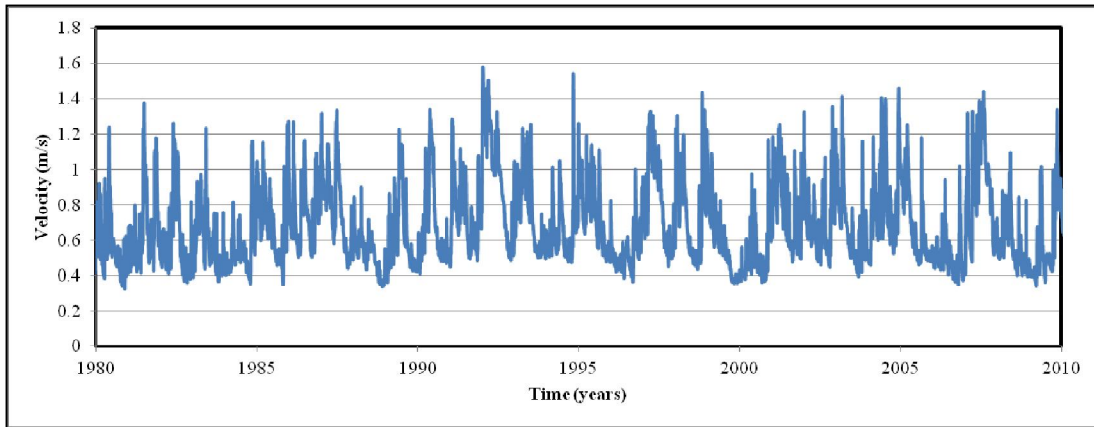


Figure 95. Velocity hydrograph for the selected period

3. Generate the EFA curve and obtain the β parameters.
 - a. There are two options to generate the EFA curve that will be used in the model to obtain the critical velocity: using a line from the Erosion Categories or using the results of an EFA test. Both methods can also be used to compare results and a sheet is included to obtain the parameters for each method in the Excel file.
 - b. The first sheet in the Excel file corresponds to the Erosion Categories (Figure 96). The input values in this sheet are the critical velocity corresponding to an erosion rate of 0.1 mm/hr or $2.78e-8$ m/s, and a higher velocity (upper bound velocity) to create a line. An erosion rate that corresponds to this velocity is selected as well and the line is generated in both graphs. The slope of this EFA curve needs to be compared to the other 5 lines to see where this generated line is. Also, a table with the five lines that divide the categories is included. These lines can also be used. The β parameters are automatically calculated.

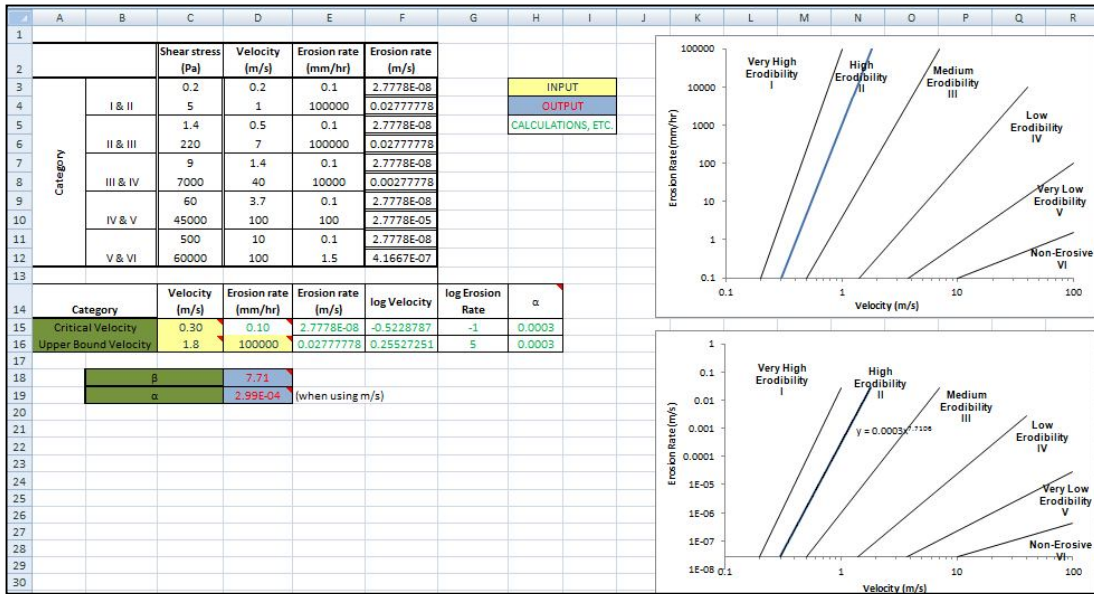


Figure 96. Erosion function categories spreadsheet

- c. The second sheet in the Excel file is used to obtain the β parameter with the EFA test results (Figure 97). The results of the EFA test are entered in the columns of velocity in meters per second and erosion rate in millimeters per hour. The Excel sheet obtains the critical velocity by extrapolation and calculates the β parameter automatically.

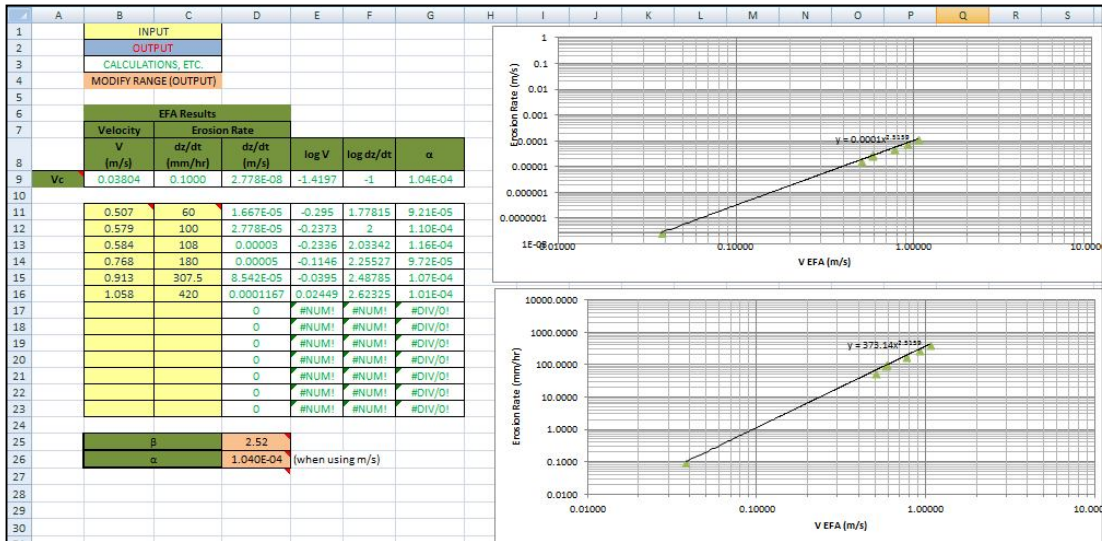


Figure 97. Erosion function results and parameters

4. Use the observed data to obtain the maximum movement of the river.
 - a. Use the overlay technique to prepare a sequence of maps and/or aerial photos to study the meander migration or use different cross-sections of the river at the bridge location for vertical degradation. Recent aerial photos (from 1990 to present) can be accessed with Google Earth. Older photos and maps can be found online or from other sources.
 - b. For the meander migration case, draw a line to obtain the movement of the point along the line through time. This point is a point of interest or a critical point (or direction). Using a program such as AutoCAD for meander migration can be convenient. This technique can also be done by hand.
 - c. Prepare a table as Table 7, with the years of the observations and the movement of the river in units of distance (the units have to be consistent with the units of daily average velocity).

Table 7. Observed data in a table

Time (years)	Mo (m)
1995	0
2003	19.8
2008	31.6
2013	37.1

6.3 USE OF EXCEL SPREADSHEET

After performing the previous steps, the critical velocity of the river at the field needs to be found. This step is called the calibration step. The calibration step to find the critical velocity can be done using the Excel file or the MATLAB code. Only the Excel file can be used for the prediction step (after finding the critical velocity). This section explains the use of the Excel file for the calculation of the critical velocity.

1. Enter the erosion rate at critical velocity \dot{z}_c , β exponent, delta t (Δt), and the initial position of the river in the space provided (Table 8). The erosion rate at critical velocity is $2.78\text{e-}8$ m/s or 0.1 mm/hr. This has to be consistent with the units used for daily velocities. The β parameter is obtained from the previous section, and the delta t is the increments in time between each velocity. Because the velocity data is in meters per second and there is only one average velocity per day, the delta t is 86400 seconds (seconds in one day). This assumes that the velocity is constant for every second of the day. The initial position of the river is always 0, unless a different reference as starting position is used for the point of interest.

Table 8. Erosion function parameters and increment in time

I.	Erosion function parameters	
	\dot{z}_c (m/s)	2.78E-08
	β (no units)	8.58
	delta t (s)	86400
	Initial Position of River	0

- Enter the daily average velocity, the date in year format and the date in the format provided by the USGS (Table 9). The M column is the daily erosion and M_c (or $M_{\text{calibration}}$) is the total accumulated erosion. Both are automatically calculated and generated after step 4.

Table 9. Velocity hydrograph input and output of movement

II.	Velocity Hydrograph Input					
	Total Number of Readings (Days)			6585	M (m)	Mc (m)
	Day Number	Time (Date)	Time (years)	Velocity (m/s)		0
	1		1995	1.02994537	0.0153	0.0153
	2		1995.00274	1.014652403	0.0135	0.0288
	3		1995.005479	0.986100558	0.0105	0.0393
	4		1995.008219	0.95483608	0.0080	0.0473
	5		1995.010959	0.921909847	0.0059	0.0532
	6		1995.013699	0.88108341	0.0040	0.0572
	7		1995.016438	0.860490583	0.0033	0.0605
	8		1995.019178	0.896578111	0.0047	0.0651
	9		1995.021918	1.018540372	0.0139	0.0791
	10		1995.024658	1.071049067	0.0214	0.1005

- Enter the observed data from the meander migration or vertical degradation (Table 10). A column for time and position of the river is provided. The time and position of the river have to be all consistent with the data entered in the previous two steps.

Table 10. Observed data

III.	Comparison of Observed Data and Calibrated Data			
		Number of Data Points		4
	Time (years)	Mo (m)	Time (years)	Mc(m)
	1995	0	0	0.000
	2003	19.8	0	0.000
	2008	31.6	0	0.000
	2013	37.1	0	0.000

4. Enter the first critical velocity to evaluate (Table 11). Start with a low velocity and click the run button. Modify the range of values that have valid numbers for the mean and standard deviation values of the RI (orange cells in Excel). The Ranking Index will be calculated based on this velocity. The method will be more precise as this Ranking Index approximates to zero. The α' coefficient is automatically calculated for every critical velocity used. A graph on the right is generated (Figure 98) and the position of the river M_c can be compared with the observed data M_o (Table 12). Use a larger velocity and run again. The Ranking Index and the α' coefficient will be different. Increase and decrease the critical velocity until it has the smallest possible RI. This critical velocity is the optimum critical velocity and is used, along with the α' parameter, in the prediction step.

Table 11. Critical velocity and ranking index

IV.	v_c	0.83	m/s	Run!
	Ranking Index (RI)	0.2342889		
	Mean for RI	0.024552693		
	Strd Deviation for RI	0.209736159		
	α' (no units)	3.35E-08		

Table 12. Calibrated data output

III. Comparison of Observed Data and Calibrated Data				
		Number of Data Points		4
Time (years)	M_o (m)	Time (years)	M_c (m)	$\ln(M_c/M_o)$
1995	0	1995	0.015	#DIV/0!
2003	19.8	2002.99726	15.177	-0.265919797
2008	31.6	2007.99726	35.392	0.113326705
2013	37.1	2012.99726	40.147	0.078935013

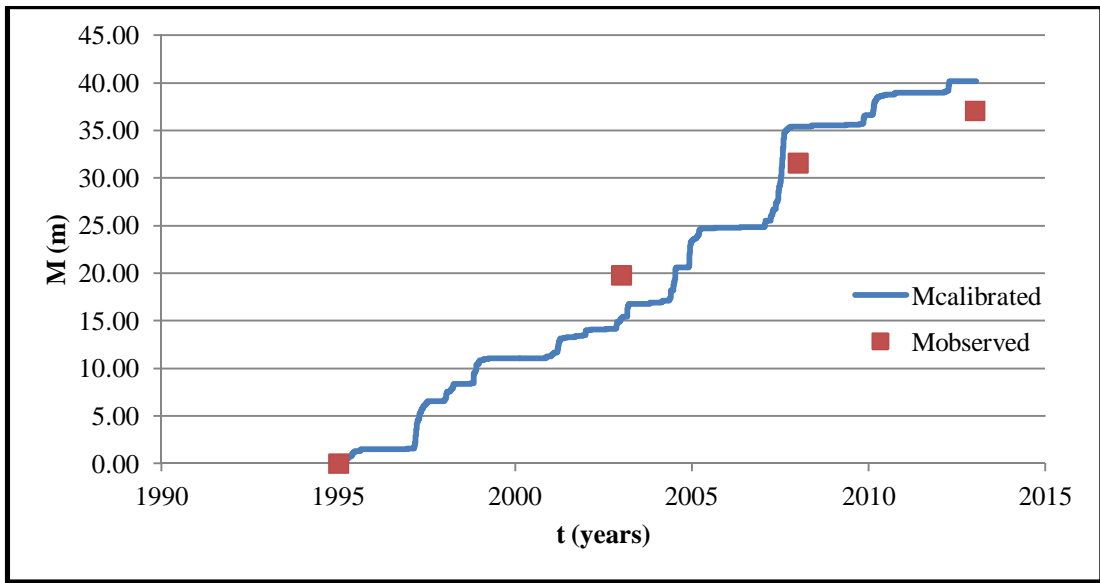
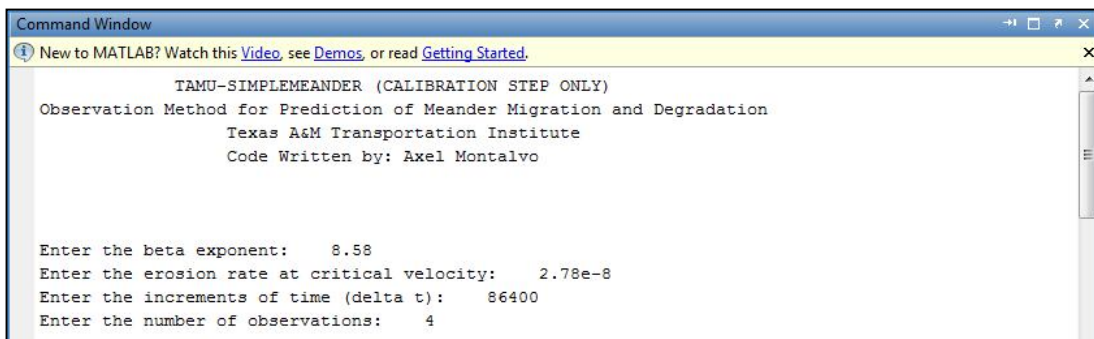


Figure 98. Observed and calibrated data

6.4 USE OF MATLAB CODE

The MATLAB code written for this project is an alternative to the Excel File. If this method is used, the section 6.3 can be skipped. If the Excel file is used, this section can be ignored. However, both methods yield the same results and can be used for verification. The advantage of this method is that the MATLAB code iterates and calculates everything without the iterating process of step 4 from the previous section. The disadvantage of this method is that it is not as visual as Excel, where data can be manipulated more easily. The MATLAB file comes with blank velocity.txt and time.txt files.

1. Copy the velocity column to the text file velocity.txt.
2. Copy the dates in year format to the text file time.txt.
3. Run the program and follow the instructions to enter the data (Figure 99).
4. Enter the β exponent (beta exponent) and press Enter.
5. Enter the erosion rate at critical velocity, z_c .
6. Enter the increments of time or delta t (86400) and press Enter.
7. Enter the total number of observations. In the case of the Brazos River, the number of observations is 4.



```
Command Window
New to MATLAB? Watch this Video, see Demos, or read Getting Started.

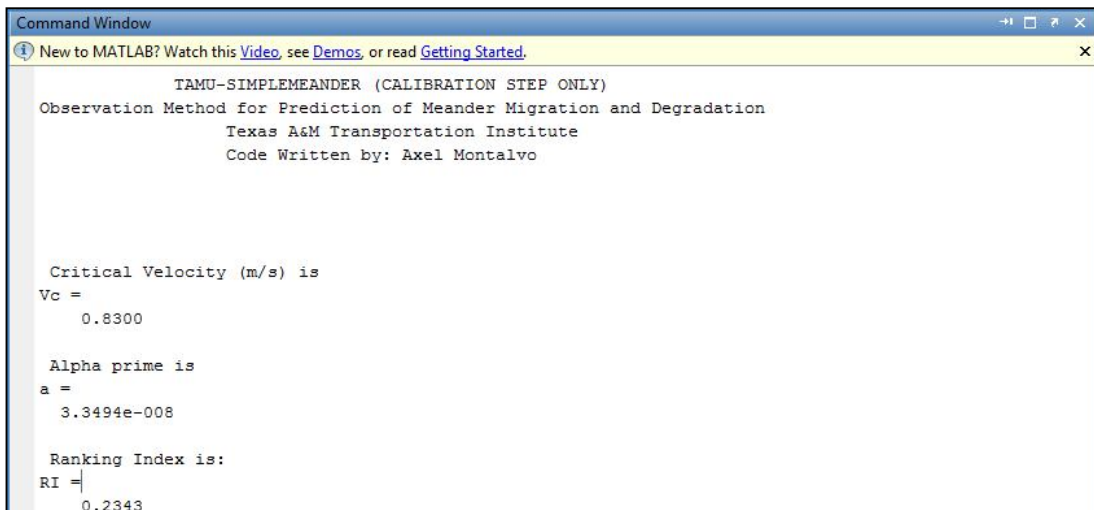
TAMU-SIMPLEMEANDER (CALIBRATION STEP ONLY)
Observation Method for Prediction of Meander Migration and Degradation
Texas A&M Transportation Institute
Code Written by: Axel Montalvo

Enter the beta exponent:      8.58
Enter the erosion rate at critical velocity:  2.78e-8
Enter the increments of time (delta t):      86400
Enter the number of observations:      4
```

Figure 99. Input of erosion parameters, time increments and number of observations

8. Enter the year of the first observation and press Enter.
9. Enter the position of the river at this year, which is 0, and press Enter.

10. The program will ask for the second year and the position of the river for that year. Enter the data and press enter. The program will keep asking for the data until it reaches the total number of observations.
11. The program shows the lowest Ranking Index and the corresponding critical velocity and alpha prime coefficient found (Figure 100). The two parameters are used in the prediction step (prediction step is available only in Excel).



```
Command Window
New to MATLAB? Watch this Video, see Demos, or read Getting Started.

TAMU-SIMPLEMEANDER (CALIBRATION STEP ONLY)
Observation Method for Prediction of Meander Migration and Degradation
Texas A&M Transportation Institute
Code Written by: Axel Montalvo

Critical Velocity (m/s) is
Vc =
    0.8300

Alpha prime is
a =
    3.3494e-008

Ranking Index is:
RI =
    0.2343
```

Figure 100. Results of critical velocity and ranking index

12. The program shows 4 figures: position of the river through time with the observed data (Figure 101); the dimensionless EFA curve (Figure 102); the velocity hydrograph (Figure 103); and the observed versus predicted data compared to a 1:1 line (Figure 104).

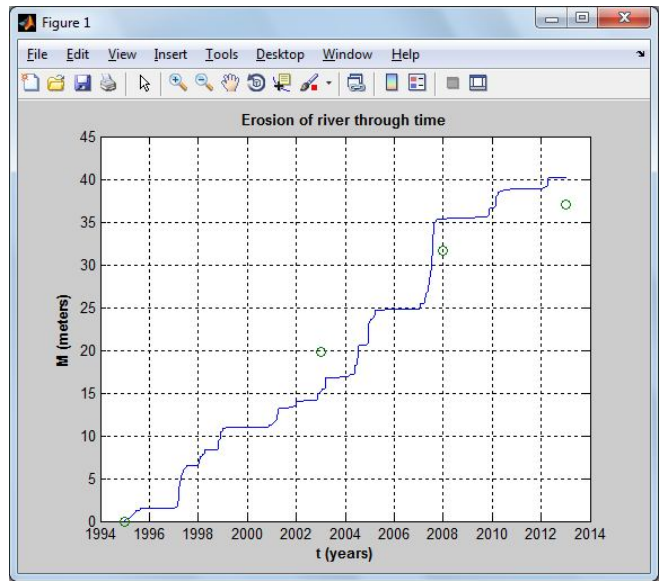


Figure 101. Movement of point with time

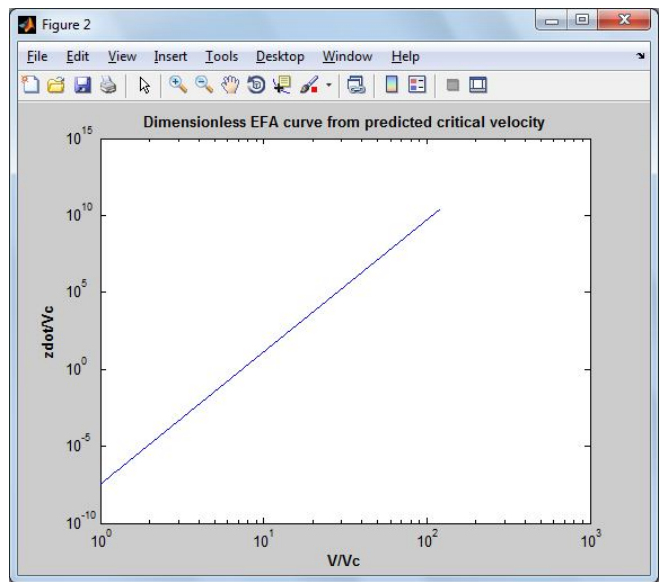


Figure 102. Dimensionless EFA curve

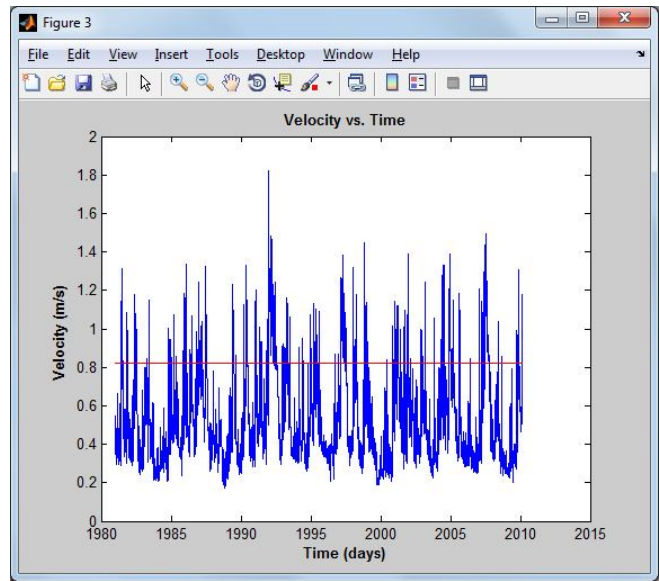


Figure 103. Velocity hydrograph and critical velocity

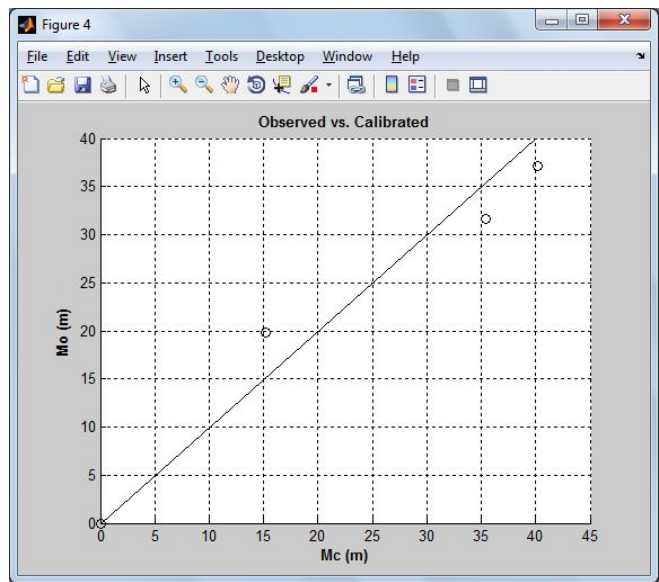


Figure 104. 1:1 slope line with results of observed data vs. calibrated data

6.5 PREDICTION STEP

After obtaining the parameters α' , β , and critical velocity, the next step is to use the same model of erosion to make a prediction of the meander migration or vertical degradation. Only the Excel spreadsheet can be used for this step, even if MATLAB was used to obtain the critical velocity. The sheet used for the prediction step looks very similar to the sheet used in Section 6.3. It also works in a similar fashion, but now the iteration process is not necessary because the critical velocity has already been found. The following steps describe the process of the prediction step.

1. In the input boxes (Table 13), enter the α' and β parameters, the increment in time delta t, the critical velocity obtained from the calibration step and the initial position of the point. Because it is a prediction, the last observed data can be used or it can be 0 instead. It is recommended to use 0 for simplification.

Table 13. Input data for prediction step

I.	Erosion function parameters	
	α'	3.35E-08
	β	8.58
	delta t	86400
	v_c	0.83
	Initial Position of River	0

s
m/s
m

2. There are two options to enter the velocity data: use a complete hydrograph or just a few velocities (Table 14). For this project (Chapter VII), the data that was used was from the last 10 years and was repeated to predict the movement of the point, starting from the last observed data point. If the last data observed was (for example) from 2010, and the velocities used are from 2000 to 2010, the dates have to be changed to correspond to the period that will be extrapolated, if the data was copied from the previous period (the dates are changed to 2010 to 2020). The spreadsheet also lets you use a few velocities, like for example, if only one or two velocities need to be evaluated (24 or 48-hour flood).

Table 14. Input of velocity hydrograph for prediction step

II.	Velocity Hydrograph Input		
	Number of Readings (Days)		3653
Day Number	Time (Date)	Time (years)	Velocity (m/s)
1		2013	0.905869735
2		2013.00274	0.907694233
3		2013.005479	0.896578111
4		2013.008219	0.892779432
5		2013.010959	1.032429161
6		2013.013699	1.04815386
7		2013.016438	1.08411278
8		2013.019178	1.06433434
9		2013.021918	1.013346452
10		2013.024658	0.9579475

- The figure obtained represents the magnitude of the movement for the period of time designated after the last observation. In this example, the period is 2013 to 2023 (Figure 105). M corresponds to the predicted data.

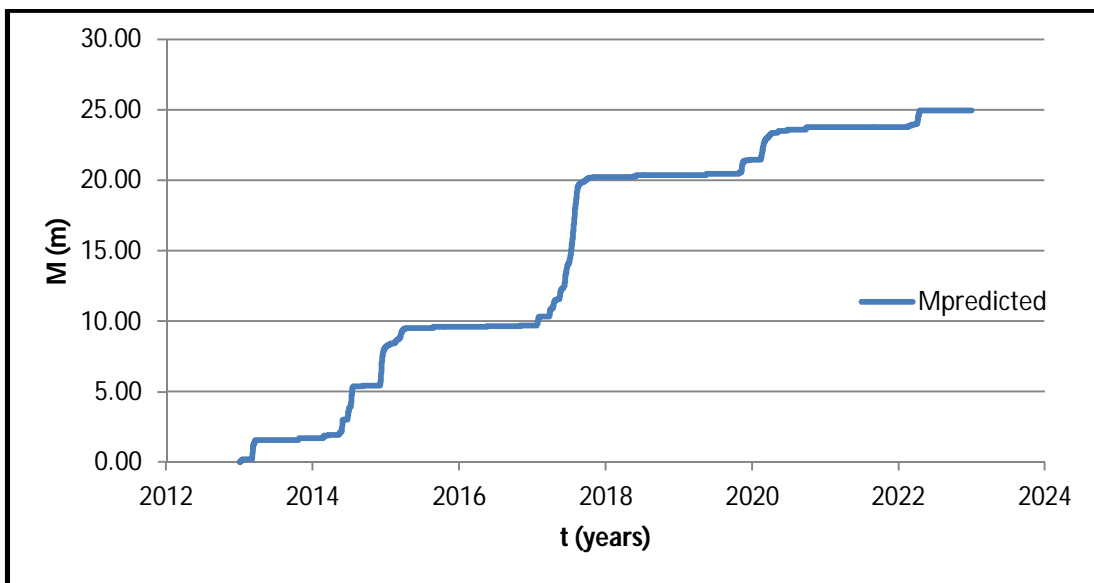


Figure 105. Predicted data versus time

6.6 VERIFICATION OF THE OBSERVATION METHOD

It is very important to verify the results of a mathematical model when it is used to compare predicted data versus observed data. In the previous step, the critical velocity is used to make a prediction of the position of the river in the future by using the same equation and the same parameters. One way to study the effectiveness of the Observation Method is to obtain the critical velocity by calibration and then make a prediction, but with knowledge of the real position of the river. For example, if data is known from 1990 to 2005, with four points of observation in 1990, 1995, 2000 and 2005, the calibration step can be used to obtain the critical velocity between 1990 and 2000. Using this velocity and the real hydrograph between 2000 and 2005, the position of the river can be predicted for 2005 and then compared with the observed data of 2005.

Figure 106 through Figure 109 correspond to several runs of the Observation Method that were performed for verification of the method and used to observe the predicted data versus the observed data. The dots in the figures are known values of observed data and the predicted line was obtained using the field critical velocity found in the calibration step with of all the observed data minus the last one. This verification step was performed for the Brazos, Trinity, Sabine and Nueces Rivers. The other two rivers, North Sulfur and Colorado, only had two points and this verification step could not be applied.

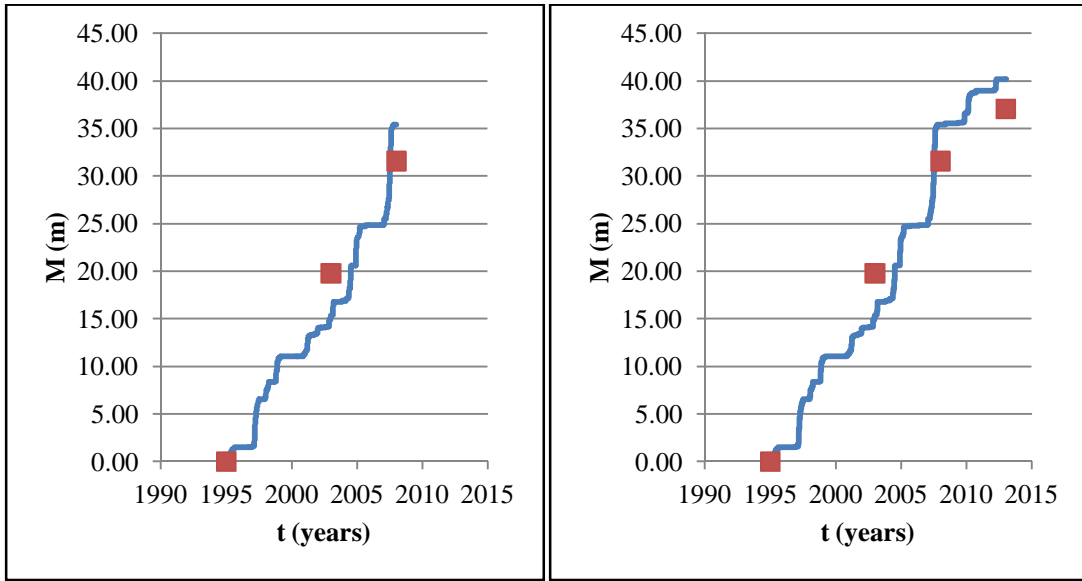


Figure 106. Brazos River verification of prediction with field critical velocity of 0.83 m/s

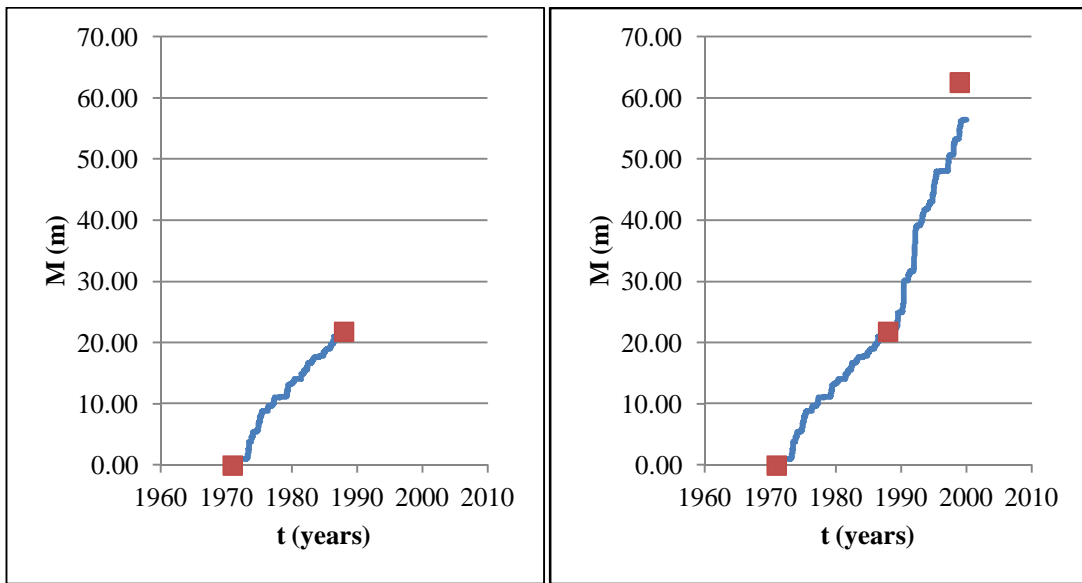


Figure 107. Trinity River verification of prediction with field critical velocity of 0.77 m/s

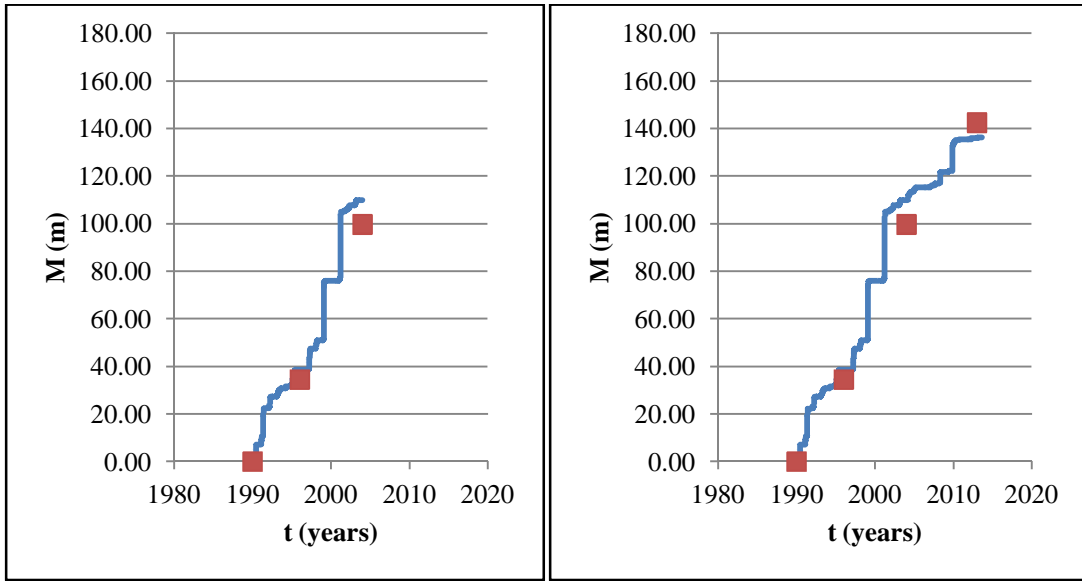


Figure 108. Sabine River verification of prediction with field critical velocity of 0.91 m/s

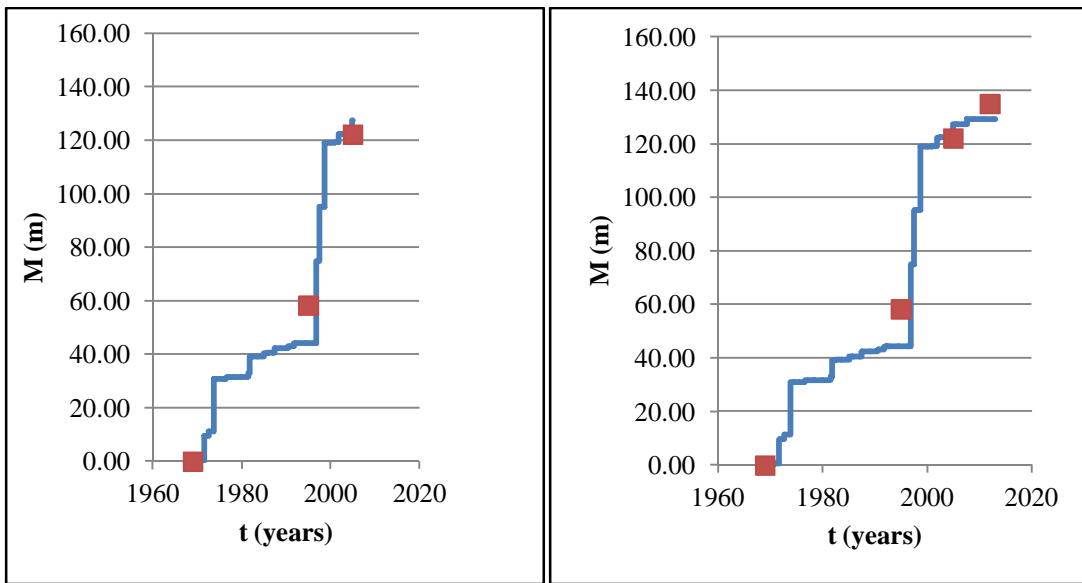


Figure 109. Nueces River verification of prediction with field critical velocity of 0.54 m/s

CHAPTER VII

RESULTS USING THE OBSERVATION METHOD

7.1 INTRODUCTION

The following figures and tables show the results for the critical velocity of each case history (Figures 110 through 125 and Tables 15 through 26). The critical velocity for each case was found by using the Excel spreadsheet and the MATLAB code written for this project and then using the Excel spreadsheet for prediction. Two sets of results are shown for each case: one using the results obtained from the EFA test and another using the chart of erosion categories. For the second set of results of each river, the meander migration cases (Brazos, Trinity, Sabine and Nueces) use the line that separate Categories I and II of the erosion categories chart and the vertical degradation cases (North Sulfur and Colorado) use the line that separate Categories II and III. The calibration step and prediction step results are shown in the next two sections.

7.2 RESULTS FOR CRITICAL VELOCITY (CALIBRATION STEP)

The first step before predicting the magnitude of the movement of the river (meander migration or vertical degradation) is finding the critical velocity at the site. Following the steps in the previous chapter, the critical velocity is found for each site using the EFA results or a line from the erosion categories chart. The first set of results for each river corresponds to the parameters obtained from the EFA curves after testing the samples obtained at the site. The second set of results of each river corresponds to the line obtained from the erosion categories chart. The critical velocity varies when using both methods. The observed data and the calibrated data are included in a table and plotted in their corresponding figure. The critical velocity and the parameters are then used in the prediction step.

7.2.1 Brazos River

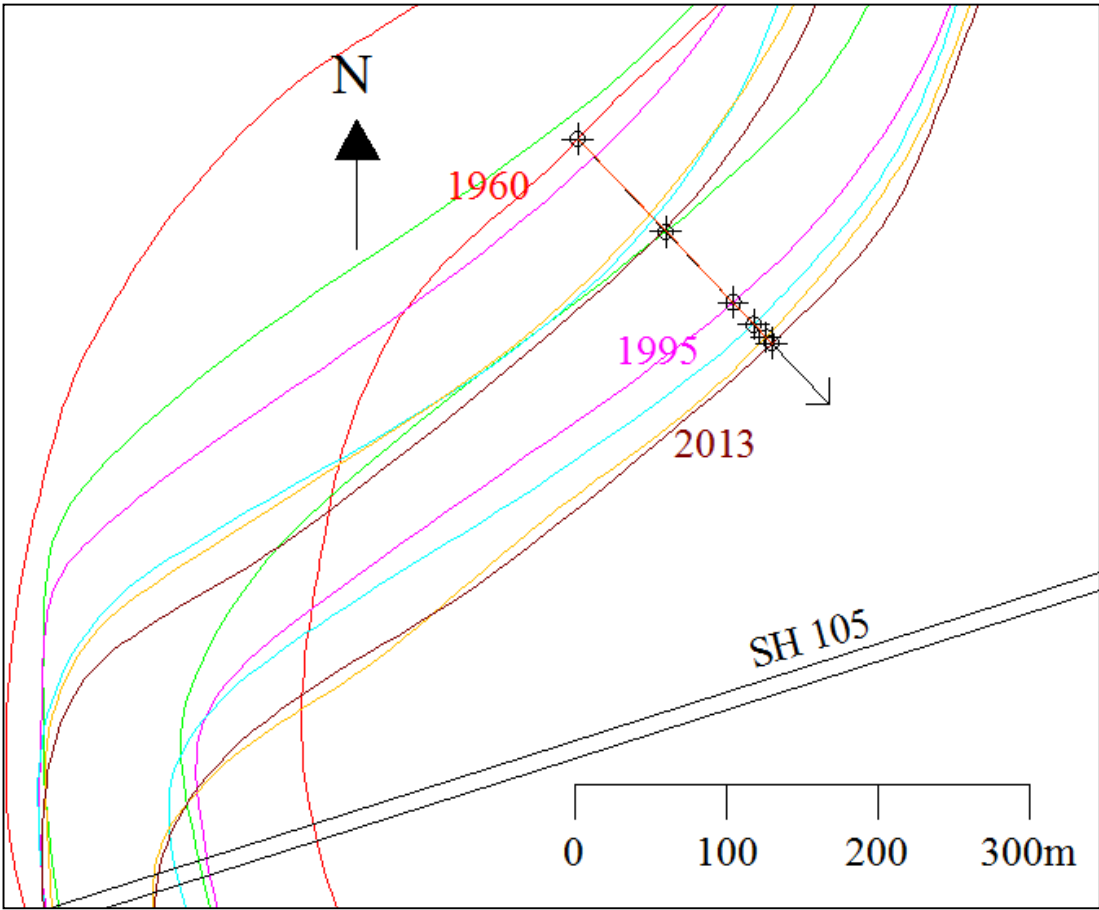


Figure 110. Brazos River meander migration

7.2.1.1 Results Using the EFA Curve from the Soil Samples for the Brazos River Case

Table 15. Brazos River data with parameters from EFA curve

α'	5.67E-08	
β	2.51	
v_c	0.49 m/s	
RI	0.069339	
Time (years)	M_o (m)	M_c(m)
1995	0	0
2003	19.8	18.344
2008	31.6	31.973
2013	37.1	38.854

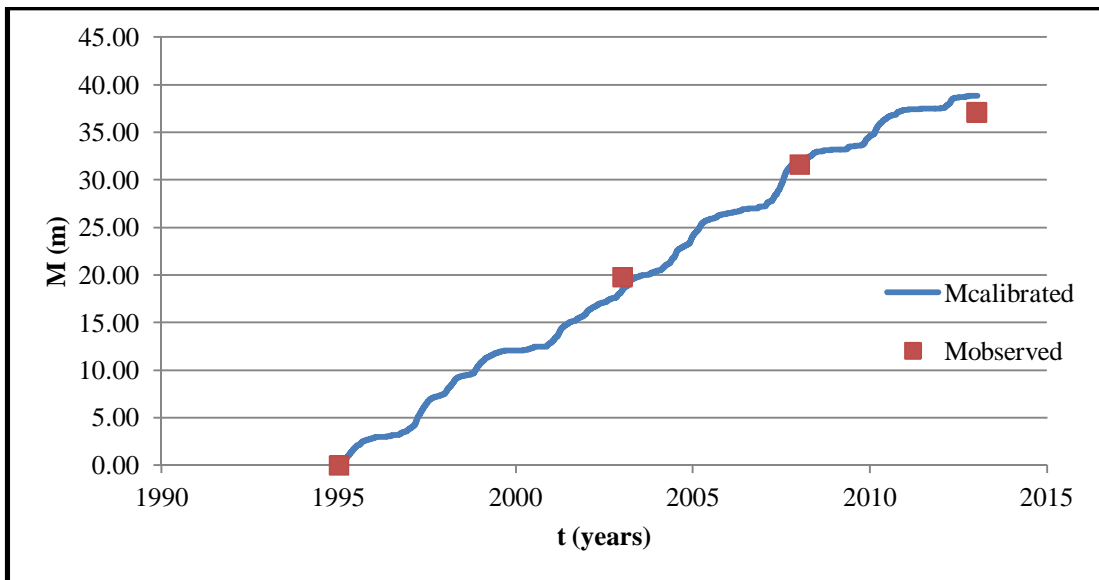


Figure 111. Brazos River meander migration with parameters from EFA curve

7.2.1.2 Results Using the Parameters from Erosion Categories Chart for the Brazos River Case

Table 16. Brazos River data with parameters from erosion categories chart

α'	3.35E-08	
β	8.58	
v_c	0.83 m/s	
RI	0.341770	
Time (years)	M_o (m)	M_c(m)
1995	0	0
2003	19.8	15.177
2008	31.6	35.392
2013	37.1	40.147

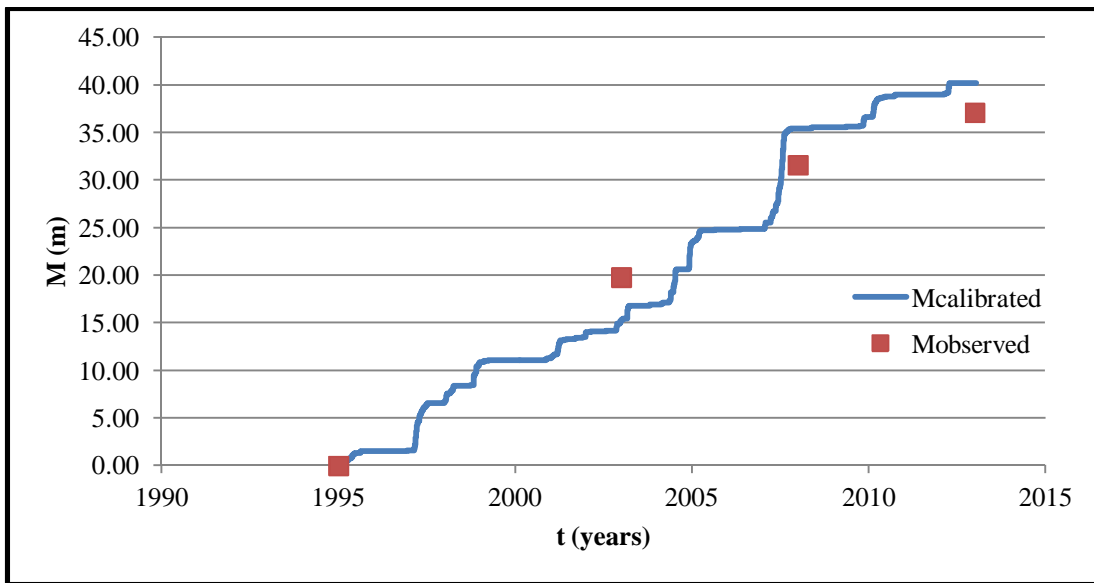


Figure 112. Brazos River meander migration with parameters from erosion categories chart

7.2.2 Trinity River

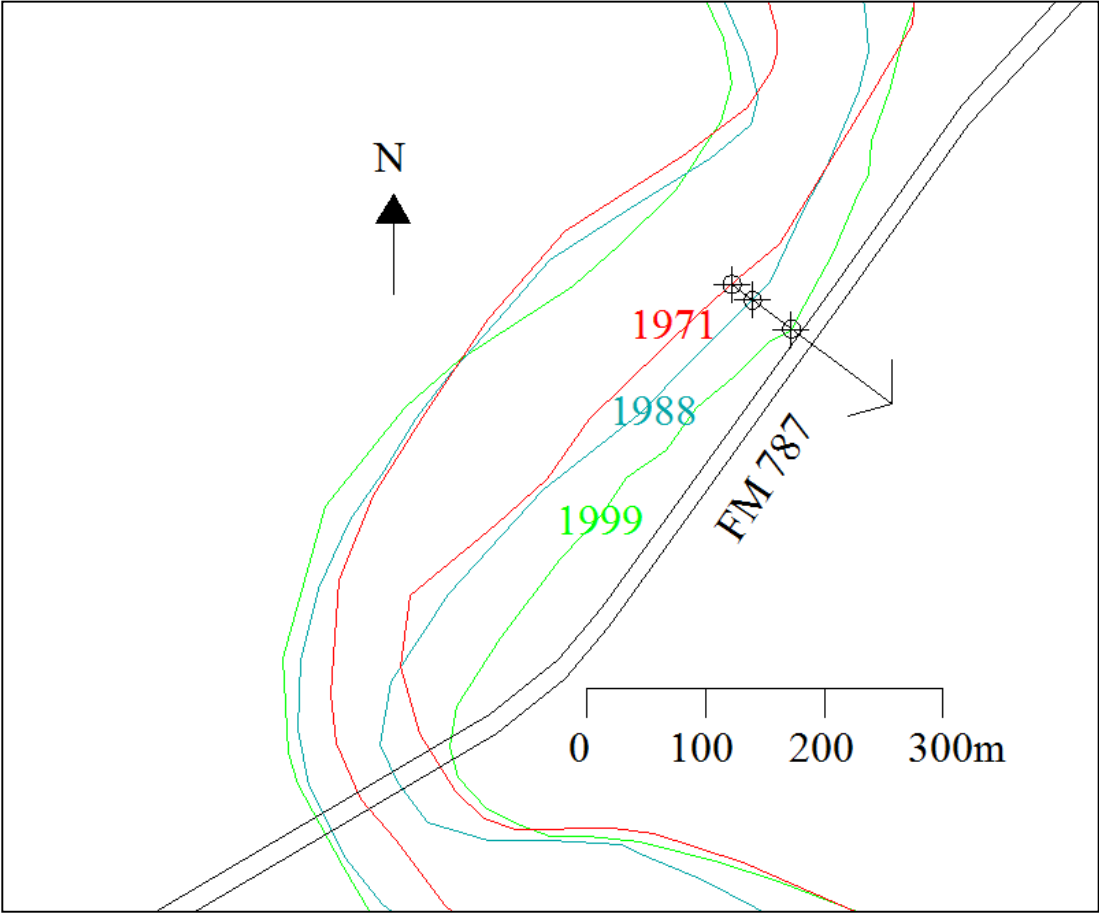


Figure 113. Trinity River meander migration

7.2.2.1 Results Using the EFA Curve from the Soil Samples for the Trinity River Case

Table 17. Trinity River data with parameters from EFA curve

α'	4.63E-08	
β	4.21	
v_c	0.6 m/s	
RI	0.364132	
Time (years)	M_o (m)	M_c(m)
1971	0	0
1988	21.85	29.173
1999	62.6	58.167

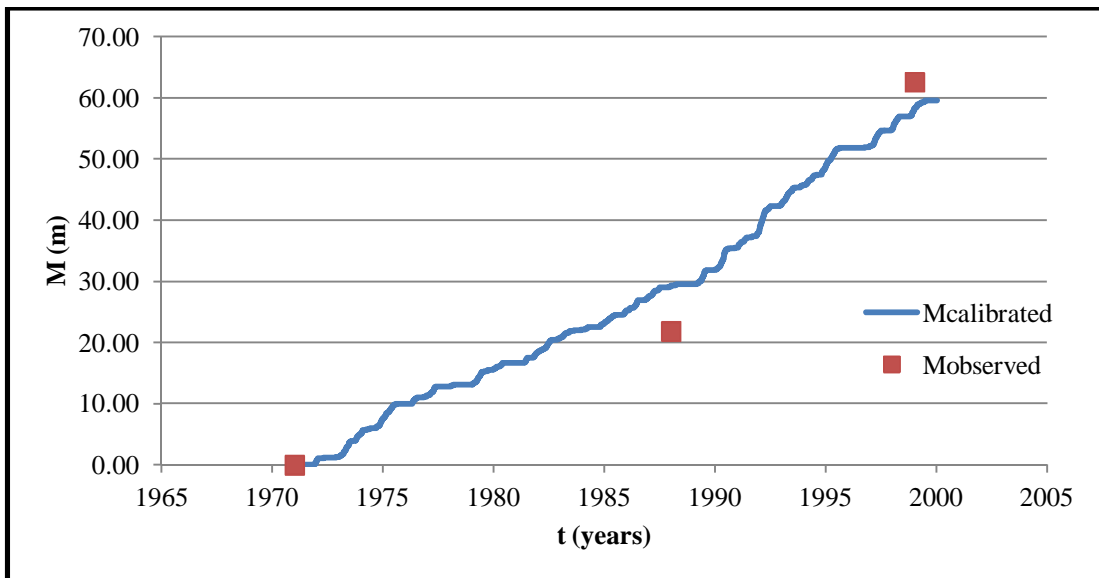


Figure 114. Trinity River meander migration with parameters from EFA curve

7.2.2.2 Results Using the Parameters from Erosion Categories Chart for the Trinity River Case

Table 18. Trinity River data with parameters from erosion categories chart

α'	3.66E-08	
β	8.58	
v_c	0.76 m/s	
RI	0.165800	
Time (years)	M_o (m)	M_c(m)
1971	0	0
1988	21.85	25.025
1999	62.6	61.994

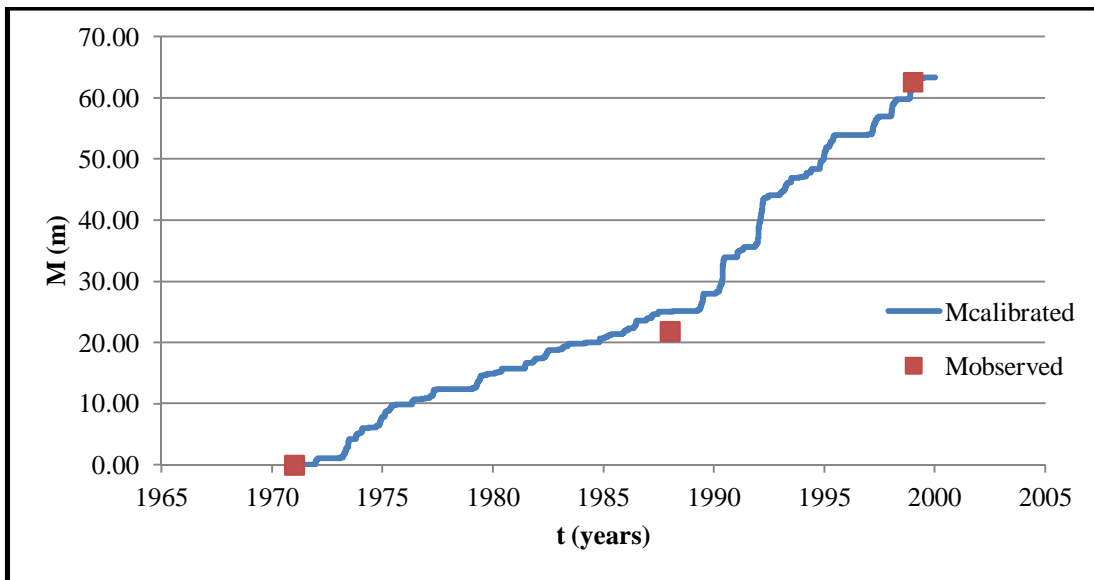


Figure 115. Trinity River meander migration with parameters from erosion categories chart

7.2.3 Sabine River

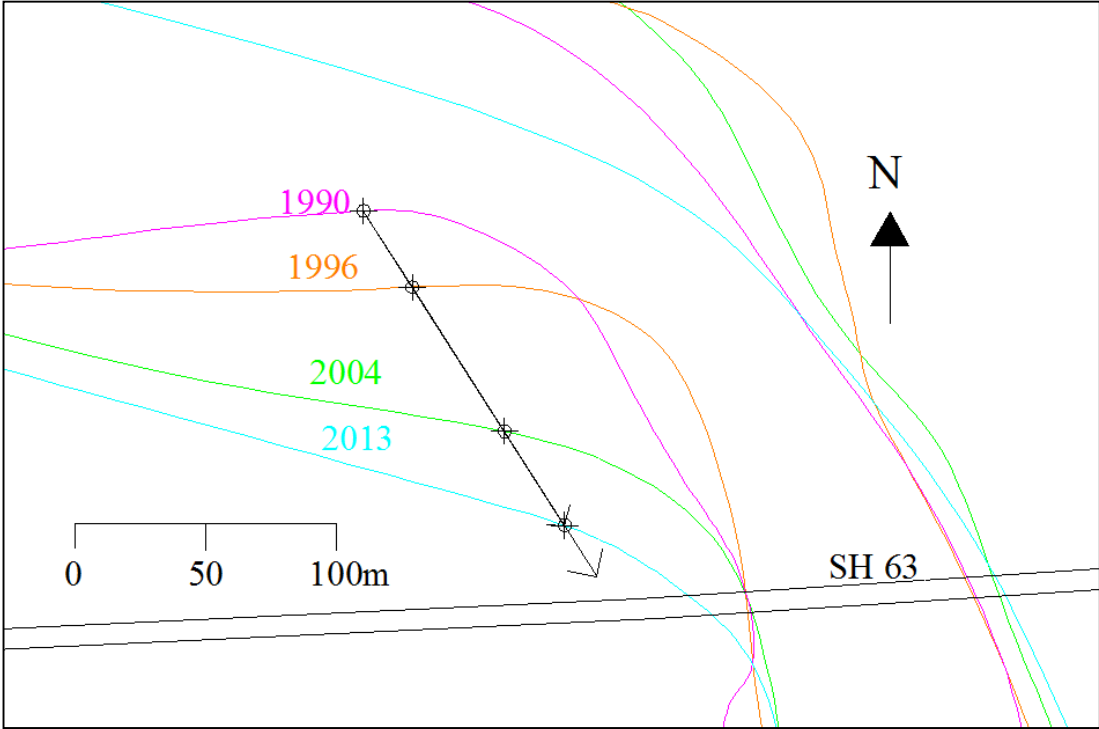


Figure 116. Sabine River meander migration

7.2.3.1 Results Using the EFA Curve from the Soil Samples for the Sabine River Case

Table 19. Sabine River data with parameters from EFA curve

α'	5.79E-08	
β	3.23	
v_c	0.48 m/s	
RI	0.347526	
Time (years)	M_o (m)	M_c(m)
1990	0	0
1996	34.6	50.901
2004	99.8	96.490
2013	142.55	130.879

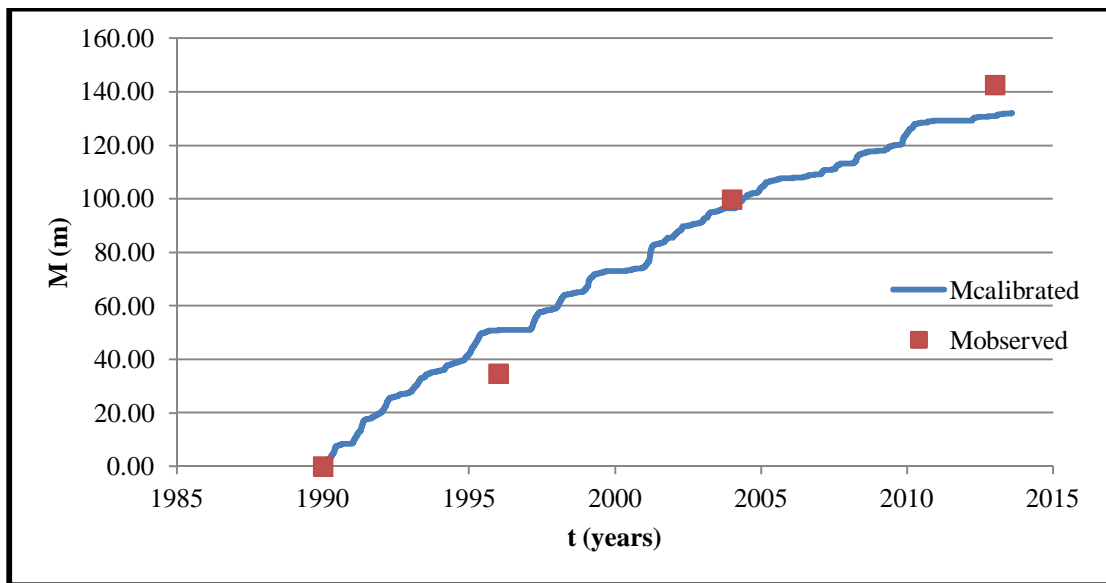


Figure 117. Sabine River meander migration with parameters from EFA curve

7.2.3.2 Results Using the Parameters from Erosion Categories Chart for the Sabine River Case

Table 20. Sabine River data with parameters from erosion categories chart

α'	3.05E-08	
β	8.58	
v_c	0.91 m/s	
RI	0.138600	
Time (years)	Mo (m)	Mc(m)
1990	0	0
1996	34.6	38.577
2004	99.8	109.743
2013	142.55	135.918

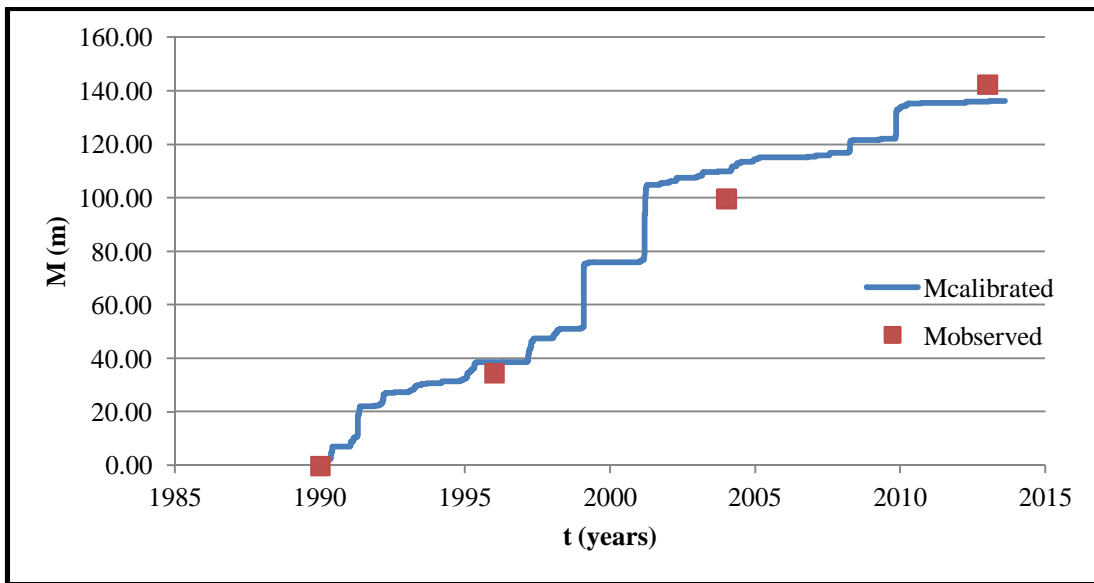


Figure 118. Sabine River meander migration with parameters from erosion categories chart

7.2.4 North Sulfur River

7.2.4.1 Results Using the EFA Curve from the Soil Samples for the North Sulfur River Case

Table 21. North Sulfur River data with parameters from EFA curve

α'	2.44E-08	
β	1.76	
v_c	1.14 m/s	
RI	0.003213	
Time (years)	Mo (m)	Mc(m)
1959	0	0
1999	3.7	3.69

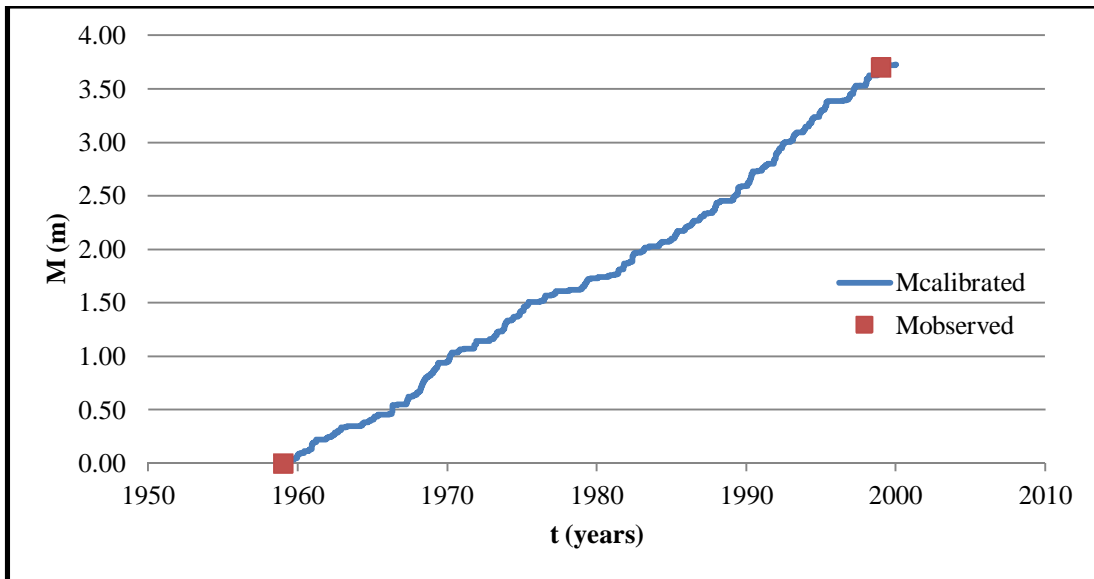


Figure 119. North Sulfur River vertical degradation with parameters from EFA curve

7.2.4.2 Results Using the Parameters from Erosion Categories Chart for the North Sulfur River Case

Table 22. North Sulfur River data with parameters from erosion categories chart

α'	1.67E-08	
β	5.24	
v_c	1.66 m/s	
RI	0.011437	
Time (years)	Mo (m)	Mc(m)
1959	0	0
1999	3.7	3.66

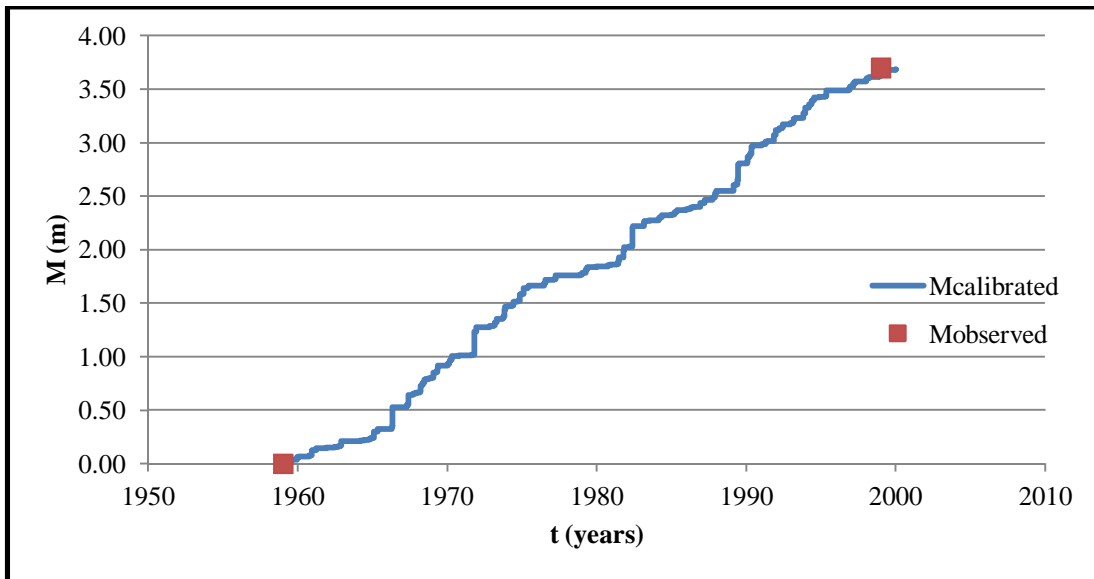


Figure 120. North Sulfur River vertical degradation with parameters from erosion categories chart

7.2.5 Nueces River

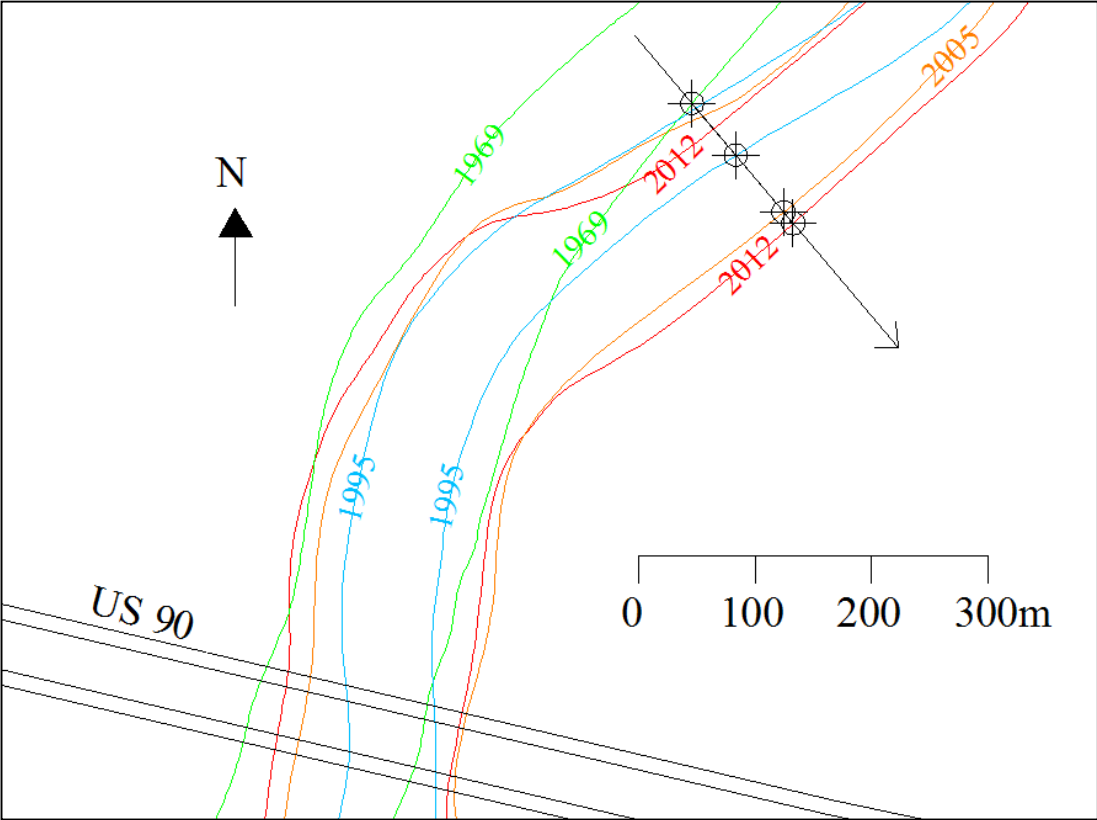


Figure 121. Nueces River meander migration

7.2.5.1 Results Using the EFA Curve from the Soil Samples for the Nueces River Case

Table 23. Nueces River data with parameters from EFA curve

α'	2.14E-07	
β	2.06	
v_c	0.13 m/s	
RI	0.357951	
Time (years)	Mo (m)	Mc(m)
1969	0	0
1995	58.3	86.427
2005	122.2	121.560
2012	135	133.927

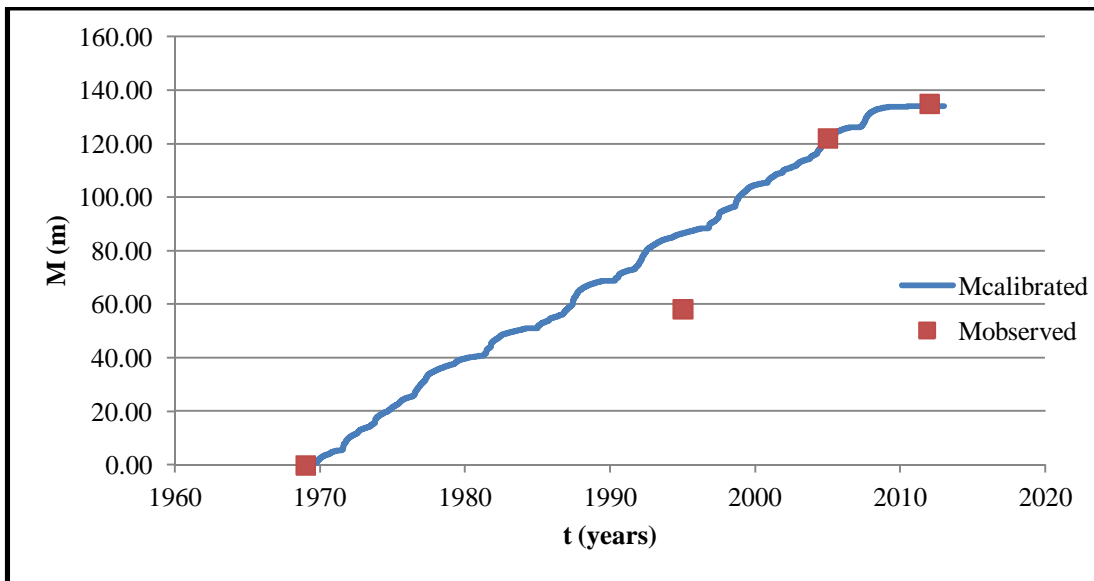


Figure 122. Nueces River meander migration with parameters from EFA curve

7.2.5.2 Results Using the Parameters from Erosion Categories Chart for the Nueces River Case

Table 24. Nueces River data with parameters from erosion categories chart

α'	5.15E-08	
β	8.58	
v_c	0.54 m/s	
RI	0.255221	
Time (years)	Mo (m)	Mc(m)
1969	0	0
1995	58.3	44.327
2005	122.2	127.472
2012	135	129.309

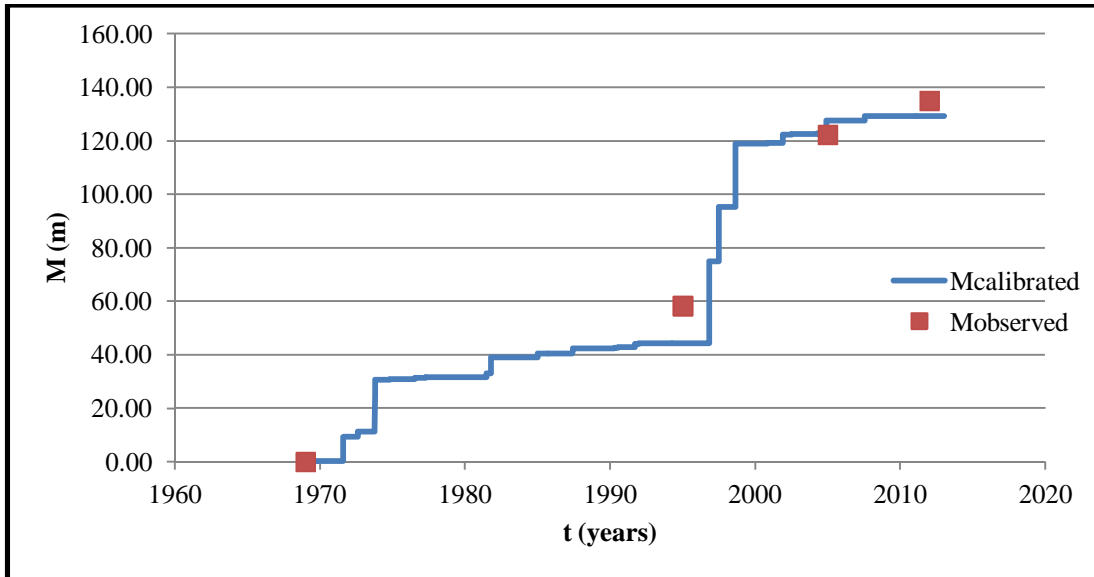


Figure 123. Nueces River meander migration with parameters from erosion categories chart

7.2.6 Colorado River

7.2.6.1 Results Using the EFA Curve from the Soil Samples for the Colorado River Case

Table 25. Colorado River data with parameters from EFA curve

α'	1.92E-08	
β	2.20	
v_c	1.45 m/s	
RI	0.003365	
Time (years)	Mo (m)	Mc(m)
1958	0	0
2005	3.65	3.63

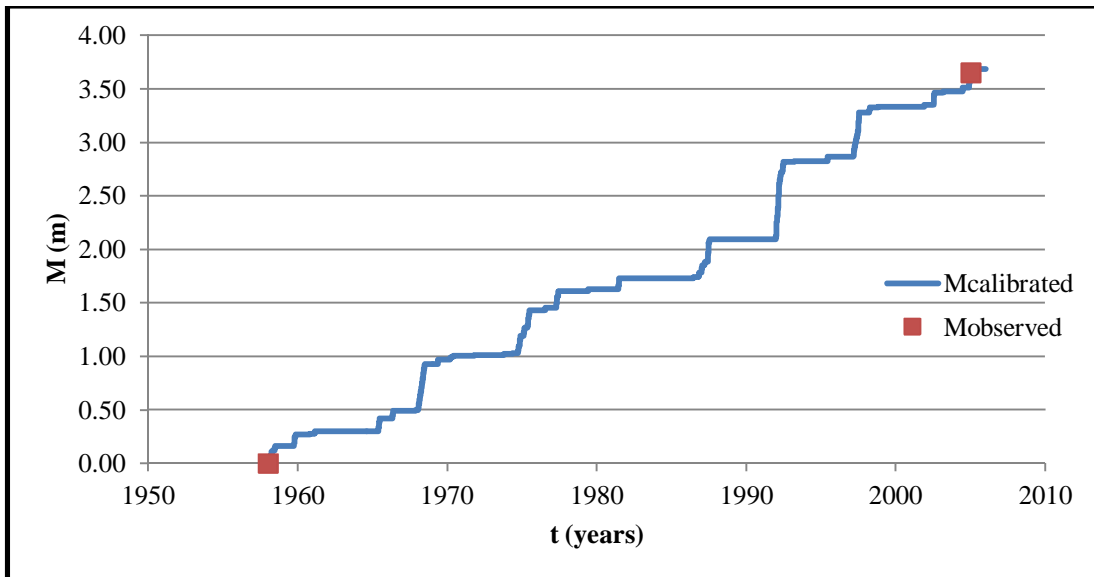


Figure 124. Colorado River vertical degradation with parameters from EFA curve

7.2.6.2 Results Using the Parameters from Erosion Categories Chart for the Colorado River Case

Table 26. Colorado River data with parameters from erosion categories chart

α'	1.72E-08	
β	5.24	
v_c	1.62 m/s	
RI	0.012824	
Time (years)	Mo (m)	Mc(m)
1958	0	0
2005	3.65	3.61

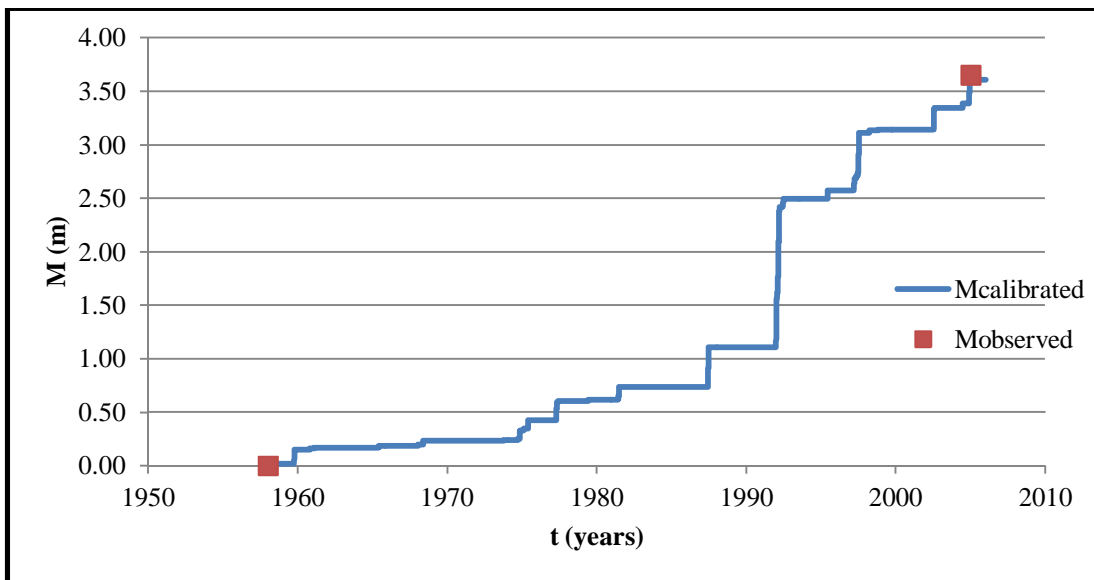


Figure 125. Colorado River vertical degradation with parameters from erosion categories chart

7.3 RESULTS FOR PREDICTION

The following assumptions and conditions were used for the prediction step (Figures 126 through 131) after the calculation of the critical velocity in the calibration step:

1. The position of the point at the last observed data was set to zero. This is not necessary, although it is easier to see the magnitude of the total predicted erosion.
2. The hydrograph used for each river corresponds to the last 10 years of velocities before the last observed data. If the last observed data corresponds to 1999, then the period of velocities used for prediction is 1989-1999, as in the North Sulfur River case.
3. Some rivers have old observed data and not recent. For example, the last Trinity River and North Sulfur River observations are from 1999. The period of 10 years are assumed from this last observed data.
4. The β exponents used are from the EFA categories chart (second set of results of each river from the calibration step). Also their corresponding critical velocity and α' coefficients were used.
5. Figures 126, 127, 128, 129, 130, and 131 correspond to the Brazos, Trinity, Sabine, North Sulfur, Trinity, and Colorado Rivers, respectively.

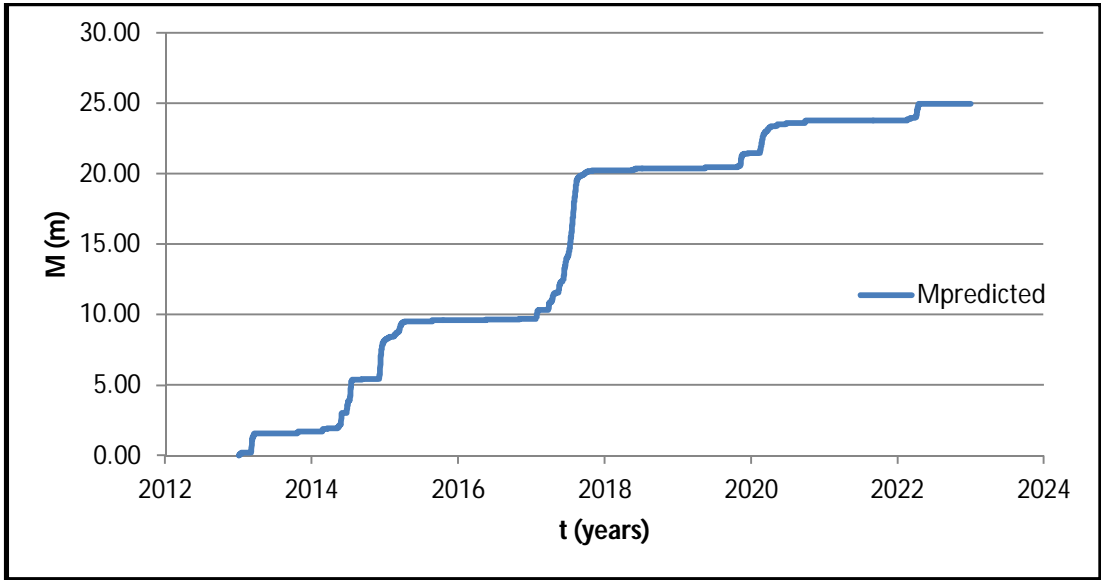


Figure 126. Brazos River prediction

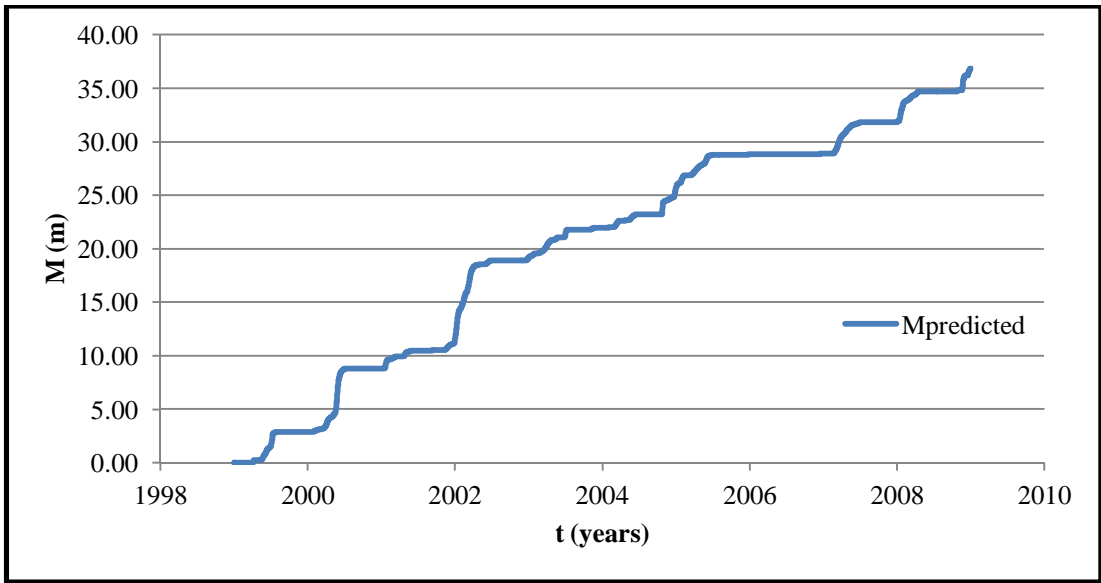


Figure 127. Trinity River prediction

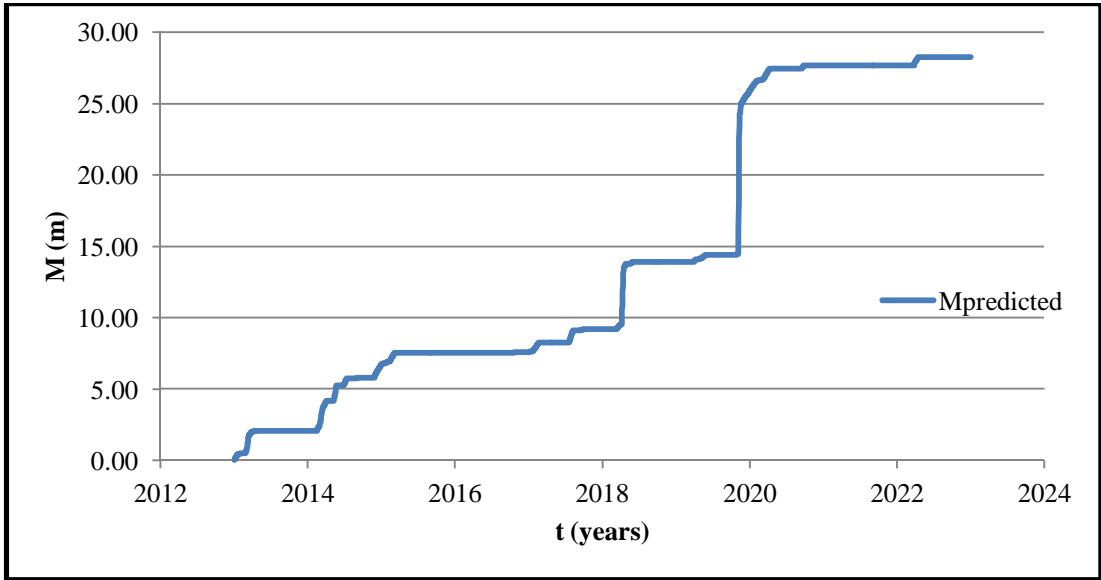


Figure 128. Sabine River prediction

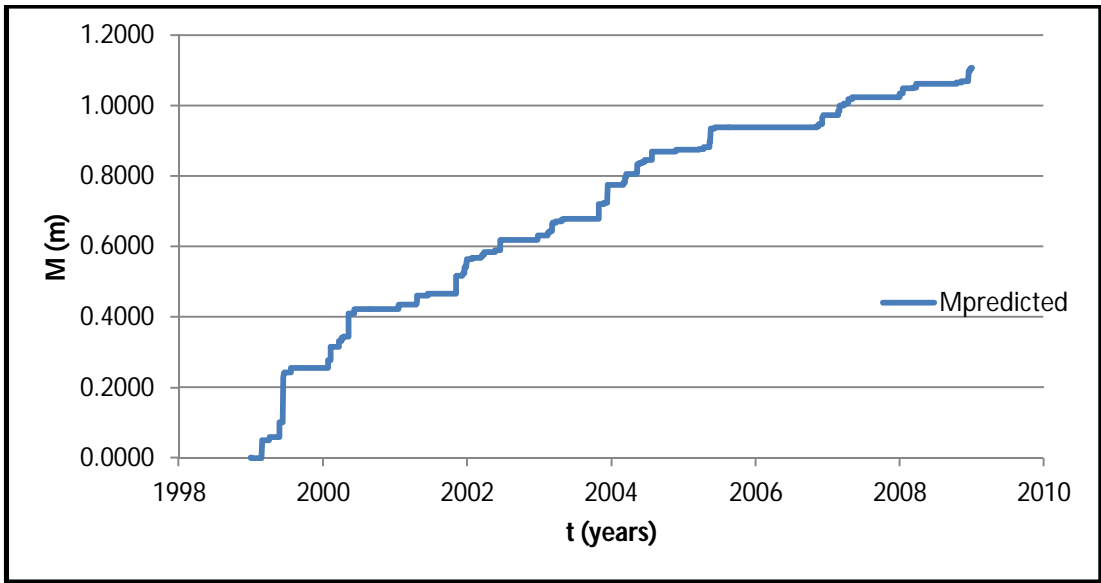


Figure 129. North Sulfur River prediction

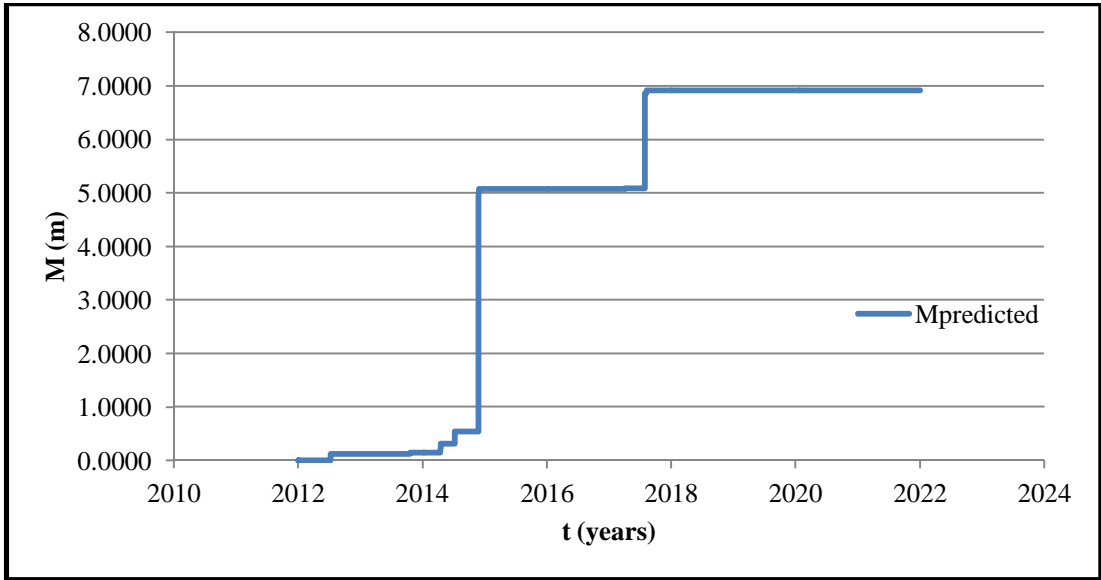


Figure 130. Nueces River prediction

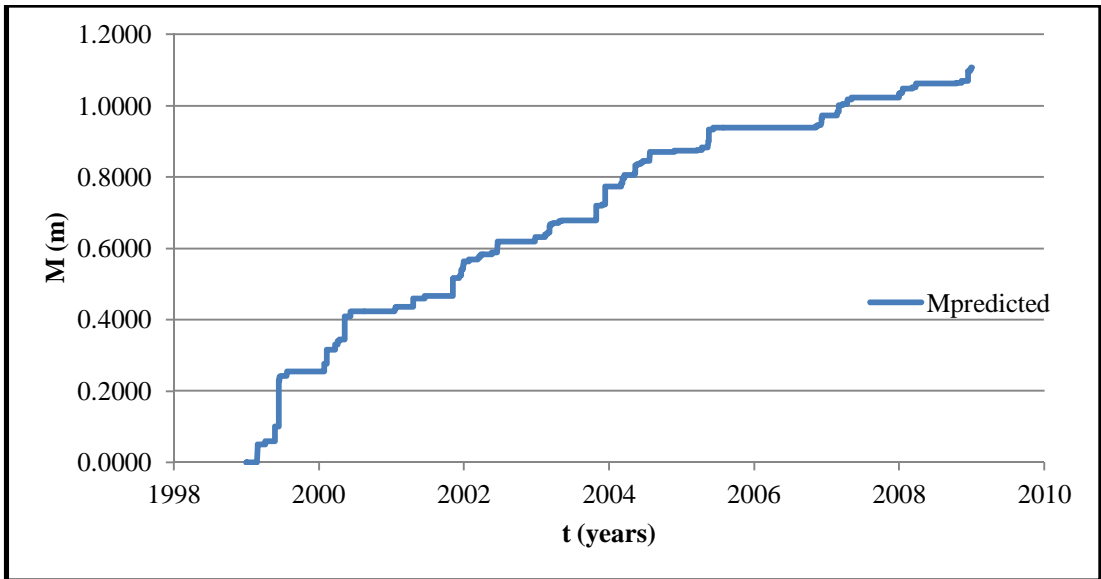


Figure 131. Colorado River prediction

7.4 DISCUSSION OF RESULTS

The results of the predictions are based on the critical velocity obtained from the calibration step. The lowest Ranking Index values were obtained from the results that used β parameters from the EFA categories chart. Only a period of 10 years was used for the hydrograph in the prediction, but this gives a general idea of how much the river will change in the period of 10 years after the last observed data. The critical velocities obtained from both methods of the calibration step used could be very different because of the difference of the slopes obtained from the samples compared to the slopes of the classification of soils chart. Besides the soil erosion parameters, the variability of the results is expected when considering all the factors such as geometry, countermeasures installed and assumptions made.

In general, the behavior of each river looks that they follow the same pattern seen in the calibration step. For the Nueces, Brazos and Sabine Rivers, the data used corresponds to recent data. The last observation for each of these rivers is from 2012 or 2013. The predictions at these sites could be accurate if it is considered that no countermeasures have been installed where the point of reference was selected, as it is the case for these rivers.

In the other cases, the prediction may not represent what will happen or what has happened. The Trinity River has not changed much since the 1990s because countermeasures such as sheet piles have been installed to decrease the erosion rate. The erosion has been controlled since the repairs at the site. Also, the vegetation at the site guards the bend of the river. This case may not be the best example to use the observation method.

As mentioned before, the North Sulfur River bridge was replaced in the 1990s and only two cross sections were used. The latest cross section found was from the 1999 and the prediction was based for the following 10 years. Two cross sections were used for the Colorado River as well. Only two points in the calibration step were used for both of these cases. At least adding one more point to the observed data for both rivers could have been more precise to obtain the critical velocity.

CHAPTER VIII

SUMMARY AND RECOMMENDATIONS

8.1 SUMMARY

Meander migration and vertical degradation have been problems that have been studied for many years, but the uncertainty has been part of its nature. The “where” and “when” involved in these problems have been approached in multiple times and solutions have been proposed to make predictions based on data available. Rivers are continuously changing and different factors in nature are responsible for their changes. Meander migration and vertical degradation are problems that depend on three main aspects: the soil at the site, the water flow conditions and the geometry of the river itself.

The method that was proposed for this project takes in consideration each of the three important aspects, while other methods proposed in the past may have ignored some of them or does not take them in consideration. Not all soils are equal and their erodibility is greatly related to the changes of the position of a river. The observation method is based on observed data (data from the past) to predict the behavior in the future. Aerial photos, maps and cross sections correspond to these observed data and tell how the river geometry has evolved with time. The river hydrograph correspond to the part of the water flow of the problem. The extrapolation method by using the aerial photos ignores the constant change of water flow. One sudden increase in water velocity may erode a few meters from the bank of a river.

The observation method was applied to 6 different rivers in Texas. Each one of them has had different problems of erosion for years and in some of them there have been remedies that were needed to avoid the exposure of the banks to big floods. The observation method consists of two important steps: calibration step and prediction step. The calibration step is used to find the critical velocity at the field, which is the minimum velocity required for erosion to occur. The most important input data to obtain the critical velocity are: the erosion parameter β from EFA curve (slope of the curve in log-log scale), the observed data from aerial maps, photos or cross sections, and the

velocity hydrograph. The critical velocity for the 6 rivers was obtained by using the EFA curve from samples and from a chart that has all the erosion categories. For the prediction step, the input data is essentially the same as in the calibration step, but there is no iteration process and the critical velocity used is the one obtained from the calibration step.

For this project, the observation method was developed considering all the factors mentioned before and it can be applied by using two programs: MATLAB or Microsoft Excel. The method is relatively simple to use and the results can be compared to other methods. It is very important to know how much a river will change with time and this method is an alternative that provides a solution to the problem.

8.2 RECOMMENDATIONS

The observation method depends on previous or observed data to obtain the prediction of the magnitude of erosion. The method is as good as the observed data. Historic maps are not as good as high resolution photos for a few reasons. First, they could be hard to find for periods of time that the user would want. Also, the bends of the river can be confused with the water level of the river when the measurements were taken at the site to prepare the map. Photos are preferred over maps, but not enough of them could be found before 1990. The results could have been better with aerial photos. Also, the method yields better results when using a short period of time (10-20 years) with many observations, preferably with aerial photos.

Also, for the vertical degradation cases, the data that was available was very limited. Only two points were used for the North Sulfur River and the Colorado River. More points could have been better to estimate the critical velocity and to obtain a better prediction. When the code compares the calibrated data with the observed, the values were almost exactly the same, which may not be necessarily true. More points for these cases need to be used. The Observation Method also does not consider the deposit of sediments at the bottom of the river and assumes constant erosion only. This simplifies the problem, but the results may be inaccurate when this is not taken into account. Other

physical or mathematical models could be used to compare the results for the vertical degradation cases.

The results from the Observation Method were not compared to other methods used for meander migration or vertical degradation. This method proved to be a simple and quick way to obtain results for the movement of one point of the river. In the future, the Observation Method could be used in conjunction with other methods to provide a solution to the prediction of meander migration and vertical degradation problems and compare the results for a better design or planning.

REFERENCES

American Society of Testing and Materials (2007). "Standard Test Method for Particle-Size Analysis of Soils." Designation: ASTM D 422-63, West Conshohocken, PA.

Briaud, J.L., and Tucker, L.M. (1988). "Measured and predicted axial response of 98 piles." *Journal of Geotechnical Engineering*, 114 (9), pp. #984–1001.

Briaud, J.L., Chen, H.C., and Park, S. (2001a). "Predicting Meander Migration: Evaluation of Some Existing Techniques." *Texas Transportation Institute Research Report 2105-1*, College Station, TX.

Briaud, J.L., Chen, H.C., Edge, B., Park, S., and Shah, A. (2001b). "Guidelines for Bridges Over Degrading and Migrating Streams, Part 1: Synthesis of Existing Knowledge." *Texas Transportation Institute Research Report 2105-2*, College Station, TX.

Briaud, J.L., Chen, H. C., Li, Y., and Nurtjahyo, P. (2004). "SRICOS-EFA method for complex piers in fine-grained soils." *Journal of Geotechnical and Geoenvironmental Engineering*, 130(11), pp. #1180-1191.

Briaud, J.L., Chen, H.C., Chang, K.A., Chung, Y.A., Park, N., Wang, W., and Yeh, P.H. (2007). "Establish Guidance for Soil-Properties Based Prediction of Meander Migration Rate." *Texas Transportation Institute Research Report 0-4378-1*, College Station, TX.

Briaud J.L., Kim, D., Gardoni, P., Olivera, Chen, F. H., and Elsbury, K. (2009). "Simplified Method for Estimating Scour at Bridges." *Texas Transportation Institute Research Report 0-5505-1*, College Station, TX.

Briaud, J.L. (2013). *Geotechnical Engineering: Unsaturated and Saturated Soils*. John Wiley & Sons, NY.

Brice, J. C. (1975). "Airphoto interpretation of the form and behavior of alluvial rivers." *Final Report to the U.S. Army Research Office*, Washington, D.C.

Brice, J.C. (1982). "Stream Channel Stability Assessment." *Federal Highway Administration Report FHWA/RD-82/021*, Washington, DC, USA, pp. #41.

Brunner, G. W. (2002). "HEC-RAS River Analysis System: Hydraulic Reference Manual, Version 3.1." U.S. Army Corps of Engineers, Hydrologic Engineering Research Center, Davis, CA.

Google Earth Version 7.1.2.2041 (2013). Google Inc., Mountain View, CA.

Hooke, J.M. (1980). "Magnitude and distribution of rates of river bank erosion." *Earth Surface Processes*, 5 (2), pp. #363-377.

Keady, P.D., and Priest M.S. (1977). "The downstream migration rate of river meandering patterns." *Proc. 12th Mississippi Water Resources Conference*, Jackson, MS, pp. #29-34.

Lagasse, P. F., Spitz, W. J., Zevenbergen, L. W., and ZachMann, D. W. (2004a). "Methodology for Predicting Channel Migration." *National Cooperative Highway Research Program Project 24-16*, Owen Ayres & Associates, Inc., Fort Collins, CO.

Lagasse, P.F., Spitz, W.J., Zevenbergen, L.W., and ZachMann, D.W. (2004b). "Handbook for Predicting Stream Meander Migration Using Aerial Photographs and Maps." *National Cooperative Highway Research Program Project 24-16*, Owen Ayres & Associates, Inc., Fort Collins, CO.

Nanson G.C., and Hickin E.J. (1983). "Channel migration and incision on the Beatton River." *Journal of Hydraulic Engineering*, 117 (7), (Discussion and Closure), ASCE, Reston, VA, pp. #942-946.

Perri, J., Shewbridge, S., Millet, R., Huang, W., Vargas, J., Inamine, M., and Mahnke, S. (2010). "Site factor for use of velocity-based EFA erosion rates." *Scour and erosion. Proceedings of the Fifth International Conference on Scour and Erosion (ICSE-5)*, San Francisco, CA, pp. #172-181.

United States Geological Survey (2013). "USGS Water-Data Site Information for the Nation." <http://waterdata.usgs.gov/nwis/inventory>. Accessed on 08/01/2013.

APPENDIX A
OBSERVATION METHOD MATLAB CODE

```
clear all;
clc;
close all;
disp('          TAMU-SIMPLEMEANDER (CALIBRATION STEP ONLY) ');
disp('Observation Method for Prediction of Meander Migration and
Degradation');
disp('          Texas A&M Transportation Institute');
disp('          Code Written by: Axel Montalvo')

disp(' ');
disp(' ');
disp(' ');

t=load('time.txt');
v=load('velocity.txt');

B=input('Enter the beta exponent: ');
zdotc=input('Enter the erosion rate at critical velocity: ');
deltat=input('Enter the increments of time (delta t): ');
number=input('Enter the number of observations: ');

disp(' ');

for i=1:number
    i
    tO(i,1)=input('Enter the year of observation: ');
    MO(i,1)=input('Enter the position of the river: ');
end

tomo=[tO,MO];

vmin=min(v);
vmin=round(vmin/.01)*.01;
vmax=max(v);
vmax=round(vmax/.01)*.01;

vec=[vmin:.01:vmax];

lt=length(t);
Ma=zeros(lt,1);
M=zeros(lt,1);
```

```

for i=1:length(vec)
a=zdotc/vec(i);
    for j=1:length(t)

        if (v(j)/vec(i))>1
            M(j)=a*((v(j)/vec(i))^B)*vec(i)*deltat;
        else
            M(j)=0;
        end

        Ma(1)=M(1);
    end

    for j=2:length(t)

        Ma(j)=Ma(j-1)+M(j);

    end

td(1,:)=[t(1),Ma(1)];

for k=1:(length(t0)-1);

    td(k+1,:)=[t(t0(k+1)*365-t0(1)*365),Ma(t0(k+1)*365-t0(1)*365)];
end

Mcp=[td(:,2)];
Mco=[tomo(:,2)];

for kk=1:(length(t0)-1);

    Mcpp(kk,1)=Mcp(kk+1,1);
    Mcoo(kk,1)=Mco(kk+1,1);

end

average=abs(mean(log(Mcpp./Mcoo)));
standard=std(log(Mcpp./Mcoo));

RI=standard+average;
results(i,:)=[vec(i),RI,standard,average];

end

[minnum,minindex]=min(results(:,2));
[row, col] = ind2sub(size(results(:,2)), minindex);

```



```

Vc=results(row,1);
RI=results(row,2);

for j=1:length(t)
a=zdotc/Vc;
    if (v(j)/Vc)>1
        M(j)=a*((v(j)/Vc)^B)*Vc*deltat;
    else
        M(j)=0;
    end
    Ma(1)=M(1);
end

for j=2:length(t)

    Ma(j)=Ma(j-1)+M(j);

end

for k=1:(length(t0)-1);

    td(k+1,:)=[t(t0(k+1)*365-t0(1)*365),Ma(t0(k+1)*365-t0(1)*365)];

end

    Mcp=[td(:,2)];
    Mco=[tomo(:,2)];

for kk=1:(length(t0)-1);

    Mcpp(kk,1)=Mcp(kk+1,1);
    Mcoo(kk,1)=Mco(kk+1,1);

end

%%%%%%%%%%%%%%%%%%%%%%%%%%%%%%%%%%%%%%%%%%%%%%%%%%%%%%%%%%%%%%%%%%%%%%%%%%FIGURES

disp(' ');
disp(' Critical Velocity (m/s) is');
Vc
disp(' ');
disp(' Alpha prime is');
a
disp(' ');
disp(' Ranking Index is: ');
RI

```

```

figure(1)
plot(t, Ma, 'linewidth', .5);
grid on;

title('Erosion of river through time', 'fontweight', 'bold');
xlabel('t (years)', 'fontweight', 'bold');
ylabel('M (meters)', 'fontweight', 'bold');

hold on
scatter(tO, MO);

figure (2)
x=[0:.01:100];
x=x';
xx=(x/Vc);
for i=1:length(x)
    if xx(i)<1
        xx(i)=0;
    else
        xx(i)=xx(i);
    end
end
yy=a.*(xx.^B);
loglog(xx, yy)

xlabel('V/Vc', 'fontweight', 'bold');
ylabel('zdot/Vc', 'fontweight', 'bold');
title('Dimensionless EFA curve from predicted critical
velocity', 'fontweight', 'bold');

figure (3)

plot(t, v)
xlabel('Time (days)', 'fontweight', 'bold');
ylabel('Velocity (m/s) ', 'fontweight', 'bold');
title('Velocity vs. Time', 'fontweight', 'bold');

hold on
plot(t, Vc, 'r')

figure(4)

scatter(Mcp, Mco, 'k');

title('Brazos River', 'fontweight', 'bold');
xlabel('Mc (m)', 'fontweight', 'bold');
ylabel('Mo (m)', 'fontweight', 'bold');
grid on;

```

```
title('Observed vs. Calibrated','fontweight','bold');

hold on

Mmax=max(Mcpp);
if max(Mcoo)>Mmax
    Mmax=max(Mcoo);
end

Mmax=round(Mmax/10)*10;
xxx=[0,Mmax];
yyy=[0,Mmax];
plot(xxx,yyy,'k');
```